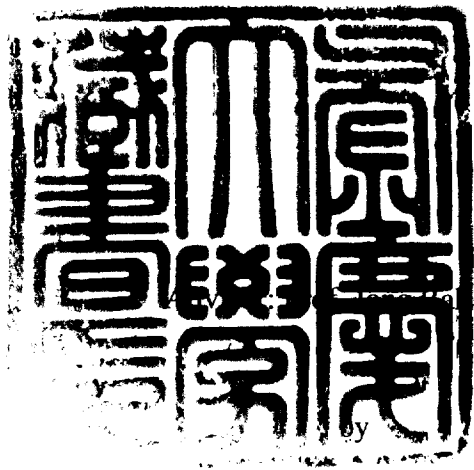


Equalizer performance of underwater acoustic communications in multipath fading channel

(다중경로 페이딩 채널에서 수중음향통신 시스템의 등화기 성능)



Yoon

Chun-Dan Lin

A thesis submitted in partial fulfillment of the requirements
for the degree of
Doctor of Philosophy
in Department of Telematics Engineering
The Graduate School,
Pukyong National University

February 2006

林春丹의 工學博士 學位論文을 認准함.

2006年 2月 26日

主 審 工學博士 鄭 信 一 印

委 員 工學博士 河 德 鎬 印

委 員 工學博士 金 錫 泰 印

委 員 工學博士 金 載 洙 印

委 員 工學博士 尹 鍾 樂 印

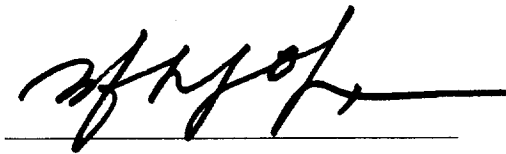
Equalizer performance of underwater acoustic communications
in multipath fading channel

A dissertation

by

Chun-Dan Lin

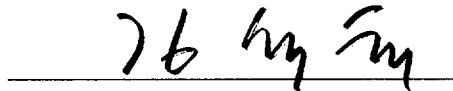
Approved by:



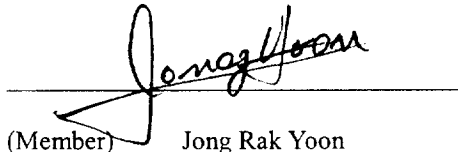
(Chairman) Shin Il Jeong



(Member) Deock-Ho Ha



(Member) Kim Seok Tae



(Member) Jong Rak Yoon



(Member) Jea-Soo Kim

February 28, 2006

Contents

Abstract

Chapter 1 Introduction	1
1.1 Background	1
1.2 Adaptive equalization	2
1.3 Diversity technique- passive phase conjugation (PPC)	3
 Chapter 2 Linear Equalizer and Nonlinear Decision Feedback Equalizer	 6
2.1 Channel model and communication system	6
2.2 LMS linear and nonlinear equalizer	11
2.3 Simulation results	15
2.4 Conclusions	30
 Chapter 3 Performance of Adaptive Equalization for QPSK System	
Over Multipath Channel	31
3.1 Background	31
3.2 Communication system and equalization	32
3.3 Simulation results	38
3.4 Conclusions	62
 Chapter 4 Performance Comparison of Passive Phase Conjugation	
and Decision Feedback Equalizer	63
4.1 Background	63

4.2 System structure and equalization algorithm -----	64
4.3 Performance comparison of PPC and DFE-----	68
4.4 Conclusions -----	79
 Chapter 5 Conclusions -----	 80
 References -----	 82
 Acknowledgements -----	 88

List of Figures

Figure 2.1	Block diagram of communication system -----	7
Figure 2.2	LMS structure -----	12
Figure 2.3	Equalizer structures -----	14
Figure 2.4	Channel response to probe signal for $R=10m$ -----	17
Figure 2.5	Output scatter for $R=10m$ -----	18
Figure 2.6	Equalizer performance for $R=10m$ -----	20
Figure 2.7	Channel response to probe signal for $R=600m$ -----	21
Figure 2.8	Output scatter for $R=600m$ -----	22
Figure 2.9	Equalizer performance for $R=600m$ -----	24
Figure 2.10	Channel response to probe signal for $R=1000m$. -----	26
Figure 2.11	Output scatter for $R=1000m$ -----	27
Figure 2.12	Equalizer performance for $R=1000m$ -----	29
Figure 2.13	BER vs. SNR for LE and DFE -----	30
Figure 3.1	Block diagram of QPSK system -----	32
Figure 3.2	Equalizer structures -----	37
Figure 3.3	Channel frequency response -----	41
Figure 3.4	LE performance for $R=10m$ -----	43
Figure 3.5	DFE performance for $R=10m$ -----	45
Figure 3.6	LE performance for $R=600m$ -----	48
Figure 3.7	DFE performance for $R=600m$ -----	50
Figure 3.8	LE performance for $R=1000m$ -----	52
Figure 3.9	DFE performance for $R=1000m$ -----	54

Figure 3.10	BER vs. SNR after LE and DFE -----	56
Figure 3.11	Correlation coefficient with respect to drifting distance -----	57
Figure 3.12	DFE performance with drifting distance for R=10m -----	59
Figure 3.13	DFE performance with drifting distance for R=600m -----	61
Figure 4.1	Multichannel DFE structure -----	67
Figure 4.2	Block diagram for PPC equalizer -----	67
Figure 4.3	PPC and DFE performance for M=3 and R=700m -----	70
Figure 4.4	PPC and DFE performance for M=13 and R=700m -----	72
Figure 4.5	PPC and DFE performance for M=3 and R=1000m -----	74
Figure 4.6	PPC and DFE performance for M=13 and R=1000m -----	77
Figure 4.7	MSE vs. number of receivers for DFE and PPC -----	78
Figure 4.8	MSE vs. number of receivers for DFE and PPC (SNR: 20dB) -----	79

List of Tables

Table 2.1	Parameters for simulation of equalizer performance-----	15
-----------	---	----

다중경로 페이딩 채널에서 수중음향통신 시스템의 등화기 성능

임춘단

부경대학교 대학원 정보통신공학과

요 약

수중음향 채널의 시-공간적 확산에 의한 다중경로의 영향은 데이터 상호간의 ISI(Inter-Symbol Interference)를 발생시킨다. 이런 수중음향채널의 ISI를 감소시키는 방법으로 적응등화기가 사용되고 있으며, 현재 많은 부분에서 활용 개발되고 있다. 수중음향 통신시스템에서 ISI에 의한 성능감소를 향상시키는 방법으로 다중경로에 강한 변조방식의 선택과 알고리즘 개발이 요구되고 있다. ISI에 의한 성능향상에 적용되는 알고리즘은 선형 등화기(LE)와 비선형 DFE(Decision Feedback Equalizer)에서 LMS(Least Mean Square) 알고리즘을 사용되고 있으며, 본 논문에서는 BPSK(Binary Phase Shift Keying)와 QPSK(Quadrature Phase Shift Keying) 변조 방식을 사용하여 다중경로에 의한 ISI의 영향을 감소시키기 위해 알고리즘을 적용하여 수치모의실험을 통해 전해에서 다중경로에 의한 심벌간의 상호간섭을 줄이고 높은 전송률을 얻을 수 있는 효과적인 방법을 연구하였다.

큰 Eigenvalue spread 가지는 채널에서 등화기를 사용할 때 학습 부분은 RLS(Recursive Least Square) 알고리즘을 사용하고 실제 데이터 전송에서는 LMS 알고리즘을 사용하여 빠른 수렴 속도와 양호한 성능을 가지도록 하였다. 논문에서 제안된 기술은 수렴속도와 MSE(Mean Square Error)의 균형을 맞출 수 있는 기술이며, 음원이 이동할 때와 이동하기 전 채널에서 높은 코히어런스를 가질 때 등화기는 채널변화를 추적하고 수렴하는 결과를 보여 줄 것이다.

마지막으로 수동 패시브 컨주게이션(PPC:Passive Phase Conjugation)과 DFE의 성능을 비교 하였다. DFE는 높은 SNR(Signal to Noise ratio)의 출력이지만 선택된 파라미터에 대해서 민감하다. PPC는 많은 수신신호를 더함으로써, 높은 SNR이 아니라도 심벌간의 상호간섭을 줄일 수 있다.

Chapter 1

Introduction

1.1 Background

In recent years more and more attention has been attracted in the underwater acoustic (UWA) communications application areas such as telemetry, remote control or speech or image transmission [1]. Consequently, high data rate transmission has become an important issue in bandlimited UWA channel.

Due to the amplitude fluctuations and time varying characteristic of received signal in underwater acoustic channel the research of noncoherent detection such as frequency shift keying (FSK) had been favored in the past. FSK modulation resorts to the method that guard times inserted between pulses of the same frequency to ensure all the channel reverberation dies out. However it is at the cost of sacrificing bandwidth[2-6].

Nowadays research focuses on the coherent detection such as multiple phase shift keying (MPSK) to achieve bandwidth efficient communication [5-7]. Multipath propagation which causes intersymbol interference (ISI) is a challenging task in UWA communication. As a result several techniques are used to suppress ISI due to multipath. Among them coherent detection such as PSK method combined with equalization techniques meets the demands of bandwidth efficiency in bandlimited UWA channel.

To recover the transmitted signals in the presence of ISI several methods have been proposed. An equalization method, i.e., maximum likelihood method, though provides the best performance in the data estimation, no doubt it is at the expense of high computation complexity and unsuitable for long time spread channel. Spread spectrum technique will sacrifice the available bandwidth to suppress ISI. Therefore adaptive equalizers are always realized in the underwater acoustic time-dispersive channel. LMS (least mean

squares) and RLS (recursive least squares) are the most commonly adopted algorithms in adaptive equalizations [7-8].

Linear filter theory, the method of least squares was first invented by Gauss in 1795. The first studies of minimum mean-square estimation in stochastic process were made by Kolmogorov, Krein and Wiener late 1930s and early 1940s. LMS algorithm which is a simple, effective method, was adopted in the adaptive transversal filter by Widrow and Hoff in 1959[8].

The RLS algorithm first appeared in the paper of Plackett in 1950. Though RLS algorithm has fast convergence rate and better tracking capability, because of its main drawback of high computational complexity, it's hard to achieve real-time implementation. Consequently modified algorithm such as square-root RLS has been developed and used in real-time implementation.

1.2 Adaptive equalization

Until the early 1960s, fixed equalization was employed to combat the degrading effects of ISI imposed on telephone channels. In 1965 Lucky proposed a zero-forcing equalizer for automatically adjusting the tap weights to suppress the ISI. In 1969 Gersho, Proakis and Miller independently used a mean-square-error criterion to solve the adaptive equalization problem[8-9].

The underwater acoustic channel is always band limited and reverberant, which poses many obstacles for reliable, high-speed digital communications. The effects of reflection from the surface and the bottom of the sea give rise to multipath propagation. The channel impulse response is considered as ray model and the time dispersion due to multipath is characterized by the normalized delay spread, i.e., root mean square (RMS) delay spread. The RMS delay spread is a parameter as defining the time extent of multipath time spread. Simultaneously coherence bandwidth which directly influences the system performance could be interpreted using the RMS delay spread. Some simulation results indicate that coherence bandwidth is not severely affected by low power signals with long excess delay like RMS delay spread. Coherence bandwidth is considered to be a more accurate approach to

predicting system performance. Coherence bandwidth is a measure of the range of frequencies over which the gain and phase are approximately equal, respectively. There is an approximate relationship between RMS delay spread and coherence bandwidth [9-13].

In this study to mitigate the distortion caused by ISI due to multipath, adaptive equalizer based on LMS algorithm is employed in bandwidth efficiency coherent MPSK communication system. To investigate the effectiveness of adaptive equalizer overcoming ISI caused by multipath, numerical experiment is conducted by employing LMS linear equalizer (LE) and nonlinear decision feedback equalizer (DFE) in shallow water acoustic channels [14-17].

Linear equalizers with simple structure have been developed and applied in suppressing ISI, however they can not achieve satisfactory performance for the channel with spectral nulls. The employment of DFE in the UWA communication system shows promising results. DFE has a similar computation complexity as the LE and can give the better performance without enhancement of noise in the feedback filter [18-24].

When the equalizer is employed in communication system, it should be kept in mind that the complexity of implementation mainly depends on the number of tap weighting coefficients of equalizer. In this case multichannel equalization has been proposed which can meet this demand of using shorter length equalizers. Stojanovic et al. [7,25,26] described a method which incorporates spatial diversity and a fractionally spaced decision-feedback equalization. This method was proved to be effective in countering the effect of phase variations and ISI by combining joint synchronization and equalization.

1.3 Diversity technique - passive phase conjugation (PPC)

In communication ISI due to multipath fading is reduced by using diversity techniques. One of these is to employ multiple transmitters or receivers. Coates in 1993 and Galvin and Coates in 1994 proposed an approach that employs transmitter arrays to excite only a single path of propagation.

However, long arrays are required and small errors in positioning can degrade performance. Consequently this technique was found to be more effective at shorter ranges [27-31].

Much of the theoretical development on phenomenon of the time reversal acoustic (TRA) has been presented by Jackson and Dowling in 1991 and 1992, Kuperman et al. in 1998 and Song et al. in 1998. This technique provides an original and relatively simple algorithm to overcome the ISI problem in a shallow water channel. This solution is not a sophisticated processing algorithm. It is equivalent to matched field processing with the filter matched to the impulse response of the ocean. This technique uses time-reversal acoustic arrays to generate a spatio-temporal focus of acoustic energy at the receiver, greatly reducing distortions caused by channel propagation [31-39].

The application of TRA to the underwater communications problem was previously proposed by Jackson and Dowling in 1992 and Kuperman et al. in 1998. The first known application of TRA which developed a signaling scheme for communication purposes was introduced by Abrantes et al. in 1999 [33]. Time-reversal signal processing was first prominently demonstrated in underwater acoustics by Parulescu. Jackson and Dowling first proposed active phase conjugation for use in the ocean waveguide and Kuperman et al. subsequently demonstrated it in an experiment in the Mediterranean. Dowling used reciprocity to show how analogous pulse compression could be achieved using a receive-only array. He further suggested that this passive version of phase conjugation could be used for underwater communication. Silva et al. independently proposed PPC and tested it in numerical simulations. Athanasiou studied communication using both active phase conjugation and PPC in laboratory experiments. As part of the SignalEx experiments, Hursky et al. demonstrated PPC with a single receiving hydrophone for a low-power low data-rate application. Rouseff et al. used a 14-element receiving array in a PPC communications experiment in Puget Sound, WA. In a later theoretical study, Jackson and Dowling considered a scenario with an active array that was capable of both reception

and transmission. They showed how the time-reversed field backpropagated from such an array would focus both in time and in space at the location of the original source. Active time reversal using a vertical source-receiver array was demonstrated by Kuperman et al. Dowling later showed how analogous pulse compression could also be achieved using a passive, receive-only array, i.e., passive phase conjugation. PPC is based on sending a probe pulse and measuring the response to reduce ISI. Simulation and experimental results reported in literatures demonstrate its strong ability to reduce ISI [40].

Chapter 2

Linear Equalizer and Nonlinear

Decision Feedback Equalizer

2.1 Channel model and communication system

The impulse response of the equivalent lowpass system corresponding to band-limited carrier modulation scheme in a multipath underwater acoustic system is modelled as [9]

$$h_c(t) = \sum_{n=0} \alpha_n e^{-j2\pi f_c \tau_n} \delta(t - \tau_n) \quad (2.1)$$

where f_c is carrier frequency, α_n and τ_n are the normalized amplitude and the propagation time difference of the signal received along the n th path to the direct path amplitude and the direct path propagation time.

It is assumed that the channel is invariant for the simplicity of channel model analysis such that Doppler spread of the channel is not necessary to consider here. The system configuration utilizing BPSK modulation is depicted in Figure 2.1.

The transmitted binary data are first shaped to match the channel bandwidth for the ideal band-limited underwater acoustic system and then modulated by the carrier [40-43]. The transmitted signal sequence of binary data with a bit interval T_b is given as

$$s(t) = \sum_i s_i p(t - iT_b) \quad (2.2)$$

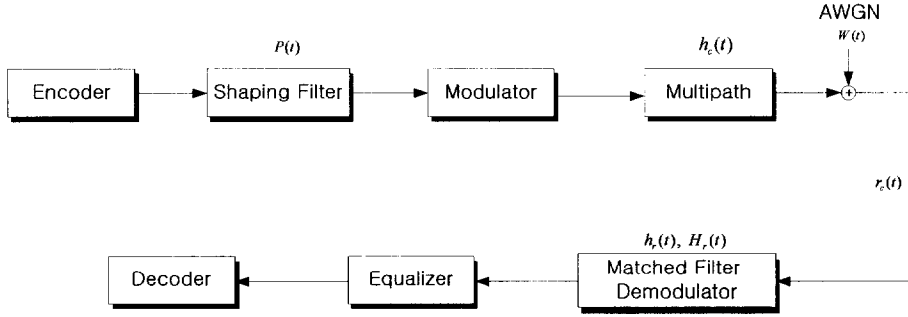


Figure 2.1. Block diagram of communication system

where s_i is the i th transmitted symbol which corresponds to bit 1, -1, which producing a phase change of 0° or 180° in BPSK modulation. The $p(t)$ is a pulse whose shape influences the spectrum of the information-bearing transmitted signal and its duration is one bit interval T_b in binary schemes. The raised cosine pulse is generally adopted as $p(t)$ and given as [9]

$$p(t) = \frac{A}{2} \left\{ 1 + \cos \frac{2\pi}{T_b} \left(t - \frac{T_b}{2} \right) \right\} \quad 0 \leq t < T_b \quad (2.3)$$

where A is the amplitude of the pulse and its spectrum $P(f)$ is given by

$$P(f) = \frac{AT_b}{2} \frac{\sin \pi f T_b}{\pi f T_b (1 - f^2 T_b^2)} e^{-j\pi f T_b} \quad (2.4)$$

In this case the effective signal bandwidth w is given to be $2/T_b$ and therefore we need a channel bandwidth w_c of $2/T_b$ or larger to transmit information sequence in ideal channel.

The equivalent low pass response $h_p(t)$ of the raised pulse $p(t)$ in multipath underwater acoustic channel is given by

$$h_p(t) = h_c(t) * p(t) \quad (2.5)$$

where $(*)$ denotes convolution operation.

In order to characterize the multipath fading and figure out its effect on the transmitted signal distortion, root mean square (RMS) delay spread should be examined, which exhibits the time-extent nature of time-dispersive multipath channel. The RMS delay spread τ_s is defined as

$$\tau_s = \sqrt{\overline{\tau^2} - (\overline{\tau})^2} \quad (2.6)$$

where average delay $\overline{\tau}$ is expressed as

$$\overline{\tau} = \frac{\sum_k f(\tau_k) \tau_k}{\sum_k f(\tau_k)} \quad (2.7)$$

where $f(\tau_k)$ is the power density for the k th path, and $\overline{\tau^2}$ is given as

$$\overline{\tau^2} = \frac{\sum_k f(\tau_k) \tau_k^2}{\sum_k f(\tau_k)} \quad (2.8)$$

RMS delay spread is interpreted as coherence bandwidth B_c in the frequency domain. Coherence bandwidth corresponds to the range of frequencies over which the channel may be considered to be flat, is given as [44]

$$B_c \approx \frac{1}{\tau_s} \quad (2.9)$$

Therefore, if the coherence bandwidth B_c is less than the signal bandwidth

W_s , then the channel is a frequency selective and the received signal is distorted. In this case, equalization should be adopted with this ISI problem encountered in multipath fading.

If Equation (2.3) is applied to Equation (2.1) then the equivalent low pass channel output of message signal $r_c(t)$ is given as

$$\begin{aligned} r_c(t) &= s(t) * h_c(t) + W(t) \\ &= \sum_i \sum_n \alpha_n e^{-j2\pi f_c \tau_n} s_i p(t - \tau_n - iT_b) + W(t) \end{aligned} \quad (2.10)$$

where $W(t)$ is white Gaussian noise.

Therefore the channel with the multipath and white Gaussian noise $W(t)$ distorts the transmitted signal in amplitude and delay so that ISI is induced. The amount of ISI depends on the multipath nature such as the normalized amplitude α_n and the propagation time difference τ_n to the direct path.

At the receiver, the receiver filter $h_r(t)$ is used for limiting the noise components outside the signal bandwidth. For the ideal transmission channel with no multipath delay and non-fading, the spectrum of the output of the receiving filter $R(f)$ is given as

$$R(f) = P(f)H_r(f) \quad (2.11)$$

where $H_r(f)$ is the Fourier transform of the receiver filter impulse response $h_r(t)$.

If we adopt the receiver filter as matched filter, then $H_r(f)$ and $h_r(t)$ are represented as

$$H_r(f) = P^*(f)e^{-j2\pi f_c T_b} \quad (2.12)$$

$$h_r(t) = p(T_b - t) \quad (2.13)$$

where superscript $()^*$ denotes complex conjugate.

The demodulated output of the raised cosine pulse $p(t)$ is given as

$$\begin{aligned}
 h_{pm}(t) &= h_p(t) * h_r(t) \\
 &= h_c(t) * p(t) * p(T_b - t) \\
 &= \sum_{n=1} \alpha_n e^{-j2\pi f_c \tau_n} p(t - \tau_n) * p(T_b - t) \\
 &= \sum_{n=1} \alpha_n e^{-j2\pi f_c \tau_n} R_{pp}(t - \tau_n - T_b)
 \end{aligned} \tag{2.14}$$

where $R_{pp}(t)$ is the autocorrelation of pulse signal $p(t)$.

The demodulated output of the received binary data signal can be expressed as

$$\begin{aligned}
 r_{sm}(t) &= r_c(t) * h_r(t) \\
 &= [\sum_i \sum_n \alpha_n e^{-j2\pi f_c \tau_n} s_i p(t - \tau_n - iT_b) + W(t)] * p(T_b - t) \\
 &= \sum_i \sum_n s_i \alpha_n e^{-j2\pi f_c \tau_n} R_{pp}(t - \tau_n - (i+1)T_b) + W(t) * p(T_b - t) \\
 &= s_k \alpha_1 R_{pp}(t - (k+1)T_b) + W_p(t) + \sum_{i \neq k} \sum_{n \neq 1} s_i \alpha_n e^{-j2\pi f_c \tau_n} R_{pp}(t - \tau_n - (i+1)T_b)
 \end{aligned} \tag{2.15}$$

where $W_p(t) = W(t) * p(T_b - t)$ is the filtered noise by the receiver filter.

The demodulated output r_k is integrated and sampled in every symbol interval T_b and the direct path signal components r_{kd} can be obtained as

$$r_{kd} = s_k \alpha_1 \int_{kT_b}^{(k+1)T_b} R_{pp}(t - (k+1)T_b) dt \tag{2.16}$$

and noise components W_{kp} is denoted as

$$W_{kp} = \int_{kT_b}^{(k+1)T_b} W_p(t) dt \quad (2.17)$$

In multipath channel,

$$\begin{aligned} r_k &= r_{kd} + W_{kp} + \sum_{i \neq k} \sum_{n \neq 1} s_i \alpha_n e^{-j2\pi f_c \tau_n} \int_{iT_b}^{(i+1)T_b} R_{pp}(t - \tau_n - (i+1)T_b) \\ &= r_{kd} + r_{km} + W_{kp} \end{aligned} \quad (2.18)$$

where r_{kd} is the wanted direct path signal, and r_{km} is ISI due to the multipath. As shown in Equation (2.18), the multipath ISI depends on the normalized amplitude and the propagation time difference of the n th path.

2.2 LMS linear and nonlinear equalizer

In order to compensate for the multipath ISI the equalizer is employed to the demodulated output. In the selection of an equalizer, Its ability to track channel characteristics changes and computation complexity are considered. LMS is one of the most popular algorithms. Therefore LMS linear equalizer and nonlinear decision feedback equalizer are used to suppress ISI.

It is assumed that there is no sampler delay, the demodulated signals is sampled in one symbol duration. The basic LMS algorithm in Figure 2.2 is expressed as the following equations.

The update tap-weight $w(k)$ at time instant kT_b is represented as

$$w(k) = w(k-1) + \mu e^*(k-1)r_{k-1} \quad (2.19)$$

where μ is step-size which controls the convergence rate and excess mean square error. In other words, the larger step size gives more rapid

convergence rate, but the larger fluctuation of tap coefficients. Estimation error $e(k)$ and filter output $y(k)$ are given as

$$e(k) = d(k) - y(k) \quad (2.20)$$

$$y(k) = w^H(k)r_k \quad (2.21)$$

where $d(k)$ and $w^H(k)$ are the desired symbol, and the tap weight coefficient, respectively. The superscript $()^H$ denotes conjugate transpose, and r_k is the tap input vector, i.e. the received demodulated binary data signal.

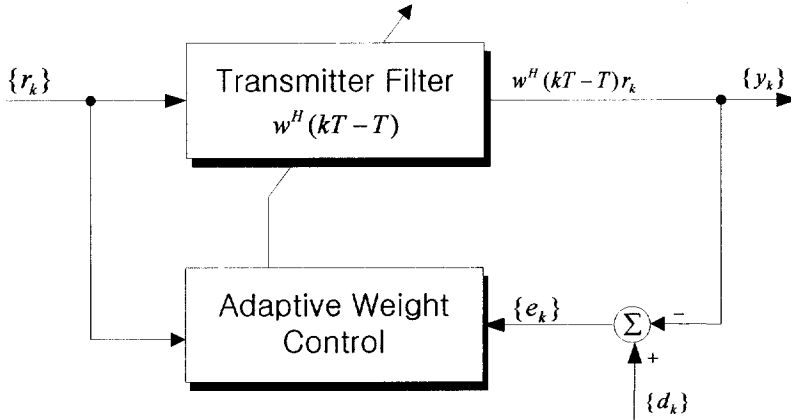


Figure 2.2. LMS structure

The tap weight coefficients of the equalizer are recursively adjusted to meet the criterion of minimizing the mean square error (MSE) with respect to the equalizer taps.

$$\min(E|e(k)|^2) = \min(E|d(k) - y(k)|^2) \quad (2.22)$$

For the linear equalizer in Figure 2.3a, filter output $y(k)$ is expressed as

$$y(k) = \sum_{j=-m}^m w_j r_{k-j} \quad (2.23)$$

where w_j is tap weighting coefficients of the equalizer.

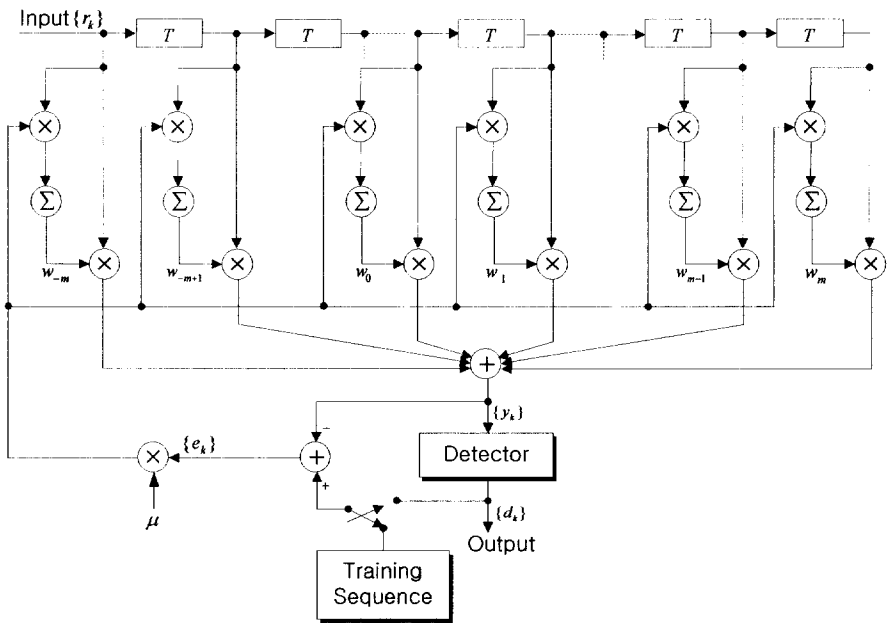
For the DFE shown in Figure 2.3b, the estimate is different from that of linear equalizer and denoted as

$$y(k) = \sum_{j=-m_1}^0 w_{ffj} r_{k-j} - \sum_{j=1}^{m_2} w_{fbj} d(k-j) \quad (2.24)$$

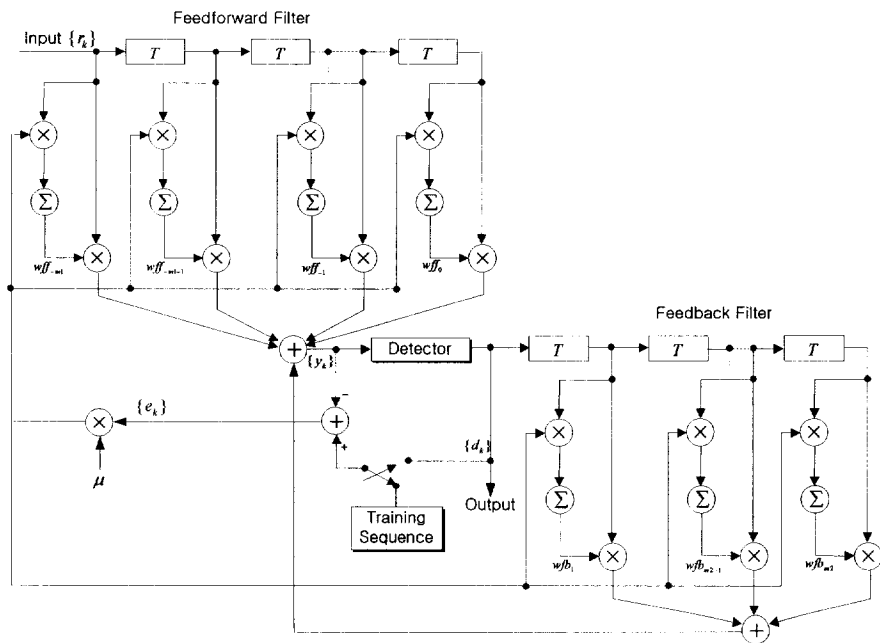
where w_{ffj} and w_{fbj} are the tap coefficients of feedforward and feedback filters.

The tap coefficients of feedforward and feedback filters are adjusted simultaneously, and the feedback filter is used to cancel out the part previously detected symbols. The input to the feedback filter is quantized signal in bit interval, thus DFE is a nonlinear equalizer. Compared with linear equalizer, DFE can not only remove ISI, but also operates on noiseless quantized levels [45].

As shown in Figures 2.3a and 2.3b, the training sequence which is a given binary data, is first transmitted to adjust the tap weights initially, then switched to decision-directed mode in which decision symbols are compared to the estimate and gives the error signal under the assumption of the decisions on information are correct.



(a) Linear equalizer.



(b) Decision feedback equalizer

Figure 2.3. Equalizer structures

2.3 Simulation results

The simulation parameters to investigate the feasibility of the equalizer for use in underwater acoustic data transmission, are given as in Table 2.1. The modulation format is BPSK. The channel model is characterized as shallow water channel since multiple reflections from surface and bottom boundaries should be considered [45-47]. The ranges between the receiver and transmitter are 10m, 600m, 1000m, respectively and the depths of the receiver and the transmitter are kept fixed to be 5m and 97m, respectively. Reflection coefficient r_b of the sandy bottom of the sea is assumed to be 0.41 [48] and reflection coefficient r_s of the sea surface with wave height of 0.05m, is calculated as 0.85. The Doppler spread and other problems are not addressed, and synchronization is assumed to be perfect. The paths with the less than -20dB of the normalized amplitude are neglected. Here ISI caused by multipath is concerned, thus signal to noise ratio (SNR) is considered as 30dB unless it's specified.

Table 2.1. Parameters for simulation of equalizer performance

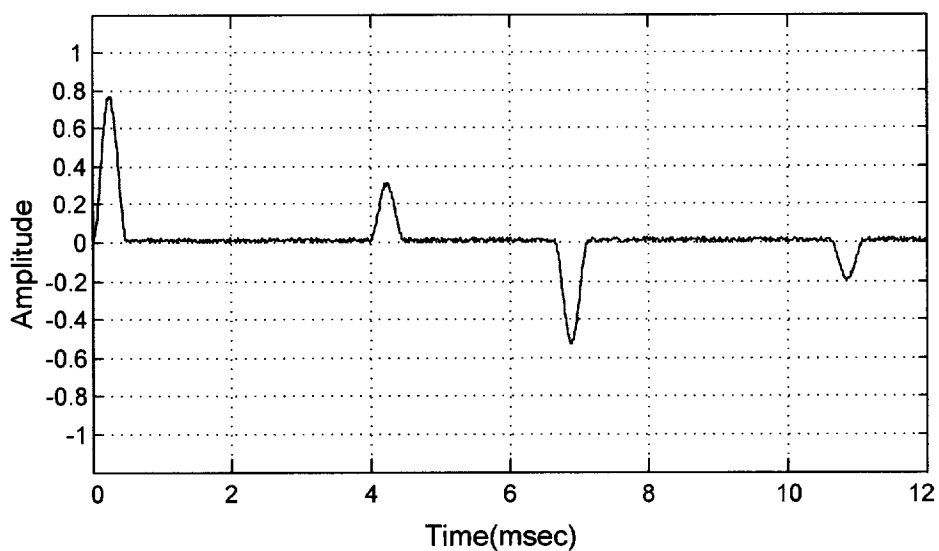
Carrier frequency	20kHz		
Symbol rate	2Kbps		
Water depth (d)	100m		
Sound speed	1500m/s		
Transmitter depth	5m		
Receiver depth	97m		
Horizontal range(R)	10m	600m	1000m

The impulse response tests are performed by transmitting the raised pulse with the bandwidth of two times bit rate. The obtained impulse response and corresponding spectra of the equivalent lowpass channel for R=10m whose range/depth ratio are shown in Figures 2.4a and 2.4b, respectively. For this channel, the multipath time dispersion extends to 10.6msec and the RMS delay spread is 3.1ms, which results in the coherence bandwidth of about

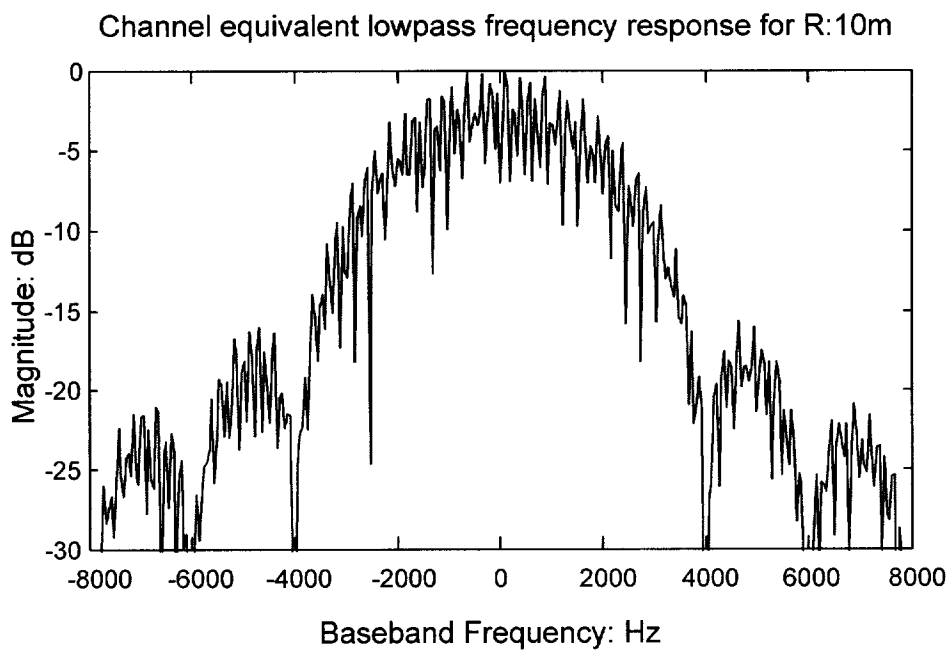
330Hz, in other words, corresponding to approximately 165bps maximum transmission rate with no equalization [63]. Error free transmission is possible in the case that the signal bandwidth is less than the coherence bandwidth. Upper part of Figure 2.5 in which signal bandwidth is about 300Hz (twice the bit rate 150bps), depicts error free transmission, but not in the lower part while transmission rate is chosen to be 300bps which occupies bandwidth of 600Hz larger than the coherence bandwidth. It's clear that this is a selective channel which causes ISI due to multipath if signal bandwidth is larger than the coherence bandwidth. In our numerical simulations to achieve error free transmission with high bit rate 2000bps in the presence of ISI, therefore compensation measure should be taken to remove ISI.

Figure 2.4b illustrates that the ISI caused by multipath is not severe since the surface reflected path's amplitude attenuates a lot and leads to the significant multipath arrivals impose less strong ISI effects. At the receiver, the received signal is demodulated, sampled by T_b , then processed by the equalizer. First the prior known training sequence 1500 symbols are transmitted to establish convergence, after which the receiver is switched to decision-directed mode. Note that "+" in the scatter plots indicates error. Figure 2.6 exhibits the received demodulated signals before and after equalization and the obtained MSE with DFE processing. It's obvious that the raw signals with no equalization representing '1' or '-1' are not separated, however, the output of linear equalizer with 25 taps shows the two clusters representing two binary signals are separated well after 400 iterations, and there are no errors detected out of 10000bits in data transmission after training sequence (for the sake of display clearly, the number of bits is limited to 2000). The linear equalizer can be enough to track the channel characteristic for $R=10m$, for comparison we further employ DFE with 2 feedforward taps and 22 feedback taps. The output of linear equalizer is more scattered than that of DFE and in addition DFE has very small MSE in rapid convergence time. Consequently DFE outperforms linear equalizer.

Then we consider the channels whose transmission ranges/water depth



(a) Channel response



(b) Frequency response for R=10m

Figure 2.4. Channel response to probe signal for R=10m

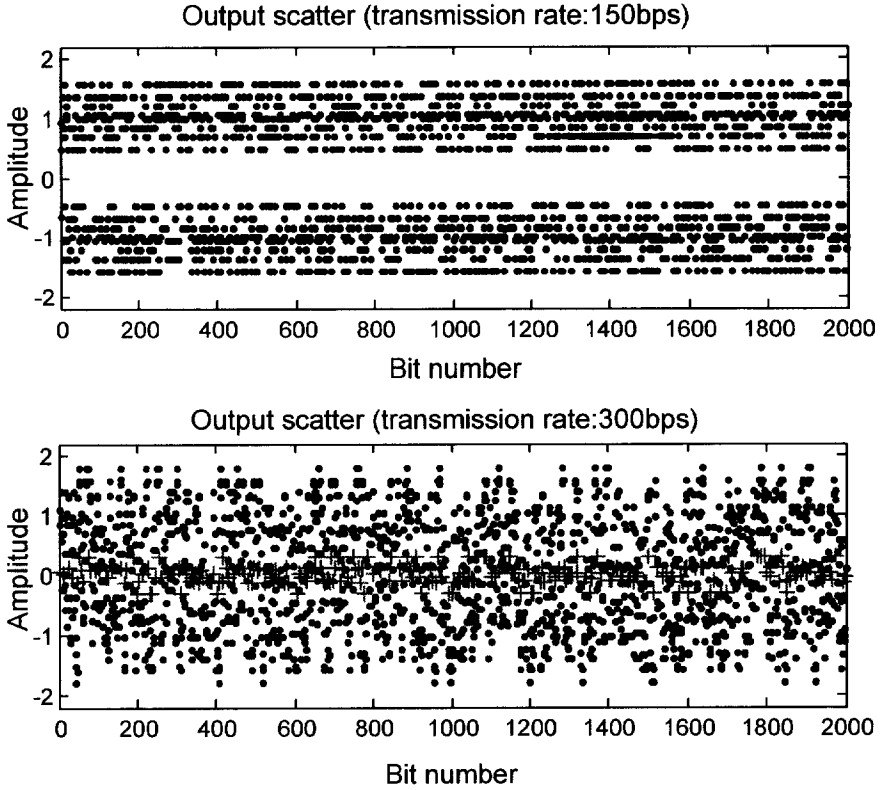
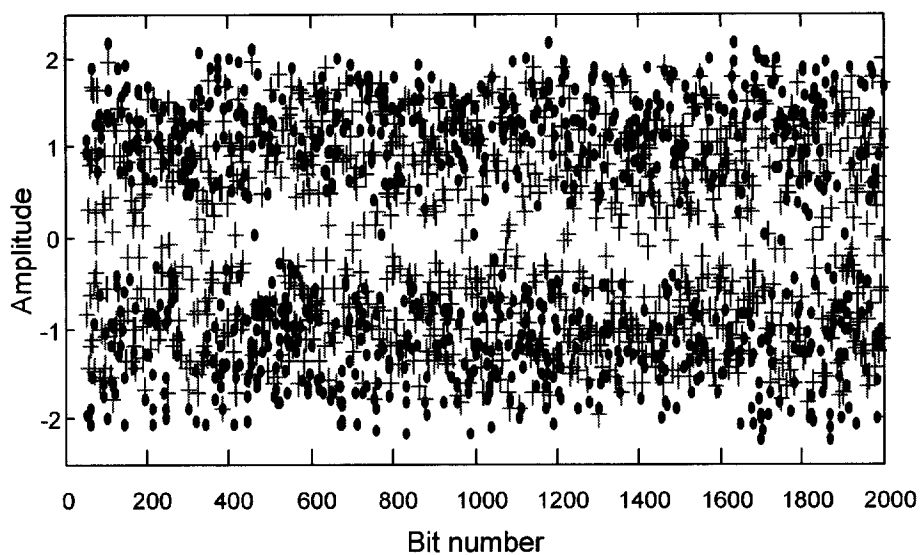
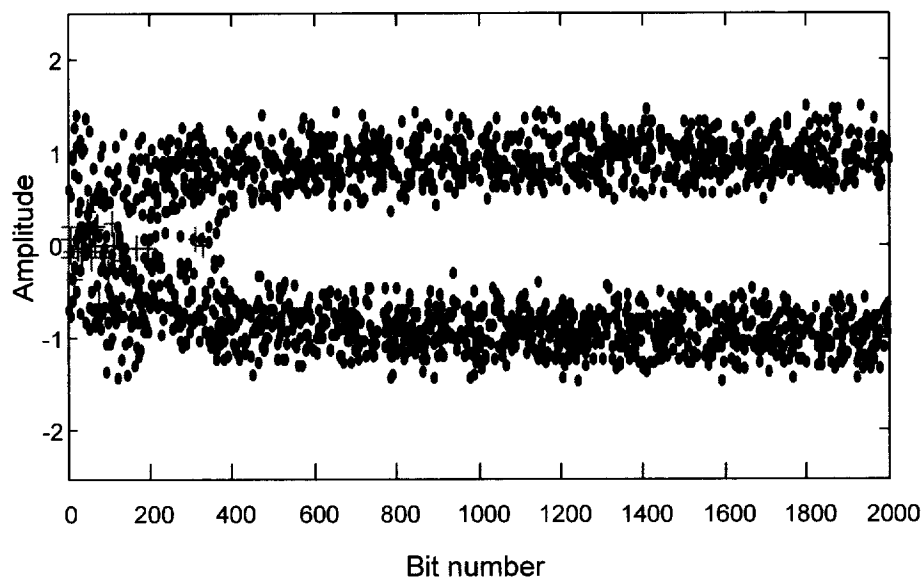


Figure 2.5. Output scatter for $R=10m$

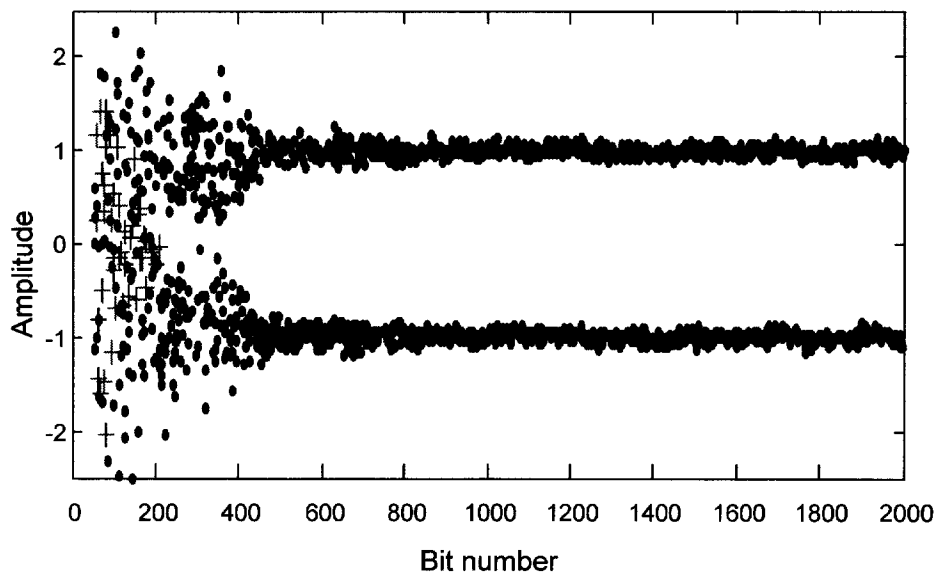
ratio. At the range of 600m, the channel impulse and the spectra with equivalent lowpass frequency response characteristic are depicted in Figures 2.7a and 2.7b. Figure 2.7a exhibits that the secondary paths delay times compared to the direct path are larger than one symbol time and separated clearly. The RMS delay spread is computed as 9.8ms, thus coherence bandwidth is approximated as 100Hz, namely 50bps maximum transmission rate with no compensation such as equalization. Figure 2.8. illustrates the estimate of coherence bandwidth is suited for this channel, the upper plot exhibits that while data bit rate is 50Hz, the two clusters which representing '1' and '-1' are separated well and there is no errors occurred, whereas at 100bps twice maximum bit rate we can not attain error free communication.



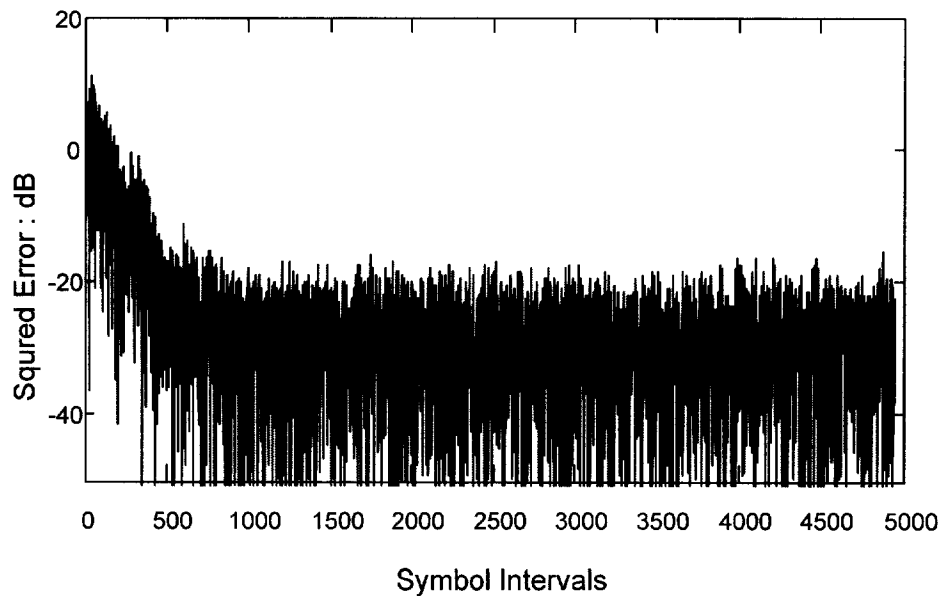
(a) Scatter plot before equalization



(b) Scatter plot after LMS LE

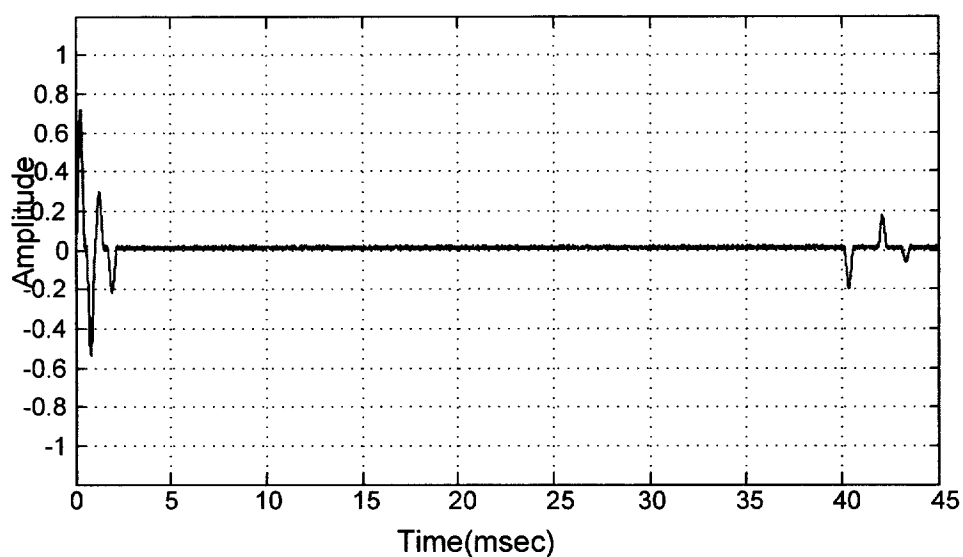


(c) Scatter plot after LMS DFE

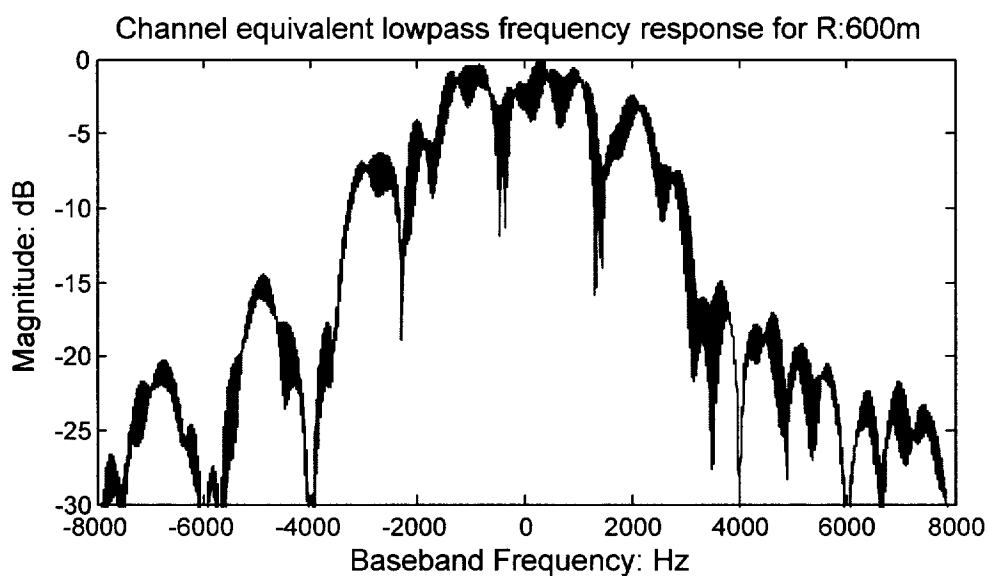


(d) MSE with LMS DFE

Figure 2.6. Equalizer performance for $R=10m$



(a) Channel response



(b) Frequency response

Figure 2.7. Channel response to probe signal for R=600m.

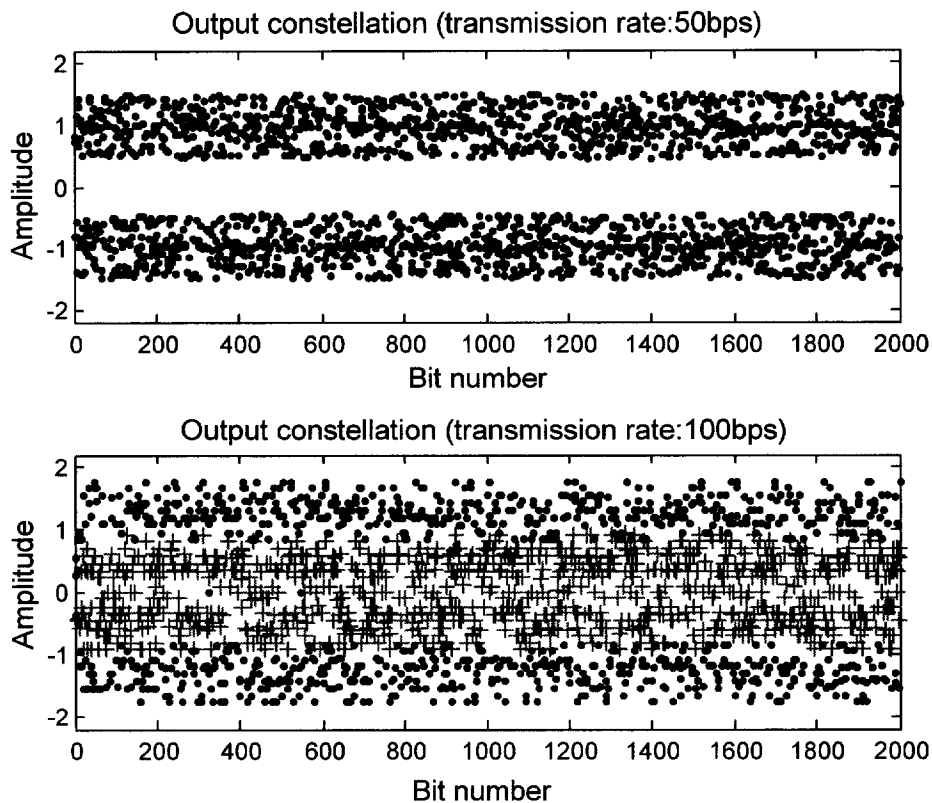
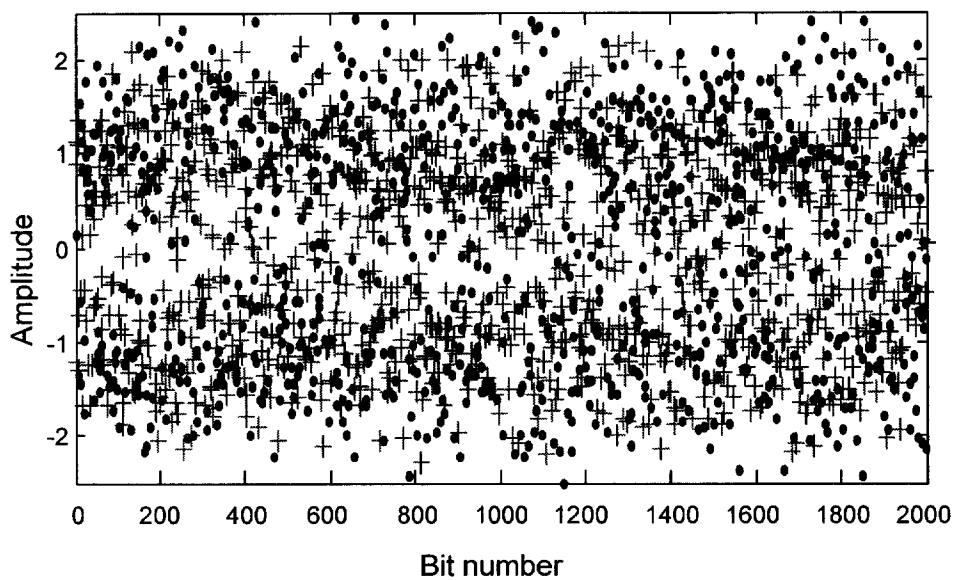
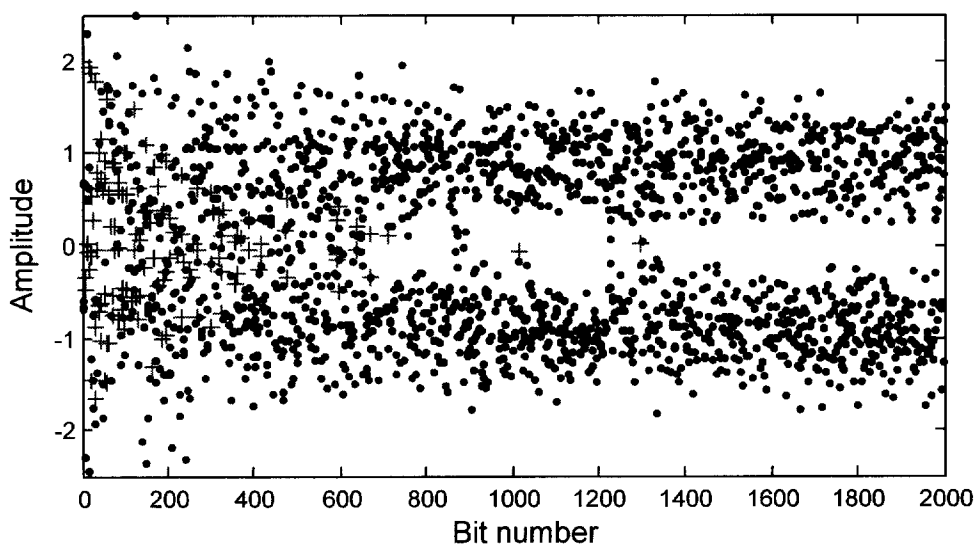


Figure 2.8. Output scatter for $R=600m$

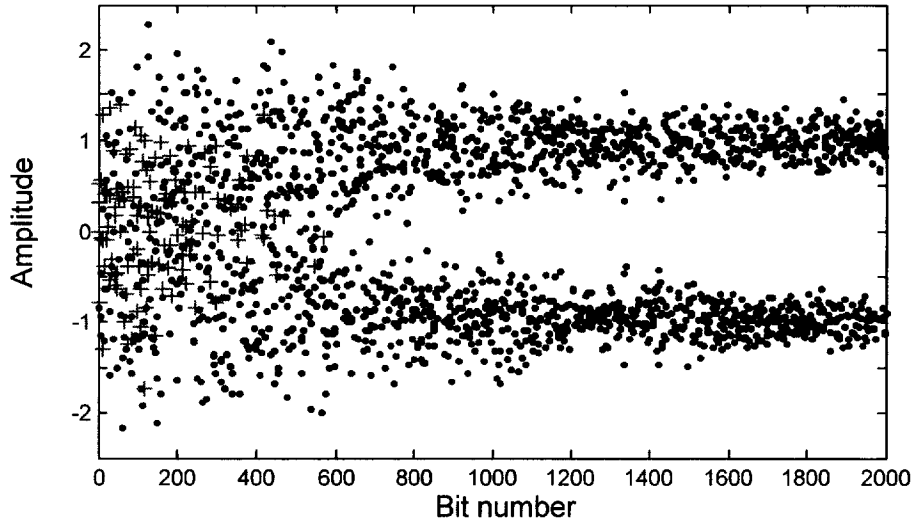
Figure 2.9 shows the input signals to the equalizer, the results of demodulated signals and MSE with equalization. Before equalization the signals can't be detected correctly due to the ISI. With the aid of the linear equalizer's (90 taps) reducing ISI effects, the received signals after a long training sequence about 1200 iterations can be separated into two clusters distinctly. For long time dispersion channel with spectral nulls, the increase of feedforward filter's coefficients leads to the noise enhancement. DFE (2 feedforward taps and 88 feedback taps) thus became a good choice in reducing the residual ISI effects. In addition DFE does not cause noise's increase since the feedback filter works on noiseless quantized levels and the feedback output is free of channel noise. We see from Figure 2.9c with DFE



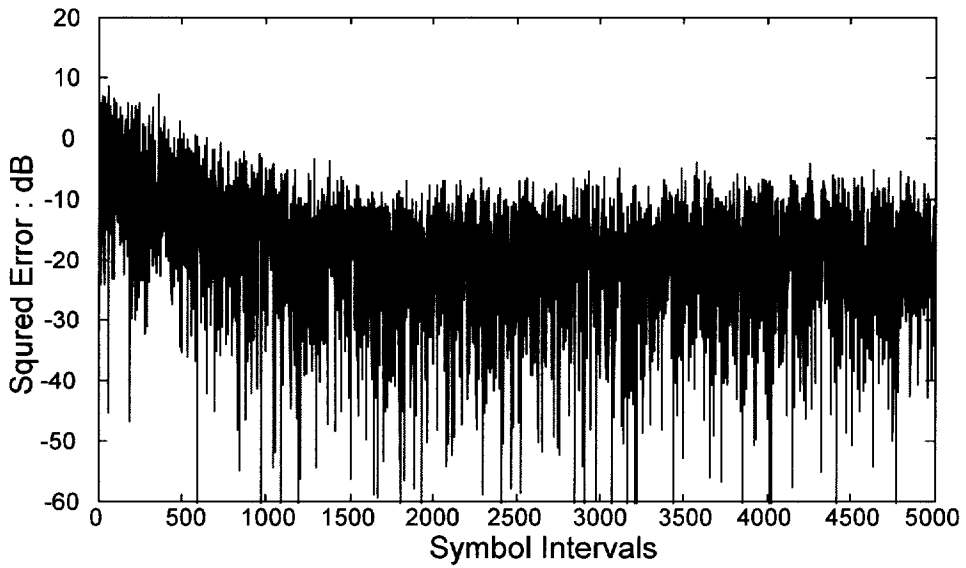
(a) Scatter plot before equalization



(b) Scatter plot after LMS LE



(c) Scatter plot after LMS DFE



(d) MSE after LMS DFE

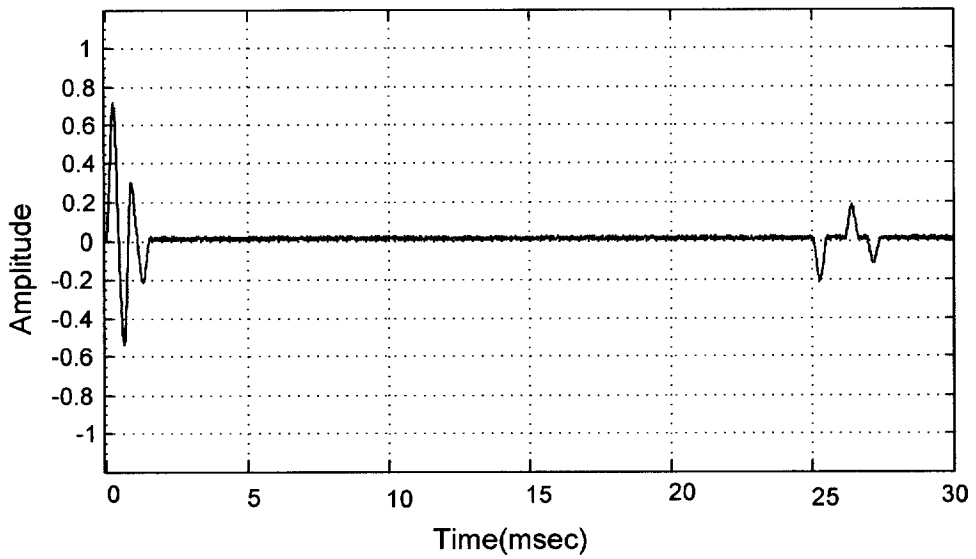
Figure 2.9. Equalizer performance for $R=600m$

processing the two clusters representing binary signals are separated clearly and we can obtain ideal transmission after 600 training symbols. It has shown the superior performance with a DFE.

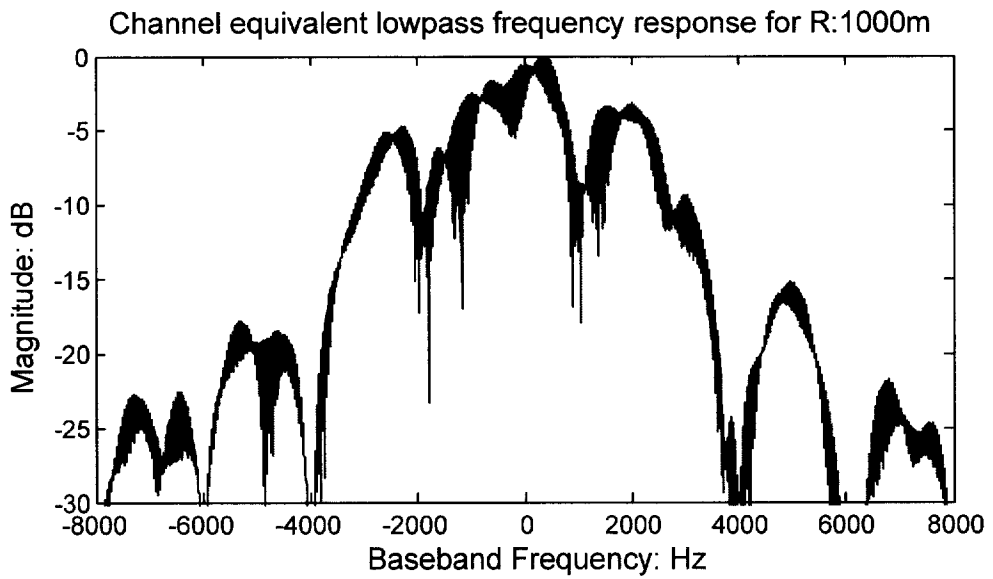
At $R=1000m$ the channel response and the spectra characteristic are depicted in Figures 2.10a and 2.10b respectively, and RMS delay spread is 7.2ms, the approximate coherence bandwidth is 130Hz, hence when the transmission rate is chosen as 50bps, 100bps smaller and larger than half of coherence bandwidth respectively. In the former case no errors is detected, whereas in the latter case there are lots of errors occurred and can't obtain error free transmission as shown in Figure 2.11. Therefore it is proved the fact that the communication with high transmission rate larger than half of the coherence bandwidth without compensation method, such as equalizer and diversity is unachievable.

For the channel $R=1000m$, the delay times of the first three multipaths compared to its former path are less than one bit duration of 0.5msec. Especially compared to the direct path, the first multipath delay time are less than one symbol duration with negative amplitude, which results in self-destructive multipath. Comparing Figures 2.7b and 2.10b, it is evidenced that the channel for $R=1000m$ possesses deeper spectral null, worse spectral characteristic and more severe ISI than the channel for $R=600m$. It reflects the fact that the severity of ISI is largely dependent on the frequency response of transmission channel [9].

To illustrate the equalizers effects in reducing ISI of the channels at different transmission ranges, both the nonlinear equalizer DFE and linear equalizer based on LMS are employed to combat against ISI effects. Due to DFE's nonlinear characteristics the output of feedback is free of channel noise [65]. As shown in Figure 2.12, for $R=1000m$ using LMS linear equalizer with 60 taps tracking the channel characteristic requires 1400 iterations, however DEF with 2 feedforward taps and 58 feedback taps just needs 800 training symbols. It's obvious that for the three different channels



(a) Channel response



(b) Frequency response

Figure 2.10. Channel response to probe signal for R=1000m.

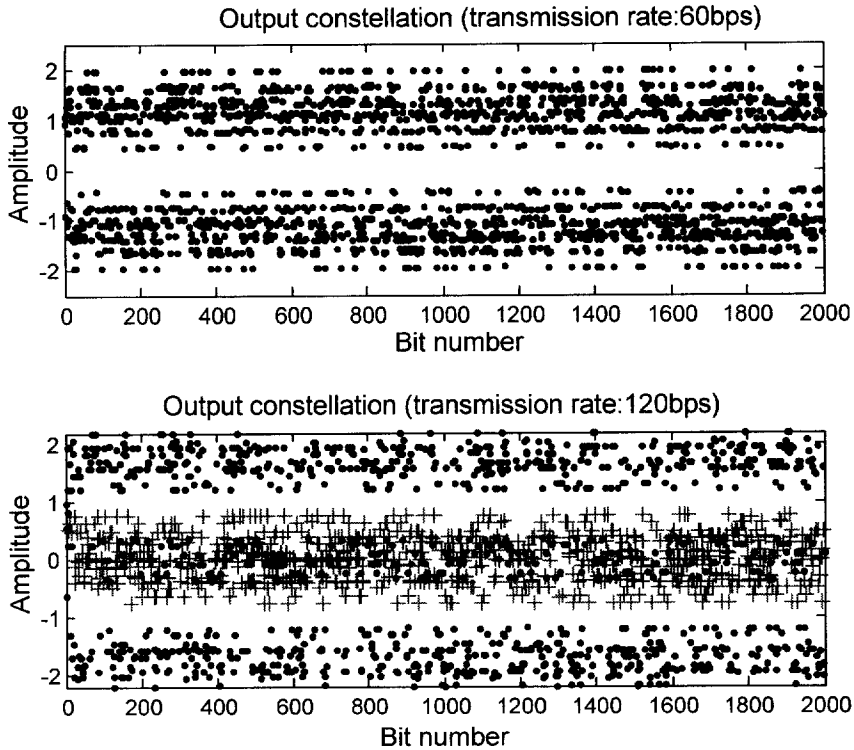
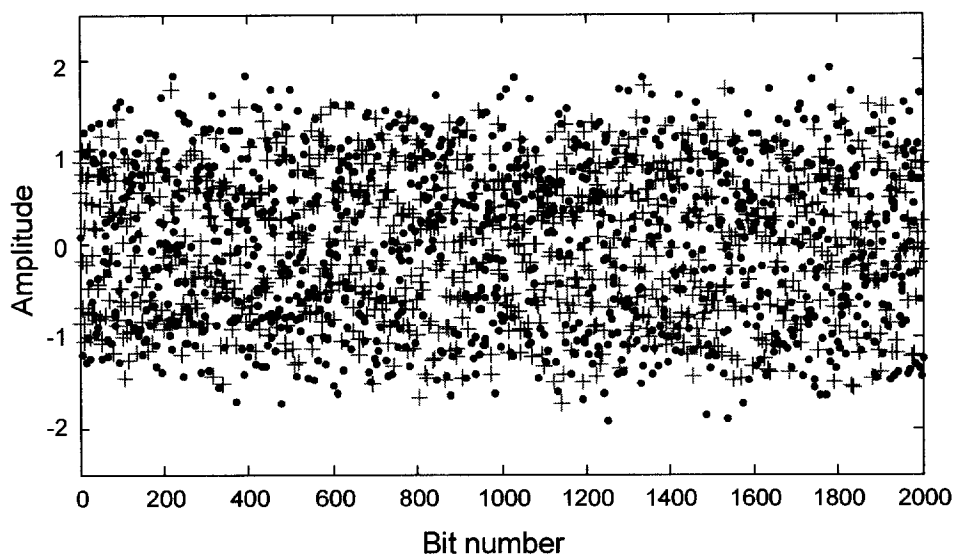


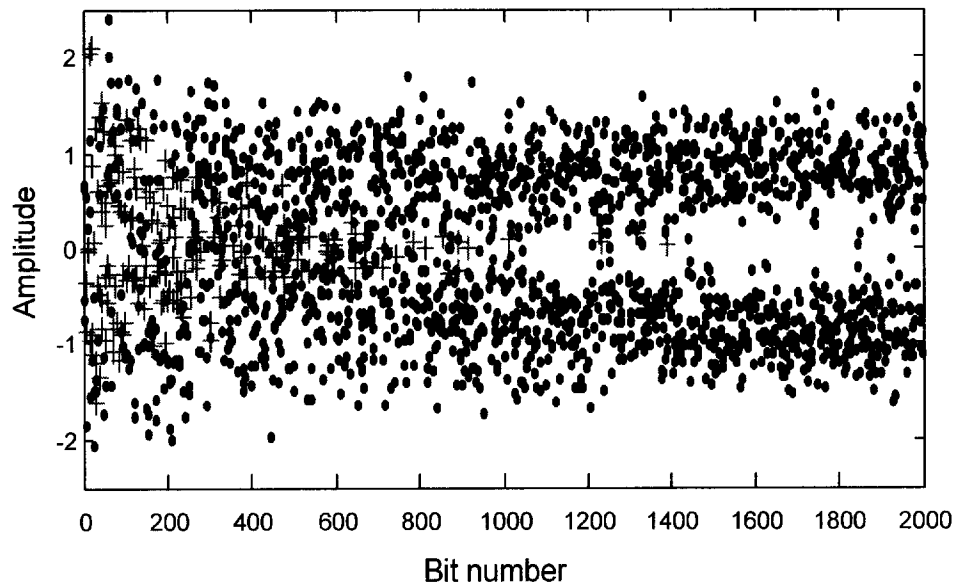
Figure 2.11. Output scatter for R=1000m

the equalizers take an important role in removing ISI. Moreover the DFE possessing nonlinear characteristic can further cancel the residual ISI completely for the channels with severe ISI such as deep spectral nulls without increasing the system's noise.

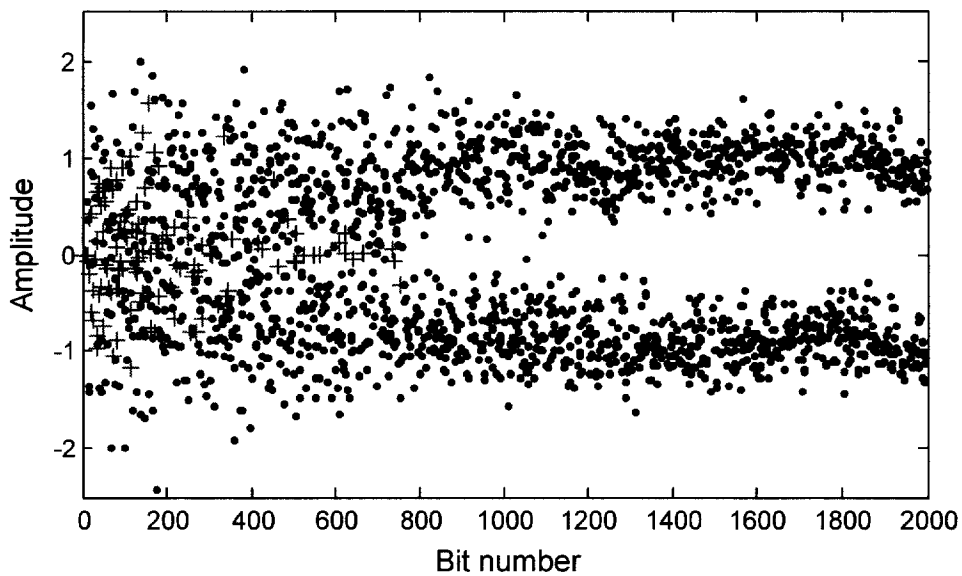
To compare the performance of DFE and linear equalizer at different values of SNR, test was performed at R=600,1000m. Figure 2.13 illustrates that for the channel R=600m in the case of employing linear equalizer there are much more errors than DFE. When SNR is not less than 16dB, the BER will satisfy the communication requirement: which is on the order of 10^{-5} . However for R=1000m when SNR is less than 14dB DFE has similar performance compared with linear equalizer possibly due to the decision errors, when SNR larger than 14dB DFE shows superiority. Therefore, DFE shows better tracking ability than linear equalizer. The advantage is that



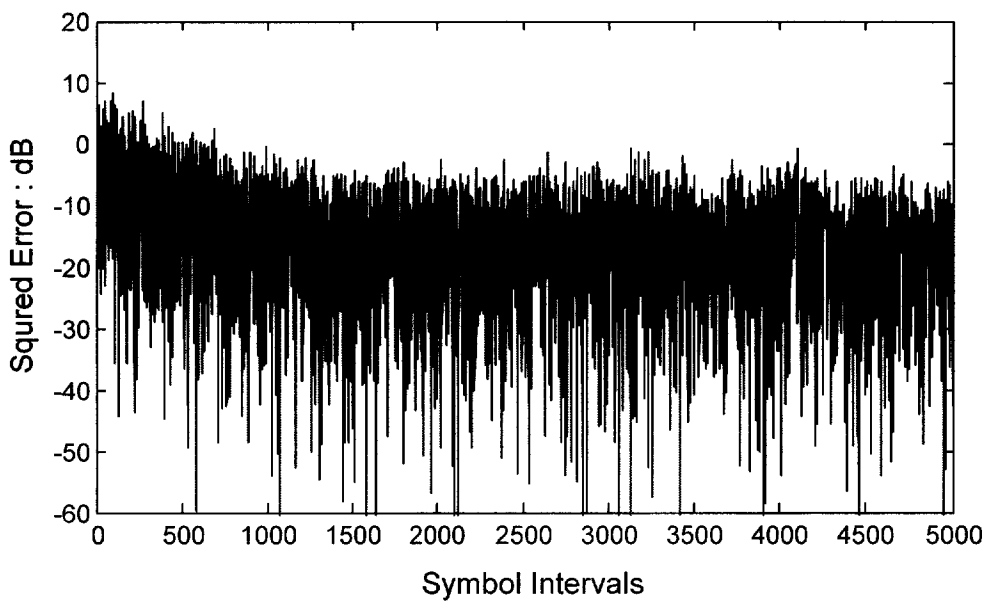
(a) Scatter plot before equalization



(b) Scatter plot after LMS LE



(c) Scatter plot after LMS DFE



(d) MSE after LMS DFE

Figure 2.12. Equalizer performance for $R=1000m$

DFE can not only cancel the ISI effects, but also can give rise to SNR enhancement.

2.4 Conclusions

ISI due to multipath is concentrated on and the responses to the transmitting signal wave-formed as raised pulse over three multipath channels are tested to know the channels characteristics, then through the numerical simulation by employing equalization it is found that linear and nonlinear LMS equalizer can be applied to combat ISI imposed on modulated signal over time dispersive channel. For the channel with weak ISI the adaptive linear equalizer is effective in reduction of ISI, but for the channel with severe ISI employing adaptive nonlinear equalizer can remove ISI completely and obtain good performance. Therefore high data rates become possible in the case where channel variance is sufficiently slow to allow for channel tracking.

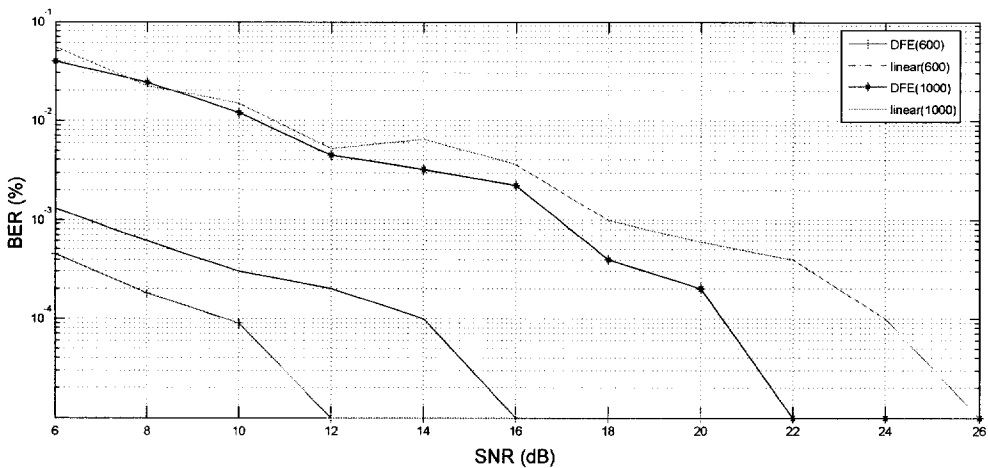


Figure 2.13. BER vs. SNR for DFE and LE

Chapter 3

Performance of Adaptive Equalization for QPSK

System over Multipath Channel

3.1 Background

Signal reverberation due to multipath is considered to be most severe in shallow water channel communication especially with high transmission rate. As a result the development of adaptive equalizer used to suppress ISI caused by time dispersion makes the coherent modulation with high transmission rate possible. For quadrature phase shift keying (QPSK) modulation the symbol rate is one half the bit rate so that the bandwidth requires one half the bandwidth occupied by BPSK with the same transmission symbol rate. Hence in this chapter QPSK modulation combined with equalization technique is employed to meet the demands of bandwidth efficiency in bandlimited UWA communication. Here the adaptive equalization algorithms' choosing is focused on and the suitable method is proposed, which can offer good performance for various channels [49-53].

LMS and RLS are the most commonly adopted algorithms in equalization. To efficiently reduce ISI effects the parameters between computational complexity, tracking abilities, convergence rate should be involved trade off. LMS algorithm is always favored because its low computational complexity and good tracking ability in slow time-varying channels. However for a channel needs large number of coefficients LMS equalizer becomes unrealistic because of its convergence time [54-58].

Though RLS algorithm has fast convergence rate and better tracking capability, due to its main drawback of high computational complexity, it's hard to achieve real-time implementation. In this study it is proposed that for a channel having large eigenvalue spread with severe ISI RLS algorithm can

be used to estimate the channel characteristics while training sequence is first sent, LMS equalizer is then employed to remove ISI after transmission being switched to decision-direct mode.

3.2 Communication system and equalization

The system configuration utilizing QPSK modulation is depicted in Figure 3.1. The binary data is first transmitted into encoder generating four-level data streams, then passing the I-channel and Q-channel pulse shaping filter to match the channel bandwidth for the ideal band-limited underwater acoustic system. After being modulated by QPSK modulator, the transmitted signal is introduced into multipath and additive white Gaussian noise (AWGN) by channel. At the receiver the received signal will be demodulated, low-pass filtered by the receiver filters matched to the transmitter filters, processed by equalizer to remove the ISI effects and noise, finally detected and decoded generating the stream of data.

The underwater acoustic model for simulation is characterized as linear

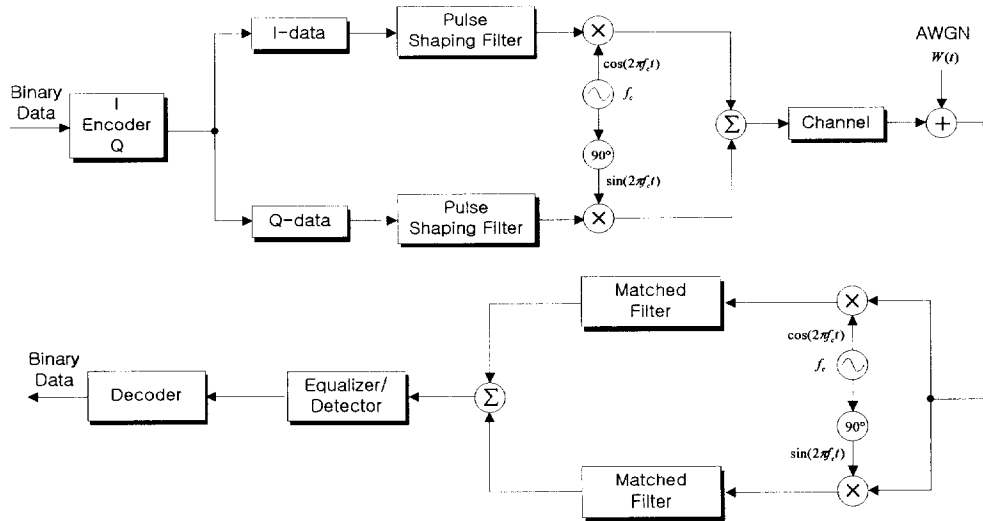


Figure 3.1. Block diagram of QPSK system

slow time-varying shallow water channel, thus data transmission will encounter ISI effects due to the channels time dispersion. The transmitted baseband signal can be given by

$$s(t) = \sum_k s_k p(t - kT) \quad (3.1)$$

where s_k is the sequence to be modulated by QPSK modulator corresponds to four levels $\{1+j, 1-j, -1+j, -1-j\}$. $1/T$ is the symbol rate, i.e., the I-data (Q-data) bit rate, $p(t)$ is the raised cosine shaping pulse adopted which had been mentioned in Chapter 2 leading to the base band signal bandwidth occupying $2/T$ two times the symbol rate for QPSK modulation[9]

$$p(t) = \frac{A}{2} \left(1 - \cos \frac{2\pi t}{T}\right) \quad 0 \leq t < T \quad (3.2)$$

The transmitted signal r_c at the equivalent discrete multipath channel end is represented as

$$r_c(t) = \sum_{n=0}^M h_n \operatorname{Re}\{s(t - nT)e^{j2\pi f_c t}\} + W(t) \quad (3.3)$$

where $W(t)$ is additive white Gaussian noise, f_c is the carrier frequency, M is the number of channel transmission paths including direct path whose delay time set to zero, and $\{h_n\}$ normalized to be unity are tap gains of channel having a transfer function $H(z)$ as

$$H(z) = \sum_{n=0}^M h_n z^{-n} \quad (3.4)$$

The demodulated signal at the receiver before low-pass filter can be expressed as [40]

$$r_o(k) = r_c * p(T - t)e^{-j2\pi f_c t} \quad (k-1)T \leq t \leq kT \quad (3.5)$$

where $r_o(k)$ represents the received signal at instant kT and $(*)$ denotes convolution operation.

The low-pass filtered signal $r(k)$ will be processed to eliminate ISI by equalizer. Let RR denote N -by- N autocorrelation matrix of the input signal vectors $r(k)$ to the linear equalizer with order of N [8]:

$$RR = E[r(k)r^H(k)] \quad (3.6)$$

where $r(k) = [r(k), r(k-1), \dots, r(k-N+1)]$ is the N -by-1 tap input vector and the superscript means transpose conjugate.

$$RR = \begin{bmatrix} rr(0) & rr(1) & \dots & rr(N-1) \\ rr(1) & rr(0) & \dots & rr(N-2) \\ \vdots & \vdots & \ddots & \vdots \\ rr(N-1) & rr(N-2) & \dots & rr(0) \end{bmatrix} \quad (3.7)$$

where $rr(i)$ is the components of correlation Hermitian matrix RR .

Let $\lambda_i (1 \leq i \leq N)$ be the eigenvalues of matrix RR , thus a concept of eigenvalue spread is defined as

$$\chi(RR) = \frac{\lambda_{\max}}{\lambda_{\min}} \quad (3.8)$$

where $\lambda_{\max}, \lambda_{\min}$ are the largest and the smallest eigenvalues of RR , respectively.

Among the equalization methods, least mean square (LMS) and RLS are most popular. RLS algorithm can be formulated as follows.

The N -by- N correlation matrix of input signal $r(k)$ is given by

$$RR_N(k) = \sum_{m=0}^k \gamma^{k-m} r(k)r^*(k) \quad (3.9)$$

where γ ($0 < \gamma < 1$) is a forgetting factor to introduce the exponential weighting into past data, superscript $()^*$ denotes complex conjugate and the cross correlation is given by

$$V_N(k) = \sum_{m=0}^k \gamma^{k-m} r(k) d^*(k) \quad (3.10)$$

where $d(k)$ is the desired signal, and the weighting coefficient vector

$$C(k) = C(k-1) + K(k) e^*(k) \quad (3.11)$$

Kalman gain vector is expressed as

$$K(k) = R R_N(k)^{-1} r(k) \quad (3.12)$$

The error between the desired signal and the estimate

$$e(k) = d(k) - w^*(k-1) r(k) \quad (3.13)$$

LMS algorithm (has been introduced in Chapter 2) can be expressed as follows.

$$w(k+1) = w(k) + \mu(k) e^*(k) \quad (3.14)$$

where μ is step size which controls convergence rate.

RLS reaches the goal of minimizing the time-average weighted squared error by adjusting the tap weight coefficients. Since the Kalman gain vector is N-dimensional, rapid convergence can be achieved due to one of the components of $K(k)$ controls each weighting vector $w(k)$, unlike LMS only one parameter step size controls the convergence rate resulting in slow

convergence rate.

The major advantage of LMS algorithm is its computational simplicity, however, its convergence rate depends on the eigenvalue spread and consequently the convergence rate will be slow when the channel results in the autocorrelation matrix of the received signal has large eigenvalue spread. In spite of its computation complexity using RLS algorithm can obtain fast convergence rate which is invariant to the eigenvalue spread. Thus tracking ability and computational complexity are important criteria to choose the update algorithm.

For the purpose of comparison, both LE and nonlinear DFE will be employed to eliminate ISI caused by multipath time dispersion. Taking one sample per symbol the tap weight coefficients of the equalizer are recursively adjusted to meet the criterion of minimizing the mean square error (MSE) with respect to the equalizer taps [59-63].

For the linear equalizer in Figure 3.2a, filter output $y(k)$ is expressed as

$$y(k) = \sum_{j=-m}^m w_j r_{k-j} \quad (3.17)$$

where w_j is tap weighting coefficients of the equalizer.

For the DFE shown in Figure 3.2b, the estimate is different from that of linear equalizer and denoted as

$$y(k) = \sum_{j=-m1}^0 w_{ffj} r_{k-j} + \sum_{j=1}^{m2} w_{fbj} d(k-j) \quad (3.18)$$

where w_{ffj} and w_{fbj} are the tap coefficients of forward and feedback filters, respectively.

Since the real UWA environment is dynamic, moving source or receiver can cause the channel variation. Thus the equalizer performance depends on

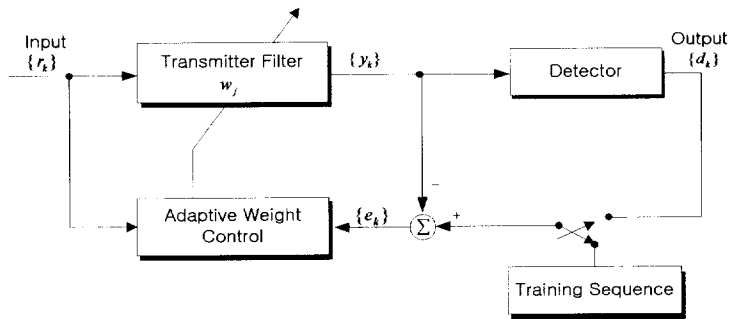
multipath structure as well as the channel coherence. The correlation coefficient ρ_h between the initial channel impulse response h_l and the changed channel response h_M whose energy have been normalized can be represented by

$$\text{Re}(\rho_h) = E[h_l h_M] \quad (3.19)$$

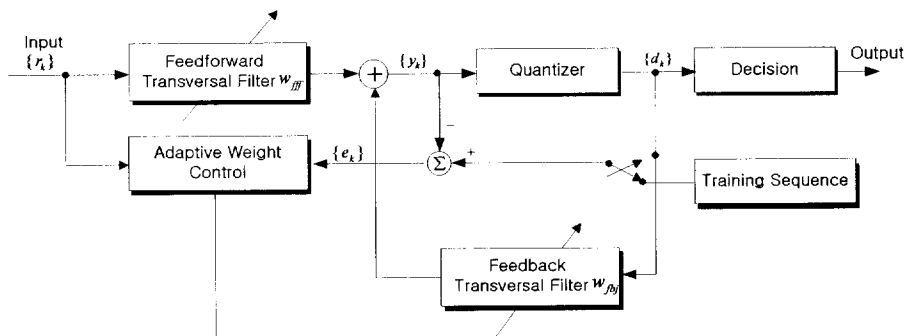
Hence Euclidean distance between the signal points can be determine by

$$d^{(e)} = \left\{ \left[\varepsilon_l + \varepsilon_M - 2\sqrt{\varepsilon_l \varepsilon_M} \text{Re}(\rho_h) \cos \frac{2\pi m}{4} \right]^{1/2} \right\} \quad m = 0, 1, 2, 3 \quad (3.20)$$

where m represents the difference between the four possible signals' phases



(a) Linear equalizer



(b) Decision feedback equalizer

Figure 3.2. Equalizer structures

of the carrier, ε denotes energy of the transmitted rectangular pulse signal $s(t)$ not considering the noise and lowpass filter [9],

$$\varepsilon_I = \int_0^T \left\{ \text{Re} \left[s(\tau) e^{j2\pi f_c \tau} \right] * h_I(\tau) \right\}^2 d\tau = \varepsilon \int_0^T [h_I(\tau)]^2 d\tau = \varepsilon \quad (3.21)$$

$$\varepsilon_M = \int_0^T \left\{ \text{Re} \left[s(\tau) e^{j2\pi f_c \tau} \right] * h_M(\tau) \right\}^2 d\tau = \varepsilon \int_0^T [h_M(\tau)]^2 d\tau = \varepsilon \quad (3.22)$$

$$\varepsilon = \int_0^T \left\{ \text{Re} \left[s(\tau) e^{j2\pi f_c \tau} \right] \right\}^2 d\tau = \frac{1}{2} \int_0^T |s(\tau)|^2 d\tau \quad (3.23)$$

Thus, Equation 3.21 can be simplified to

$$d^{(e)} = \left\{ 2\varepsilon \left[1 - \text{Re}(\rho_h) \cos \frac{2\pi m}{4} \right] \right\}^{1/2} \quad (3.24)$$

The channel coherence parameter determines signal space. When $m = 0$, $h_I \neq h_M$ causes the same demodulated signals scattered. For $m = 2$ the channel's coherence decrease contributes to the Euclidean distances between different signals points getting smaller. Therefore, the channel's coherence decrease may results in errors detected. Consequently the channel coherence parameter determines signal space and the equalizer can work well when the correlation coefficient remains high [49].

3.3 Simulation results

In this simulation the parameters are the same as those of the case mentioned in Chapter 2 except the modulation scheme. Here QPSK scheme is used leading to twice the bit rate compared to BPSK with the same symbol rate. The training sequence is selected as 300 symbols in all the cases. The

SNR is 40dB unless it is noted. We consider three cases while the horizontal ranges between the source and receiver are 10m, 600m and 1000m, respectively. For the three channels, the equivalent discrete-time channel model can be considered as

$$H_a(z) = 0.58 + 0.23z^{-8} - 0.41z^{-13} - 0.16z^{-21} \quad (3.25)$$

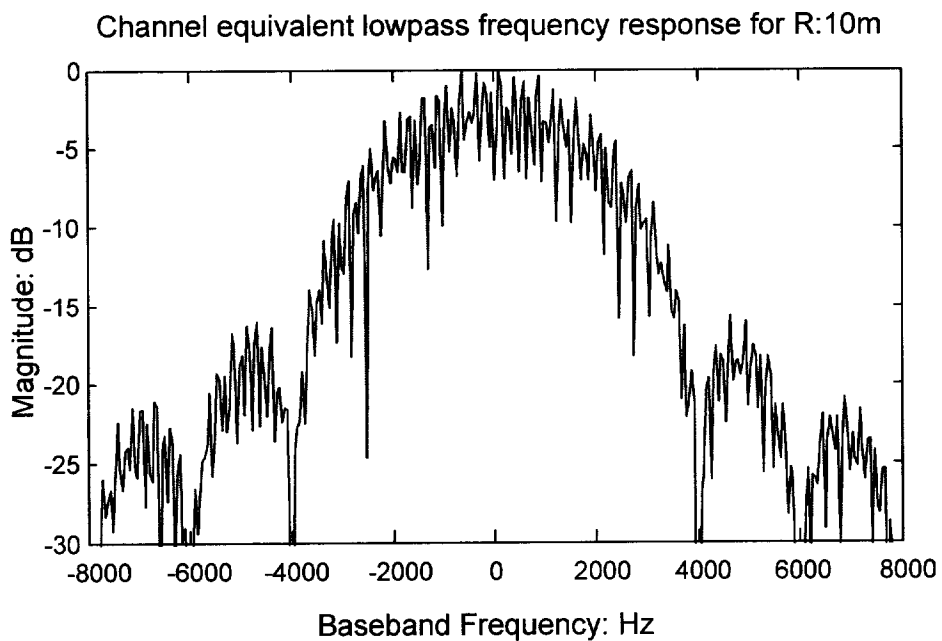
$$H_b(z) = 0.7 - 0.55z^{-1} + 0.29z^{-2} - 0.22z^{-3} - 0.2z^{-80} + 0.16z^{-84} - 0.08z^{-87} \quad (3.26)$$

$$H_c(z) = 0.7 - 0.54z^{-1} + 0.29z^{-2} - 0.22z^{-3} - 0.21z^{-51} + 0.17z^{-53} - 0.12z^{-54} \quad (3.27)$$

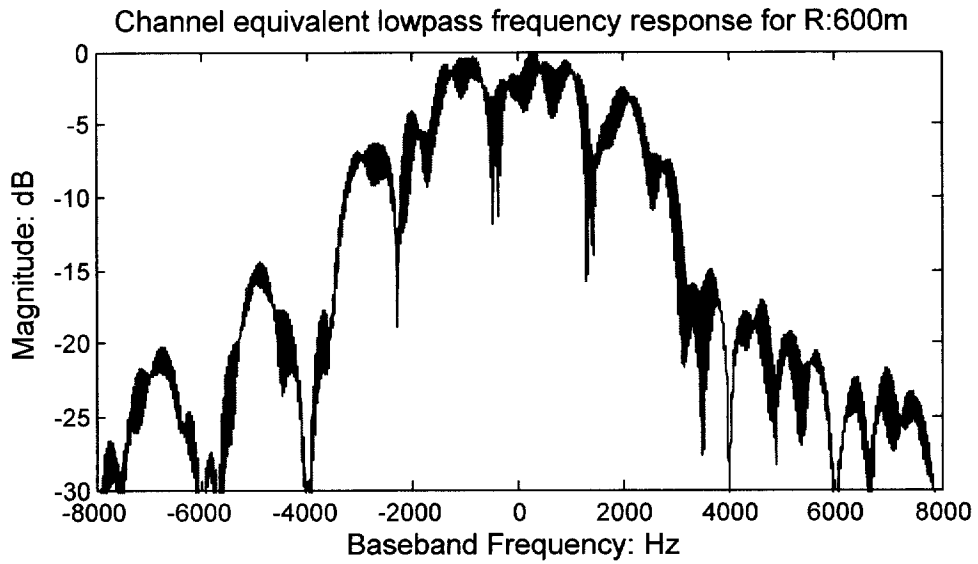
Figure 3.3 shows the frequency responses of the three channels while transmitting raised cosine pulse before QPSK signals for channel probing. It is evident that the latter two channels has deeper spectral nulls than the first channel R=10m. For the first channel when we employ a linear equalizer with 22 taps the eigenvalue spread is 3.75. Figure 3.4 shows the linear equalizer performance for the first channel. Employing LMS linear equalizer takes about 250 symbols to reach convergence and obtain an average MSE of about 18 dB, however, during the training period LMS is replaced by RLS algorithm, then in decision directed mode still using LMS algorithm to adjust the tap coefficients only needs 200 symbols to achieve the MSE of about 19dB. For R=10m, the channel does not have deep spectral nulls and small eigenvalue spread, thus linear equalizer is enough to compensate for ISI caused by multiple propagation paths. For the purpose of comparison during training time both LMS and RLS algorithms are adopted in equalization while DFE is employed. As shown in Figure 3.4, RLS used for training sequence can achieve more rapid convergence than the case of LMS. In addition the scatter diagram also shows that since RLS algorithm's employed in training mode, the equalizer output is tightly separated. While we employ

the DFE, it can remove ISI effects more completely and does not cause the noise enhancement due to its nonlinear characteristics. Figure 3.4 shows that the LMS DFE gives rise to a little degrade in MSE and much slower convergence than RLS DFE for training sequence. The average mean square error after DFE can reach 30dB, consequently the SNR of the equalizer output can be improved.

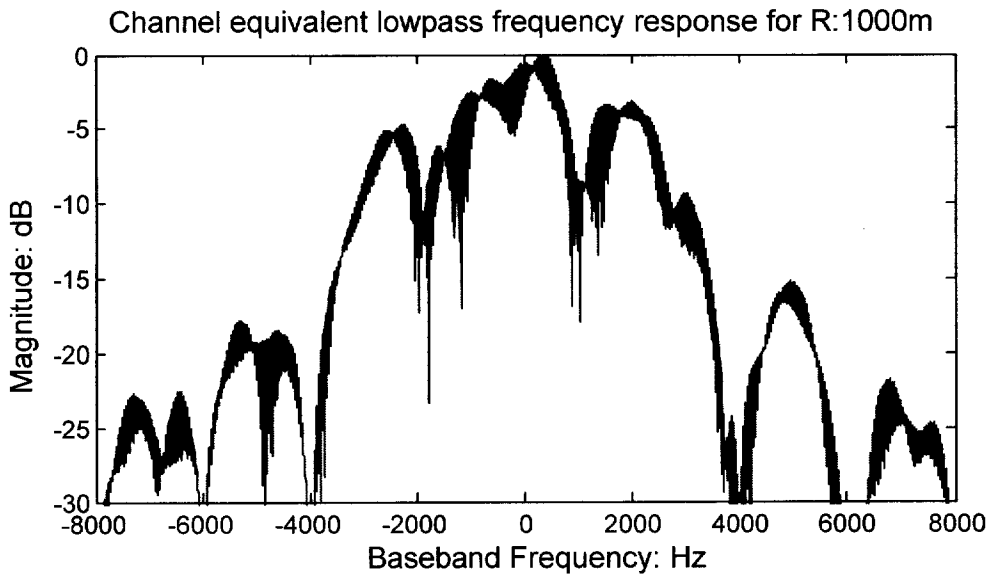
The second channel model has the eigenvalue spread of 49.17 using a linear equalizer with 88 taps to compensate for channel distortion. For the second case, large eigenvalue causes the convergence rate slow while using LMS linear equalizer. Figure 3.6 exhibits that LMS LE requires 800 iterations to reach convergence with 10dB MSE, much slower and larger average MSE compared to case 1. Thus the constellation diagram shows that



(a) Frequency response for R=10m

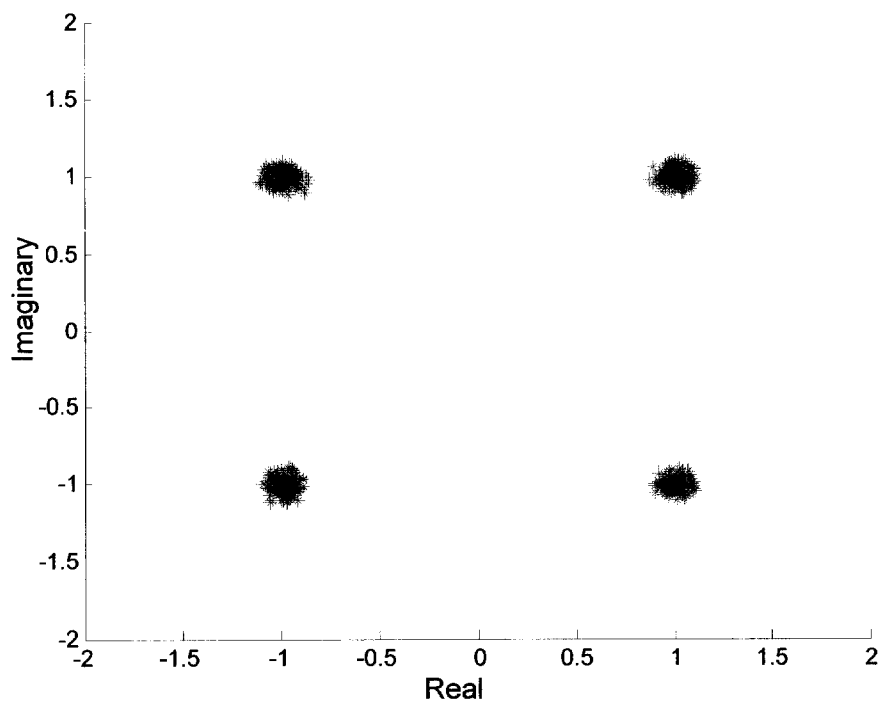


(b) Frequency response for R=600m

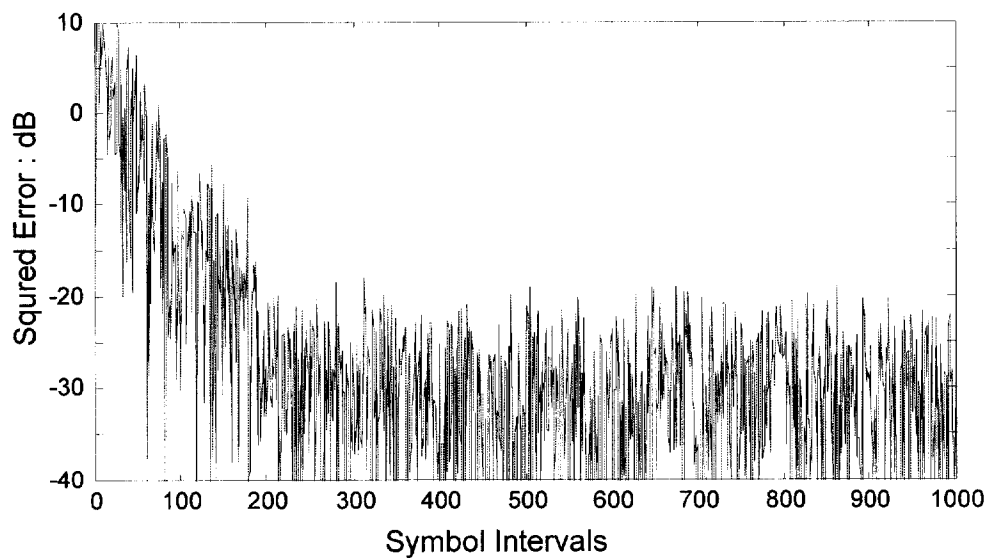


(c) Frequency response for R=1000m

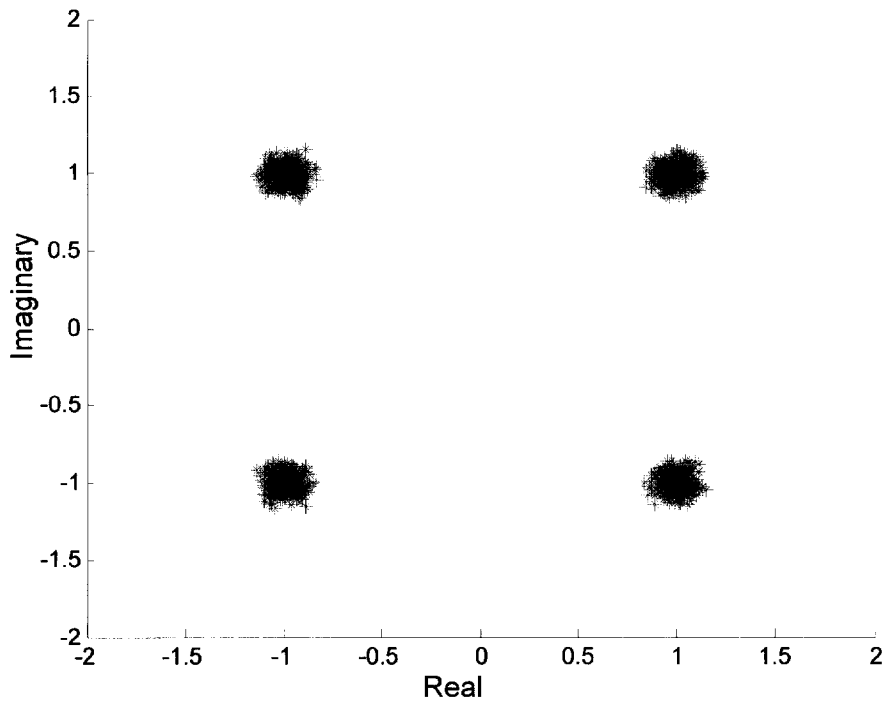
Figure 3.3. Channel frequency response



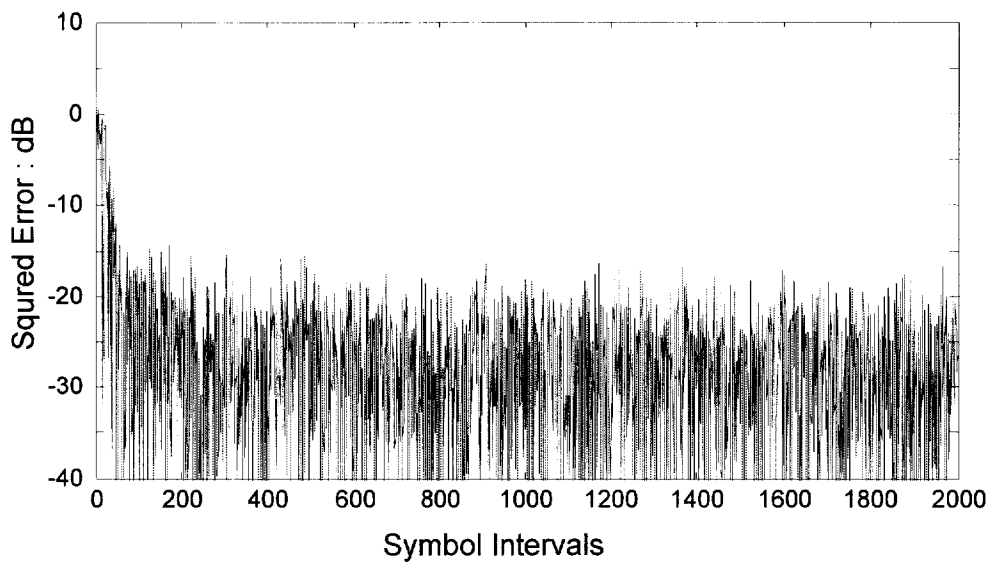
(a) LMS LE output for $R=10m$



(b) MSE after LMS LE

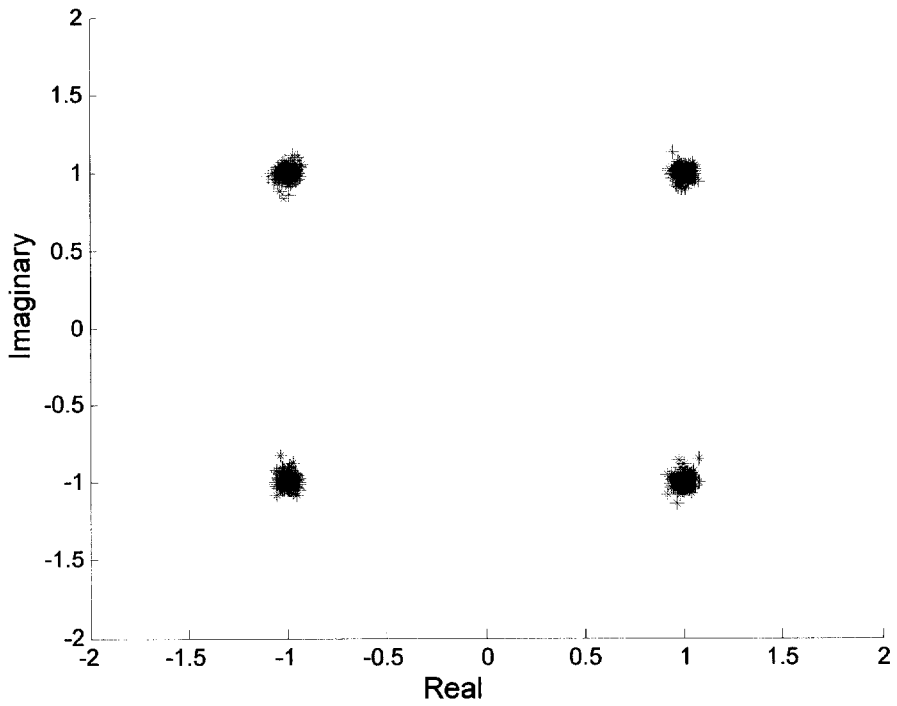


(c) RLS-LMS LE output for $R=10\text{m}$

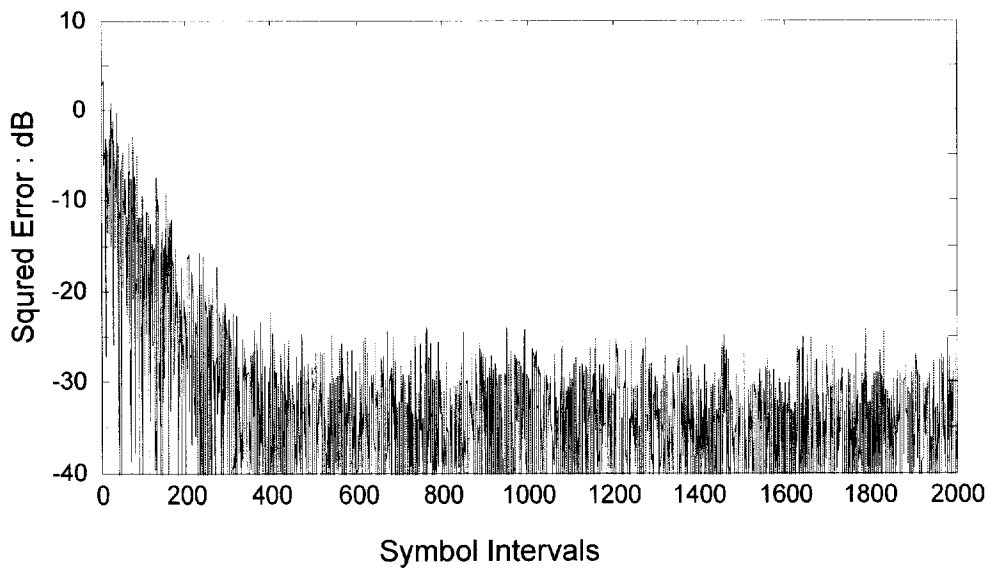


(d) MSE after RLS-LMS LE for $R=10\text{m}$

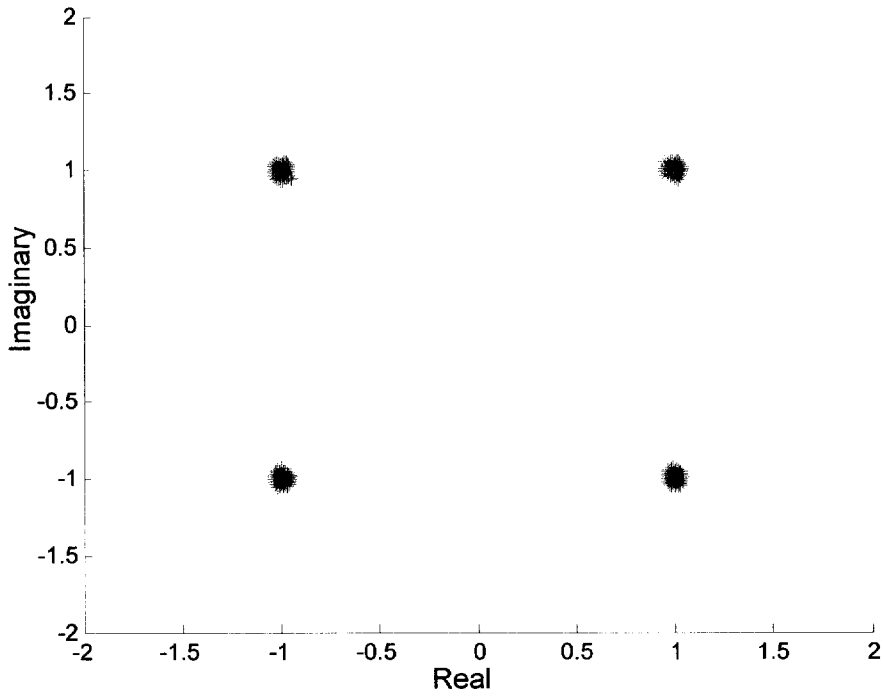
Figure 3.4. LE performance for $R=10\text{m}$



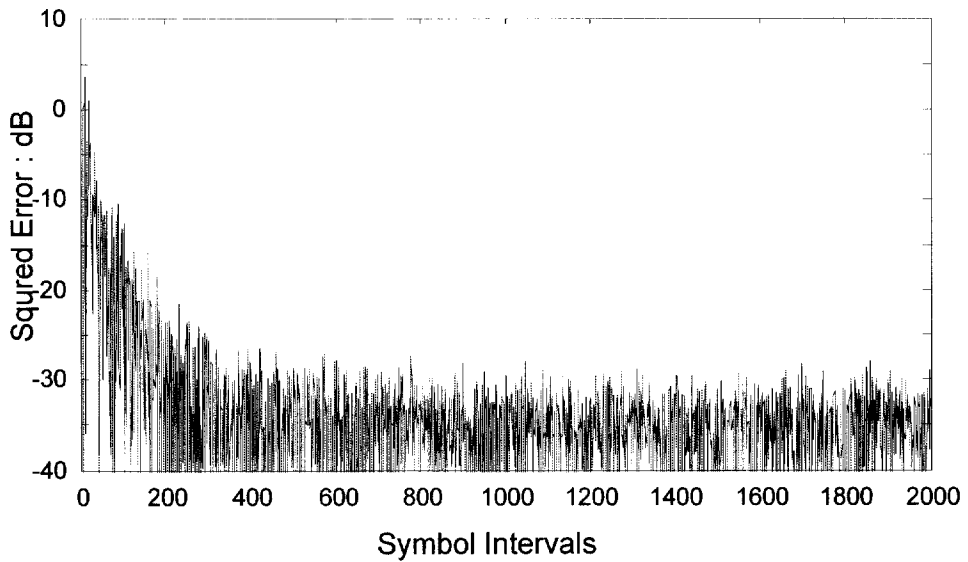
(a) LMS DFE output for $R=10m$



(b) MSE after LMS DFE for $R=10m$



(c) RLS-LMS DFE output for $R=10m$



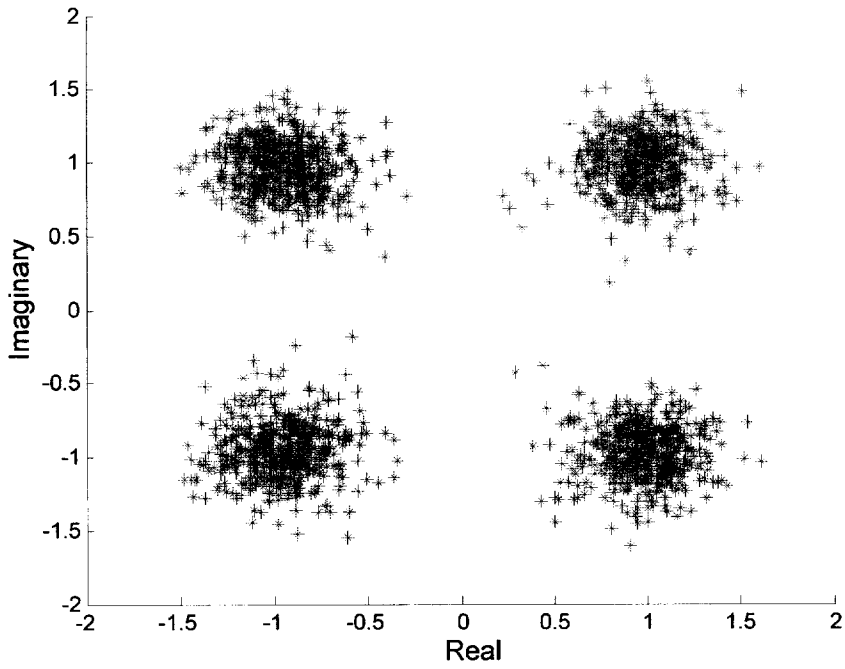
(d) MSE after RLS-LMS DFE for $R=10m$

Figure 3.5. DFE performance for $R=10m$

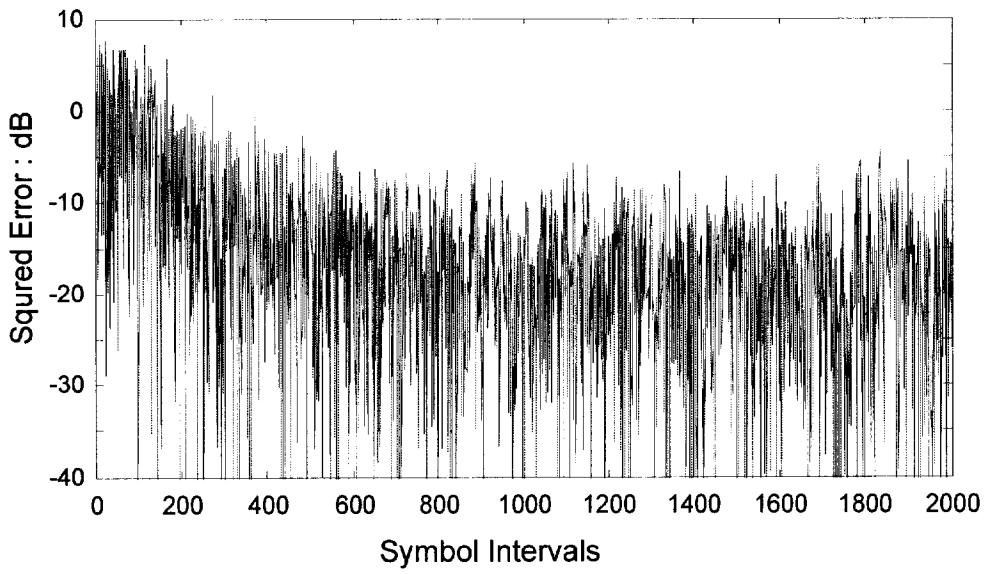
the equalizer output is more scattered and some errors detected ("+" indicates error). However while training sequence was processed using RLS algorithm, the convergence only requires about 200 symbols, and the equalizer output constellation shows better performance than that of the case LMS is first adopted during training time. After RLS equalizer processing converges within 200 iterations RLS-LMS DFE as shown in Figure 3.7 can reach much lower residue MSE. Consequently for the channel with larger eigenvalue spread the RLS equalizer is proposed to train the sequence to converge to stability, then LMS equalizer is continuously to reduce ISI can be an effective way to make a tradeoff between convergence and excess mean square error.

The third channel model for $R=1000m$ corresponds to eigenvalue ratio of 39.85 for the number of equalizer taps is chosen to be 55. Choosing RLS algorithm for training can obtain faster convergence, and constellation plots as shown in Figures 3.8 and 3.9 depict that the output of equalizer is more tightly separated compared with LMS equalizer for training sequence. Especially for the channel with deep spectral nulls and large eigenvalue spread, DFE equalizer's employment shows that RLS algorithm adopted for training can make a balance between MSE and convergence rate and achieve more ideal performance: much faster convergence and smaller MSE, i.e., larger output SNR.

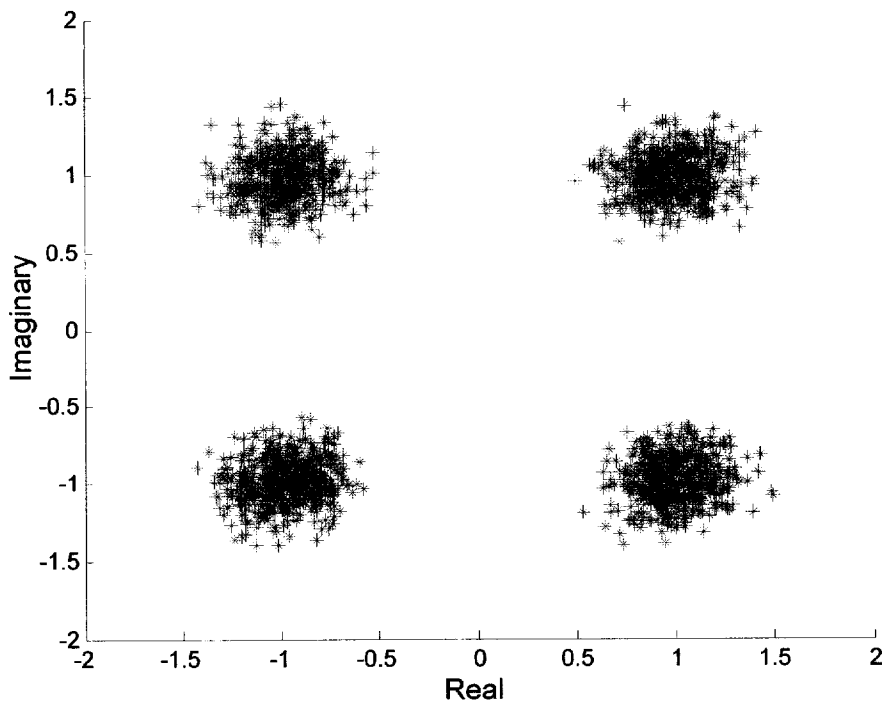
Figures 3.10a and 3.10b plot the MSE and BER as a function of input SNR for LE. It can be found that for channel $R=10m$ LE performs well and achieve smaller MSE than the other two channels. For channel $R=10m$ the higher SNR, the lower MSE. For the other two channels due to their deep spectral nulls LE can not obtain a big improvement in output SNR even at high SNR of input or noise free case. From Figure 3.11 it can be seen that DFE enhances the performance, especially at high SNR. For high SNR the MSE after DFE equalization is significantly lower than that of the linear equalizer. At low SNR the DFE performance does not show a big difference and both linear and nonlinear equalizer DFE don't supply good performance



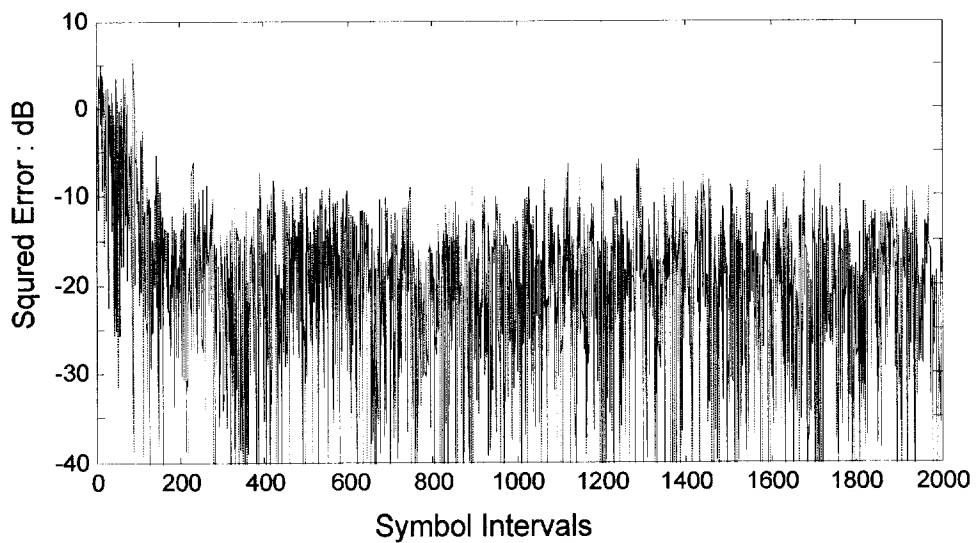
(a) LMS LE output for $R=600\text{m}$



(b) MSE after LMS LE for $R=600\text{m}$

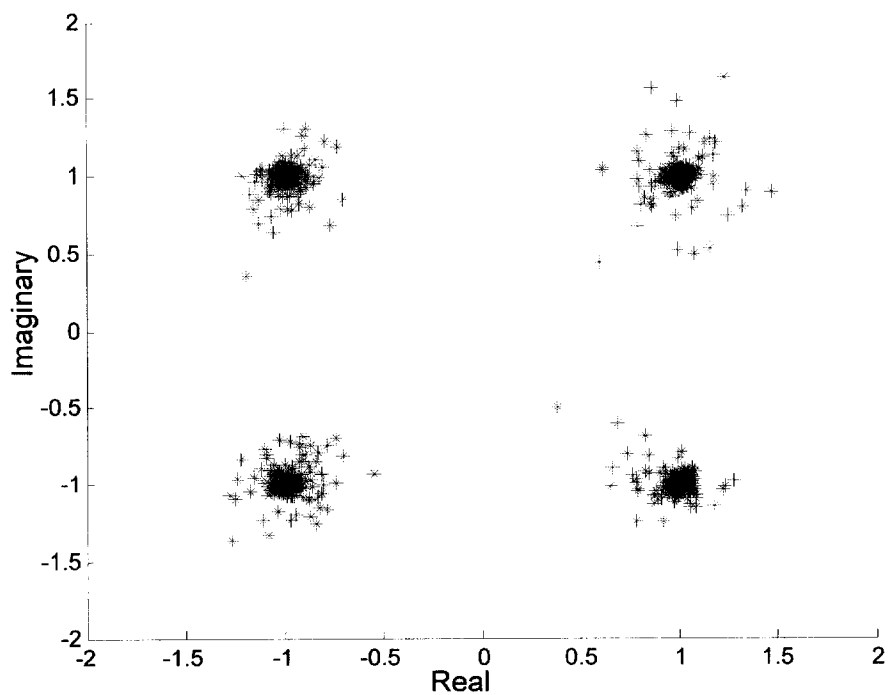


(c) RLS-LMS LE output for $R=600m$

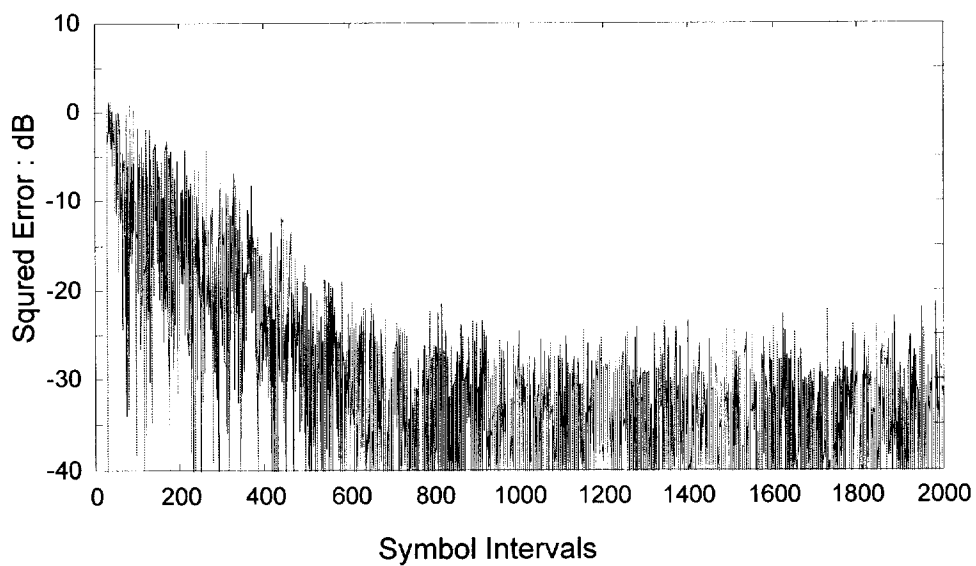


(d) MSE after RLS-LMS LE for $R=600m$

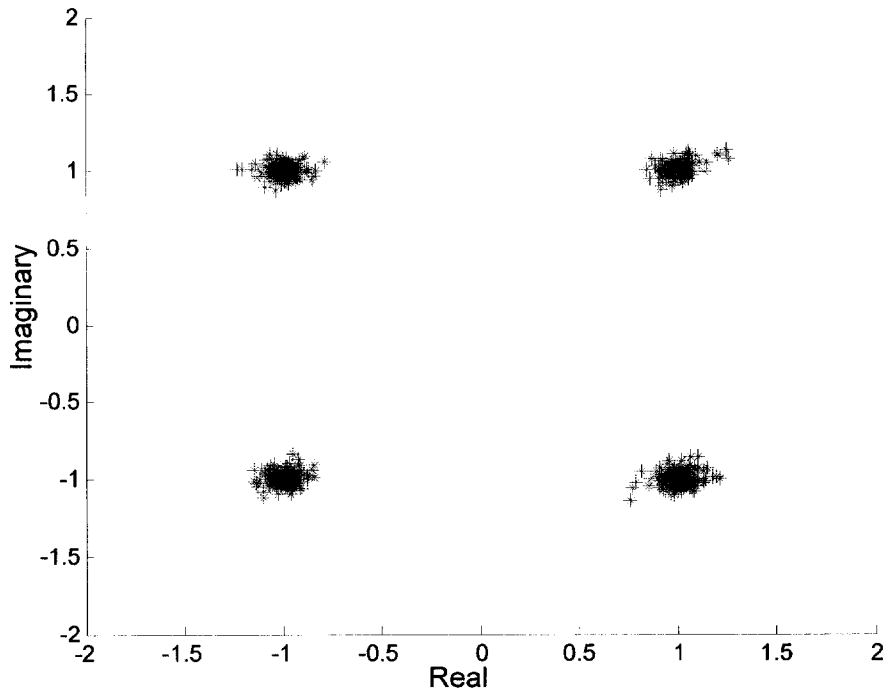
Figure 3.6. LE performance for $R=600m$



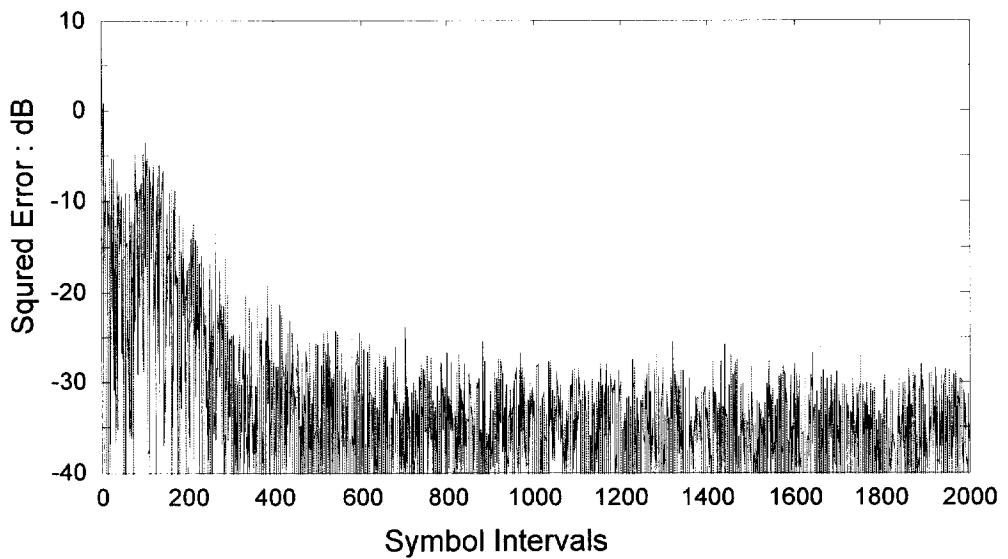
(a) LMS DFE output for $R=600m$



(b) MSE with LMS DFE for $R=600m$

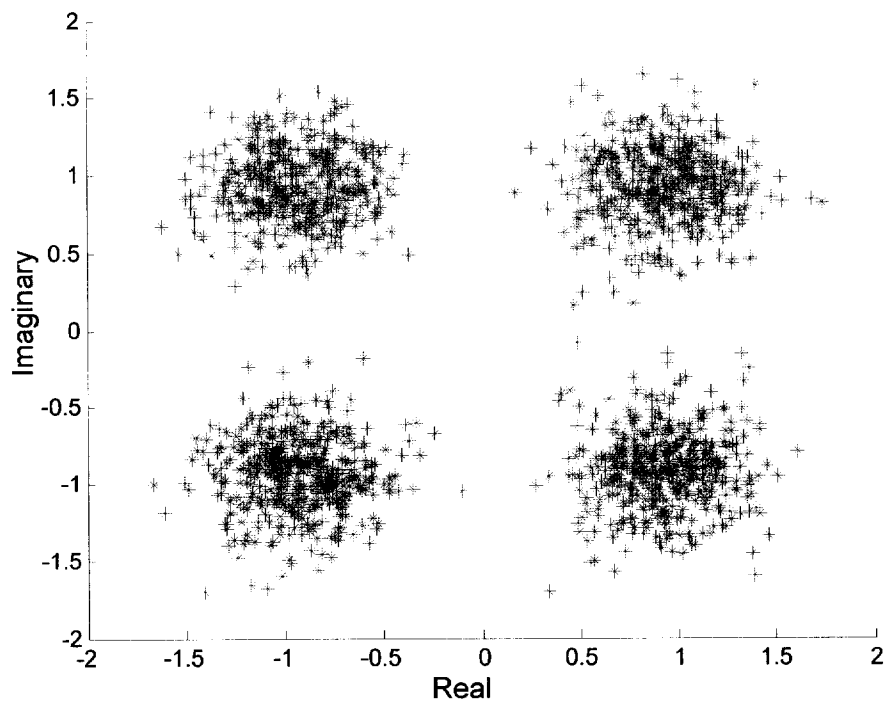


(c) RLS-LMS DFE output for $R=600m$

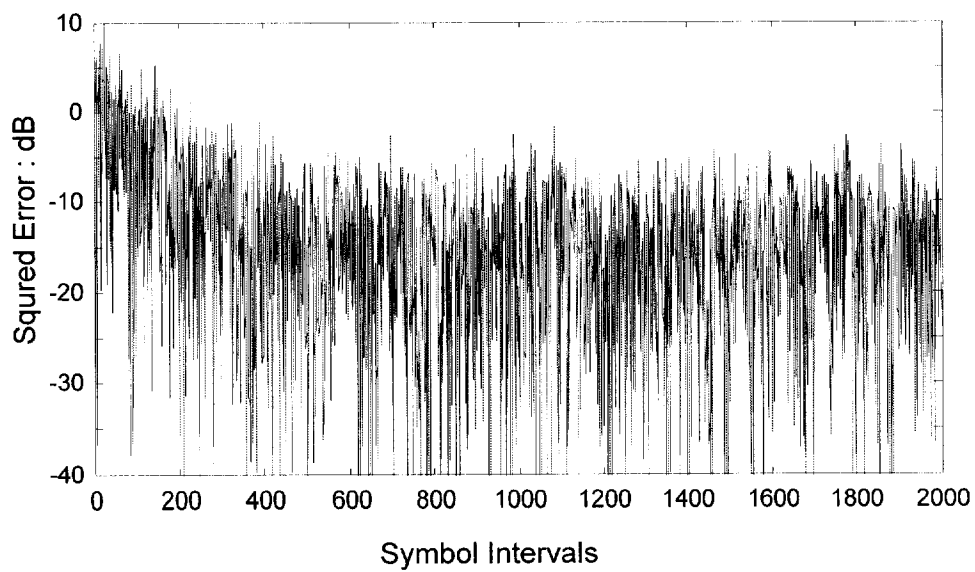


(d) MSE after RLS-LMS DFE for $R=600m$

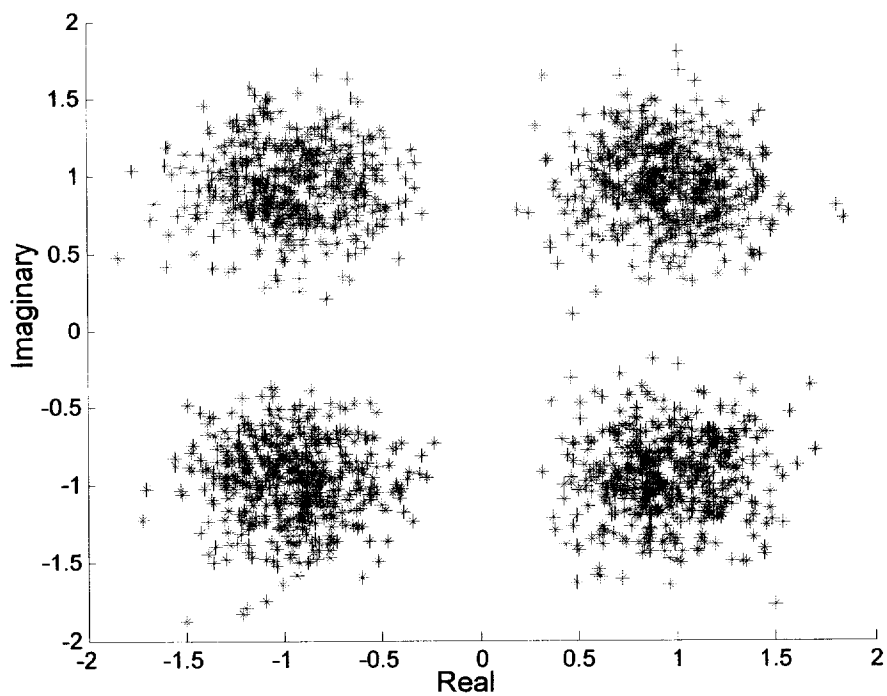
Figure 3.7. DFE performance for $R=600m$



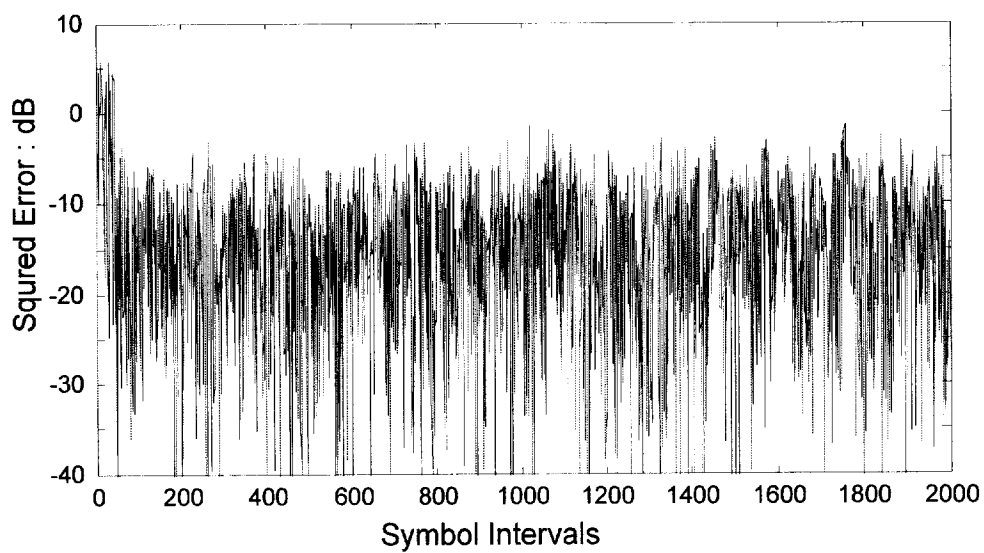
(a) LMS LE output for $R=1000m$



(b) MSE after LMS LE for $R=1000m$

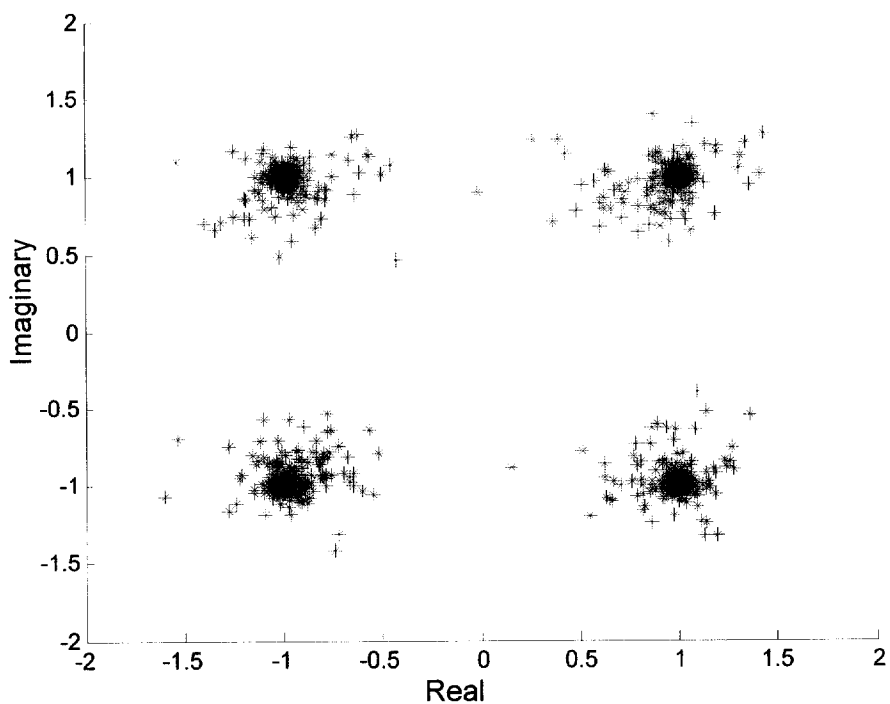


(c) RLS-LMS LE output for $R=1000m$

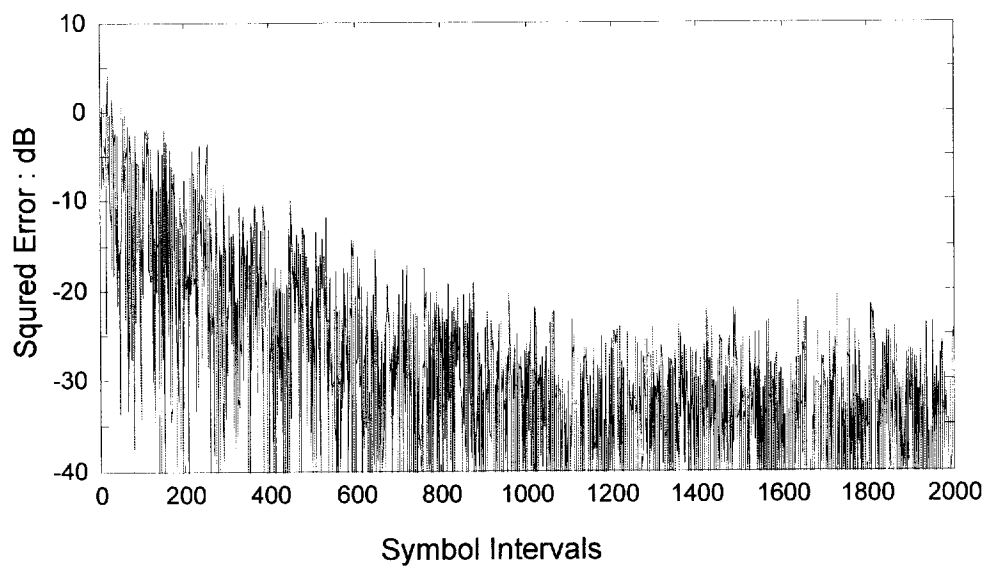


(d) MSE after RLS-LMS LE for $R=1000m$

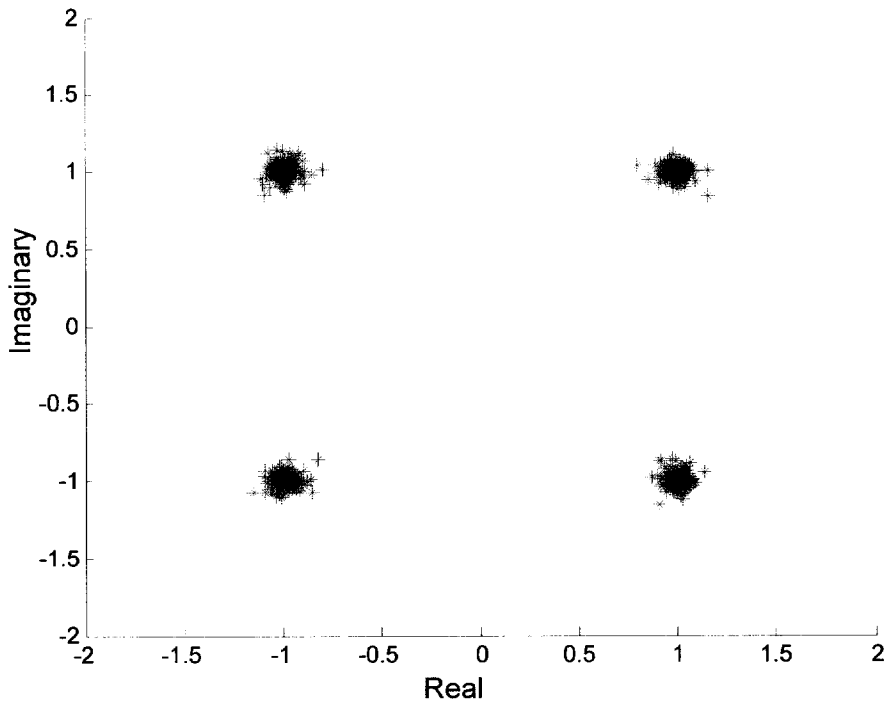
Figure 3.8. LE performance for $R=1000m$



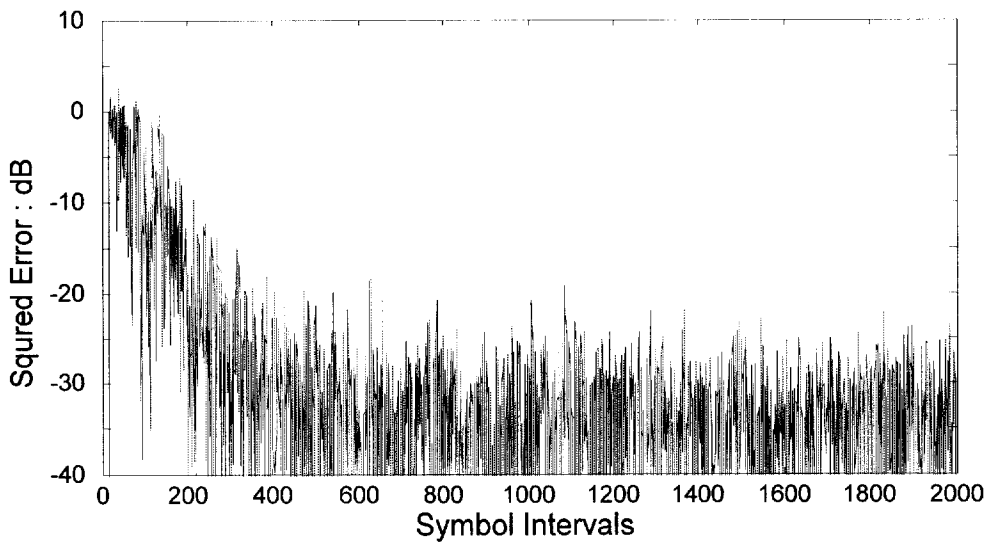
(a) LMS DFE output for $R=1000m$



(b) MSE after LMS DFE for $R=1000m$

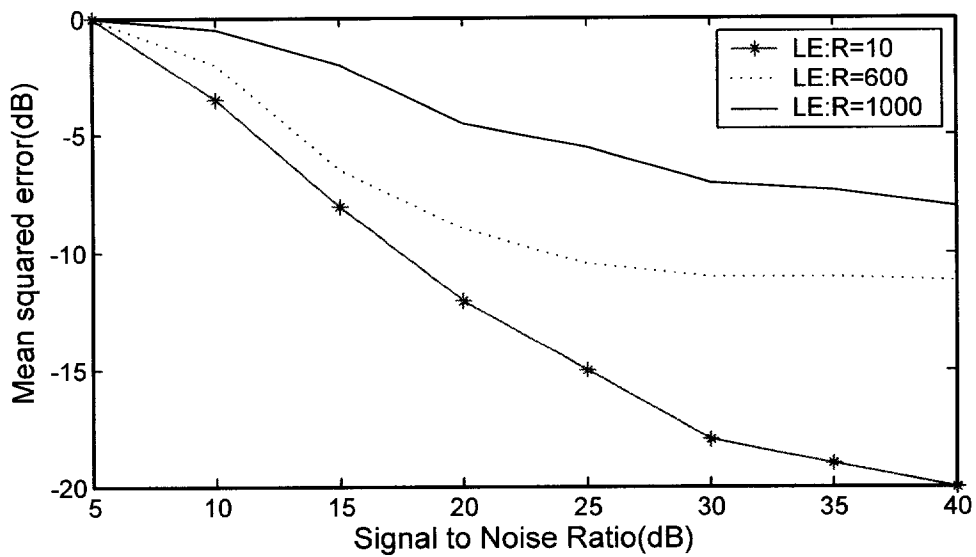


(c) RLS-LMS DFE output for $R=1000m$

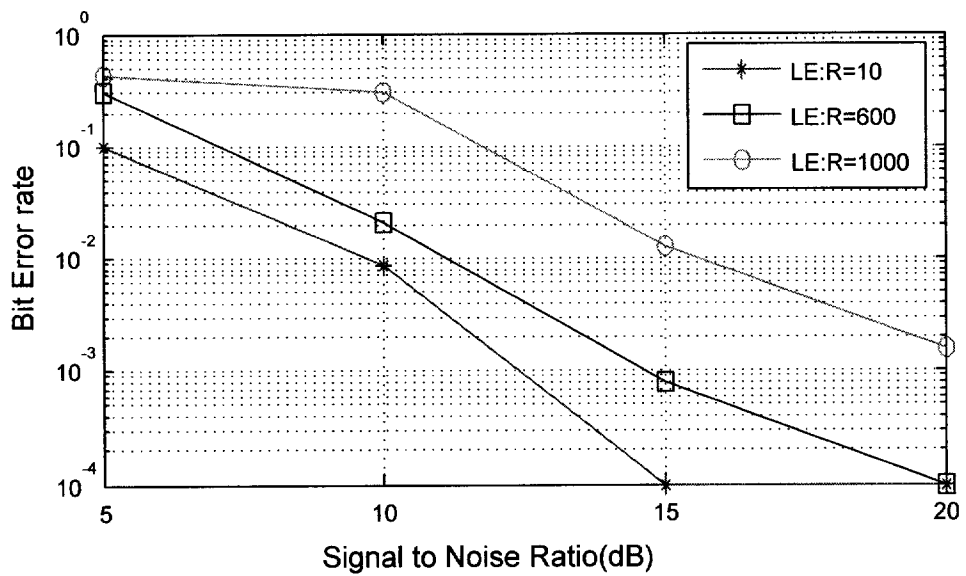


(d) MSE after RLS-LMS DFE for $R=1000m$

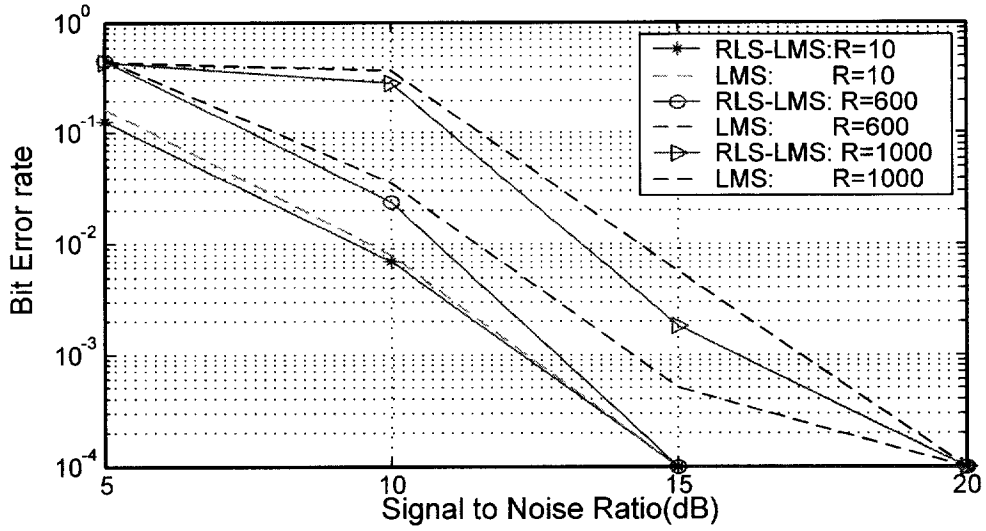
Figure 3.9. DFE performance for $R=1000m$



(a) MSE vs. SNR after RLS-LMS LE



(b) BER vs. SNR after RLS-LMS LE

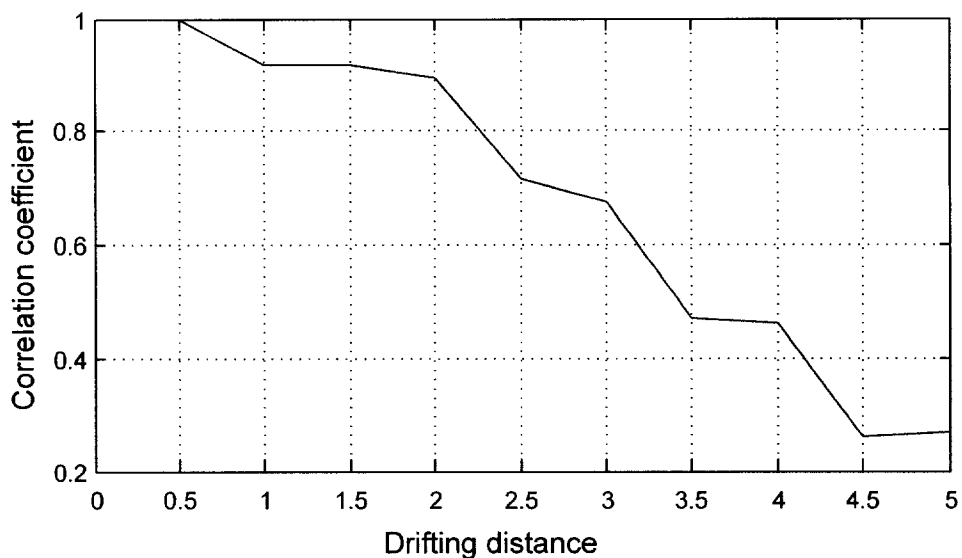


(c) BER vs. SNR after LMS and RLS-LMS DFE

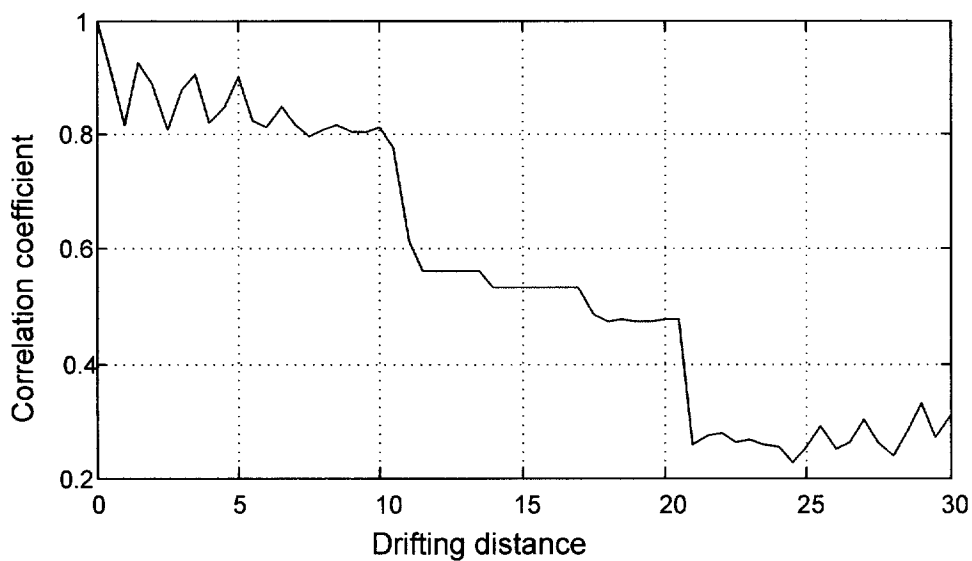
Figure 3.10. BER vs. SNR after LE and DFE

scheme always outperforms the LMS algorithm. At low SNR the DFE does not show its superiority either in convergence or in MSE. This implies that when SNR is higher than 15dB a good way for removing ISI caused by channel time dispersion is to use adaptive equalization technique.

In order to investigate the performance of equalization in slow time-varying channel, we varied the channel by changing the horizontal range between the source and receiver and plot the correlation coefficient with respect to the source's drifting distance. Figure 3.12 exhibits that the larger the drifting distance, the lower the correlation coefficient. For the channel $R=10\text{m}$ when the distance is larger than 3.5m, the coherence between the original channel and newly obtained channel due to source moving decreases to 0.67. For the second channel $R=600\text{m}$ due to the range between the source and receiver is relatively larger than the first channel, the coherence dropped to 0.53 while the moving distance reaches 15m. To study how the horizontal drifting distance influences the equalizer performance the moving

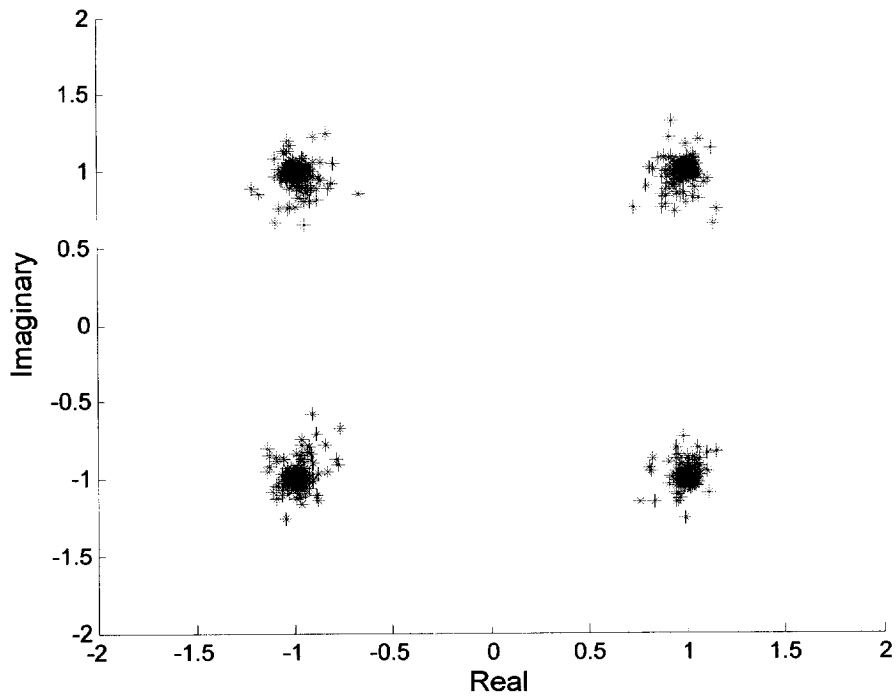


(a) For channel $R=10\text{m}$

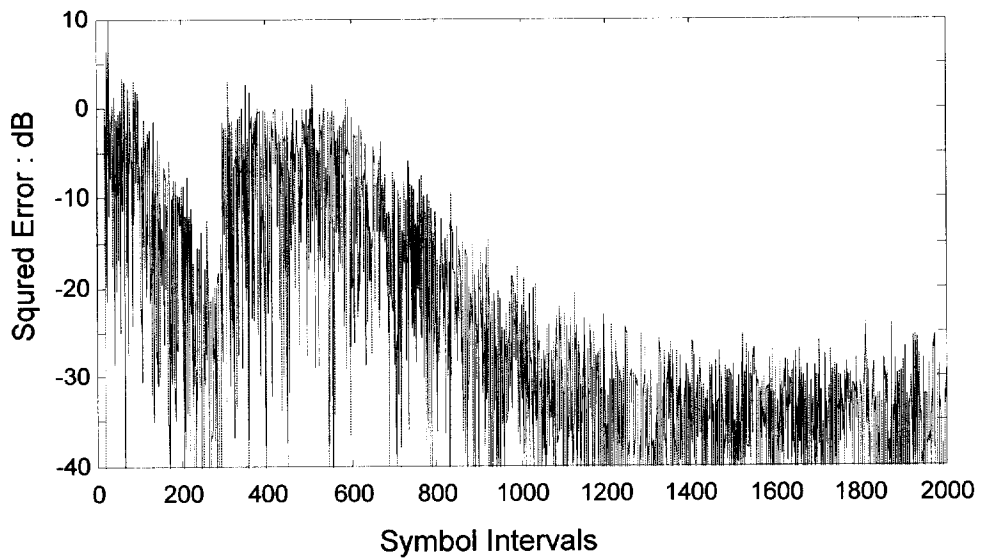


(b) For channel $R=600\text{m}$

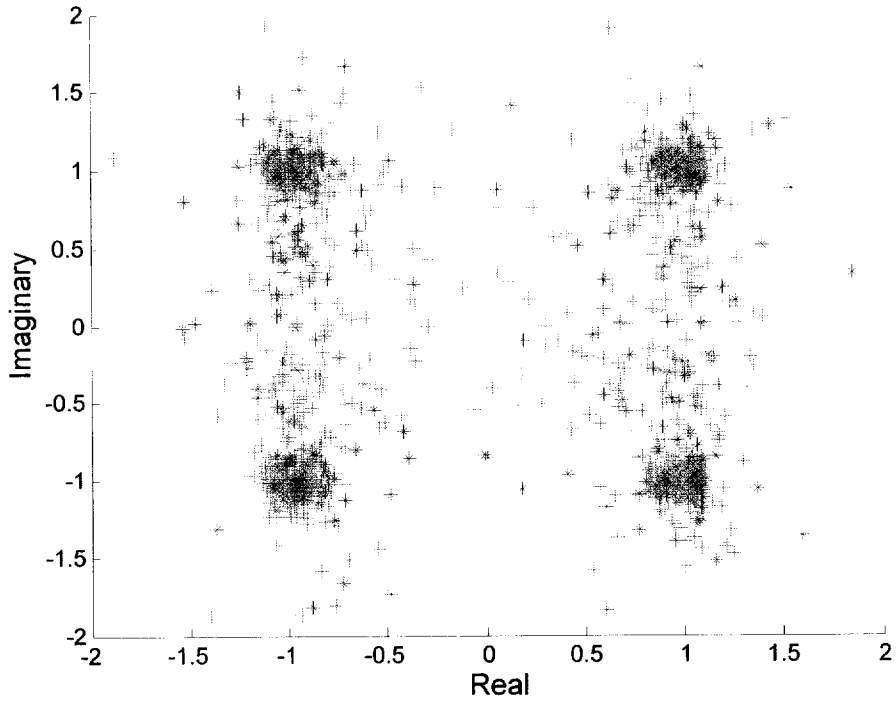
Figure 3.11. Correlation coefficient with respect to drifting distance



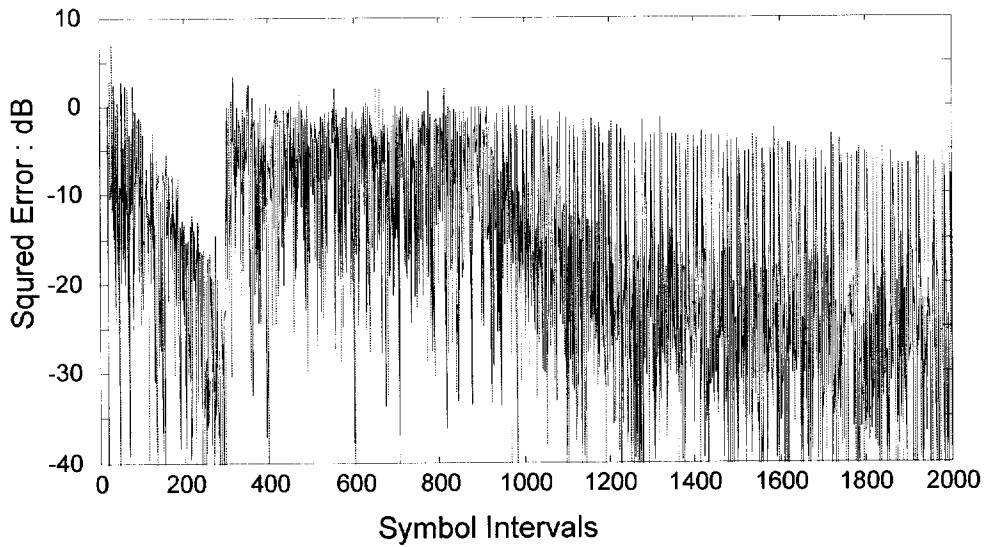
(a) RLS-LMS DFE output for R=10m (Distance: 3.5m Corr:0.67)



(b) MSE after RLS-LMS DFE

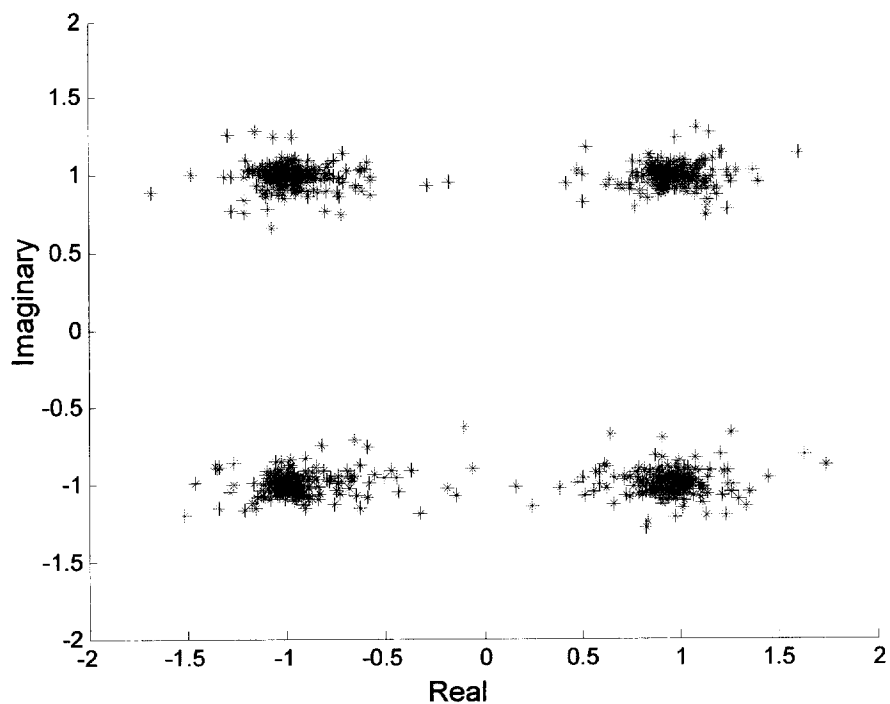


(c) RLS-LMS DFE output for R=10m (Distance: 5m Corr: 0.233)

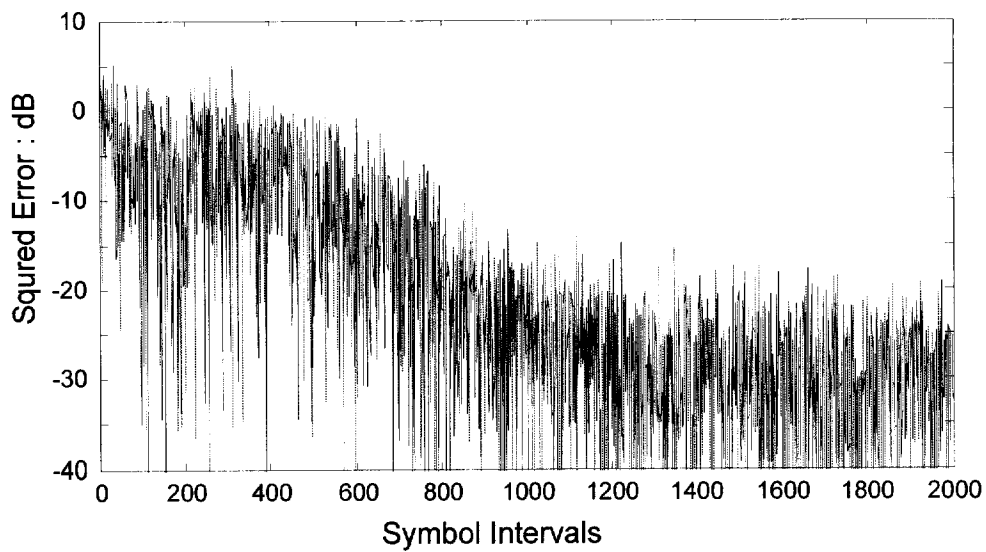


(d) MSE after RLS-LMS DFE

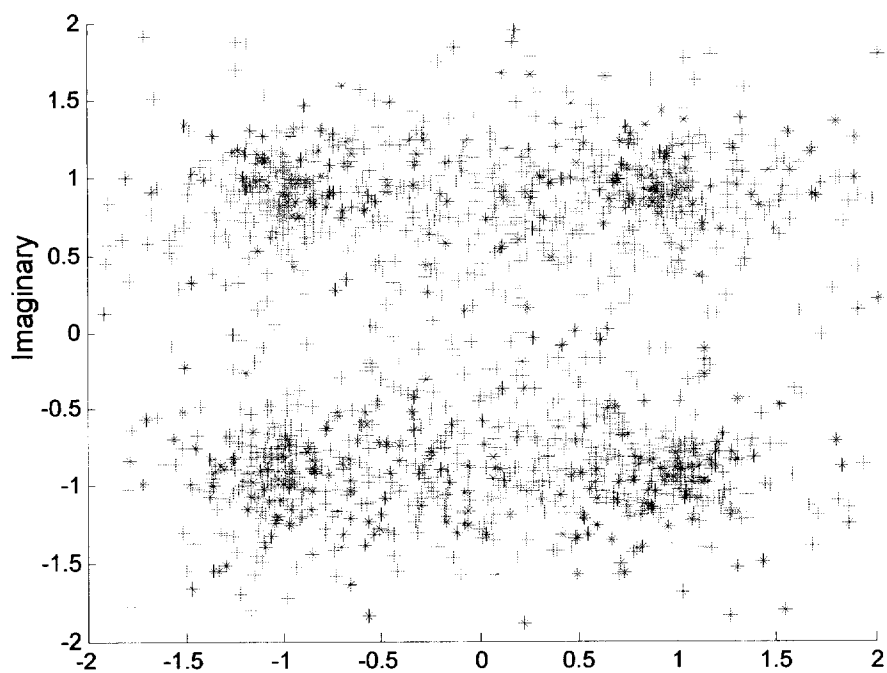
Figure 3.12 DFE performance with drifting distance for R=10m



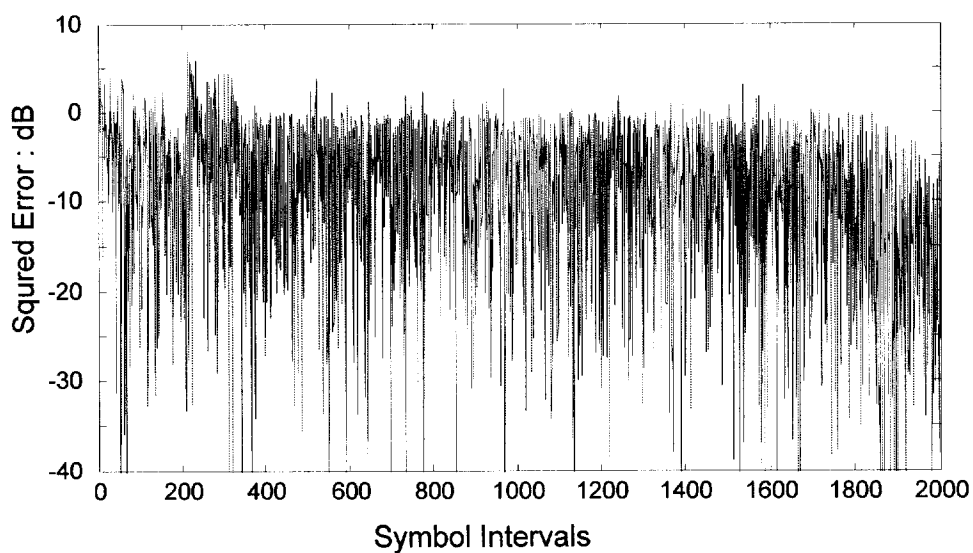
(a) RLS-LMS DFE output for R=600m (Distance: 15m Corr:0.53)



(b) MSE after RLS-LMS DFE



(c) RLS-LMS DFE output for $R=600\text{m}$ (Distance: 21m Corr:0.28)



(d) MSE after RLS-LMS DFE

Figure 3.13 DFE Performance with drifting distance for $R=600\text{m}$

Distances are selected as 3.5m and 5m, respectively for the first channel. During the training period (300 symbols) the source is assumed to be at the initial position and being switched to direct decision mode the source moves extended to 3.5m and 5m, respectively. Figure 3.13 demonstrates that while the moving distance is 3.5m whose coherence is above 0.5 the equalizer can still reach convergence and achieve error free transmission after 600 symbols transmitted. However when the drifting distance is 5m whose channel coherence decreased to 0.233, the equalizer after training will diverge, many errors are detected and can not achieve reliable communication. The same results will be obtained for the second channel, when drifting distance is 15m (coherence: 0.53), the equalizer performs well, drifting distance reaches 21m (coherence: 0.28) the equalizer does not provide satisfactory performance as shown in Figure 3.13. This result is in agreement with the experimental finding that when the channel coherence remains high channel equalizer can adapt to the variation achieving error free transmission [40].

3.4 Conclusions

Aiming at choosing appropriate equalization method to achieve ideal transmission effects, it is proposed that using RLS algorithm during the training period, then LMS algorithm is employed during the decision direct mode for the channels having large eigenvalue spread of the received signal autocorrelation matrix. The simulation results prove that it's an effective scheme to improve the equalizer performance not improving the computation complexity largely. For the channel with deep spectral nulls, it especially shows this scheme's superiority while RLS DFE is employed for training period leading to fast convergence. Equalizer performance due to drifting distance has also been analyzed and it was found that the source moving induces degrade of channel coherence resulting in smaller Euclidean distance's in signal space and more errors occurred if correlation coefficient decreases to small value.

Chapter 4

Performance Comparison of Passive Phase Conjugation and Decision Feedback Equalizer

4.1 Background

Coherent modulation schemes such as PSK offer bandwidth efficiency and power efficiency, but face the problem of multipath which causes ISI in UWA communications. Several methods deal with this problem. In Chapter 2 and Chapter 3 adaptive equalization performance has been studied. In this chapter spatial diversity will be paid attention. Building a receiver array, i.e., multichannel equalization has proved to be an efficient way of dealing with time spread UWA channels. Recently PPC was proposed, which resorts to the use of time reversal probe signal received earlier to achieve the knowledge of channel and thereby reduce the ISI. According to PPC theory multichannel matched filter can be evaluated justified for use as an equalizer in the shallow-water channel. In this chapter, the evaluations use simulated channels based on reflection functions derived from two shallow water acoustic channels. MSE is shown as a criterion for assessing the performance of the PPC and multichannel equalizers [64-68].

Adaptive channel equalization is an integral part of many digital communication receivers to combat ISI caused by multipath. Conventional adaptive equalizer design is based on the recurring transmission of known data to settle the filter coefficients. If the communication signal is received at more than one sensor, this spatial diversity can be utilized in a multichannel equalizer. The joint space-time processing usually leads to an improved performance compared to the output of signal channel receiver [69-70].

In order to account for amplitude fluctuations of the UWA channel, synchronization is assumed to be perfect and the problem of multichannel

adaptive channel equalization is concerned. Spatial diversity estimation procedures are known to yield better results than single channel estimation. In this chapter PPC and adaptive multichannel equalization is focused on and these two methods' performance efficiency is compared in the case of the time-invariant channel since PPC assumes time invariance. The simulation results of their application to shallow water channels have demonstrated the feasibility of achieving coherent communications over these channels [71-73].

4.2 System structure and equalization algorithm

4.2.1. Multichannel equalizer

In this section the problem of extracting the transmitted data sequence from the signal received over a number of propagation paths and observed across an array of sensors will be addressed. Adaptive multichannel equalization techniques can be used to first extract the channel response from a training sequence and then compensate the channel distortion during the period of the data symbols transmission.

It is assumed that the most general channel model in which each of the array sensors observes the transmitted signal passed through a different channel with some noise added. The transmitted signal is a data sequence linearly modulated onto a carrier, and it is represented in its equivalent complex baseband form as

$$s(t) = \sum_i s_i p(t - iT) \quad (4.1)$$

where s_i is the sequence of binary data symbols corresponds to bit 1, -1, $p(t)$ is the basic transmitter pulse having adopted in Chapters 2 and 3, and T the signaling interval. The channel, as seen by one of the M sensors, is described by its impulse response $h_m(t)$, which includes any transmit filtering. Both the effects of time delay and phase deviations are included in this response, and for the moment $h_m(t)$ is treated as constant in which the received signals taking one sample per symbol in the m th channel at time kT are given by

$$r_{m,k} = \left(\sum_i s(k) h_m(k-i) + \eta_m(k) \right) * p(T-t) \quad (k-1)T \leq t \leq kT \quad (4.2)$$

Assuming the constant channel impulse response in some interval, let the m th channel feedforward filter tap weight vector of multichannel equalizer whose structure is depicted in Figure 4.1 be

$$w_{m,ff} = [w_{ff-K1}^m \cdots w_{ff0}^m] \quad (4.3)$$

The feedback filter coefficients are denoted as

$$w_{fb} = [w_{fb1} \cdots w_{fbK2}] \quad (4.4)$$

The nonlinear equalizer output has the form

$$y(k) = \sum_{m=1}^M \sum_{j=-K1}^0 w_{m,ffj} r_{m,k-j} + \sum_{j=1}^{K2} w_{fbj} \tilde{d}_{k-j} \quad (4.5)$$

In order to reduce computation complexity, multichannel equalizer is a suboptimal method applicable to long range channels. It improves the limited signal-to-noise ratio at the receiver through coherent combining. In such a way, it benefits from the implicit time diversity present in the multipath propagation, as well as from the explicit, spatial diversity [74-77].

4.2.2. PPC algorithm

The block diagram for PPC is illustrated in Figure 4.2. It is clear that it is a special form of a linear equalizer where the tap coefficients are the time-reversed impulse response function. Considering only discrete multipath, the channel impulse response of m th receiver element is given as

$$h_m(t) = \sum_{n=1}^N \alpha_{m_n} \delta(t - \tau_{m_n}) \quad (4.6)$$

where α_{mn} is the amplitude of the received signal of the n th path normalized by the amplitude of the direct path signal ($n=1$) and τ_{mn} is the difference in time of arrival between the direct path signal and reflected path signal. Therefore, the probe response signal $r_{p_m}(kT)$ at m th receiver element is given as

$$r_{p_m}(kT) = p(kT) * h_m(kT) = \sum_{n=1}^N \alpha_{mn} p(kT - \tau_{mn}) \quad (4.7)$$

Output of probe signal PPC process or autocorrelation of probe response signal is given as

$$y_m(kT) = \sum_{n=1}^N (\alpha_{mn})^2 R_{pp}(kT) + \sum_{\substack{n_1=1 \\ n_1 \neq n_2}}^N \sum_{n_2=1}^N \alpha_{mn_1} \alpha_{mn_2} R_{pp}(kT + \tau_{mn_1} - \tau_{mn_2}) \quad (4.8)$$

where $R_{pp}(kT)$ is autocorrelation of the probe signal. The first term of bracket is the sum of the multipath amplitude squares defined as main lobe amplitude and the second term is a group of cross product of two different multipath amplitudes defined as side lobe.

The sum of all M-array elements PPC processes is given by

$$y(kT) = \sum_{m=1}^M \sum_{n=1}^N (\alpha_{mn})^2 R_{pp}(kT) + \sum_{m=1}^M \sum_{\substack{n_1=1 \\ n_1 \neq n_2}}^N \sum_{n_2=1}^N \alpha_{mn_1} \alpha_{mn_2} R_{pp}(kT + \tau_{mn_1} - \tau_{mn_2}) \quad (4.9)$$

The PPC method by convolving the received signal $r(kT)$ with the time-reversed impulse response function (the probe signal) can be evaluated and obtained

$$\begin{aligned} \sum_{m=1}^M h_m * r_{m,k} &= \sum_{m=1}^M \sum_i s_i \sum_{n=1}^N (\alpha_{mn})^2 R_{pp}(kT - iT) \\ &\quad + \sum_{m=1}^M \sum_i \sum_{\substack{n_1=1 \\ n_1 \neq n_2}}^N \sum_{n_2=1}^N \alpha_{mn_1} \alpha_{mn_2} R_{pp}(kT + \tau_{mn_1} - \tau_{mn_2} - iT) \end{aligned} \quad (4.10)$$

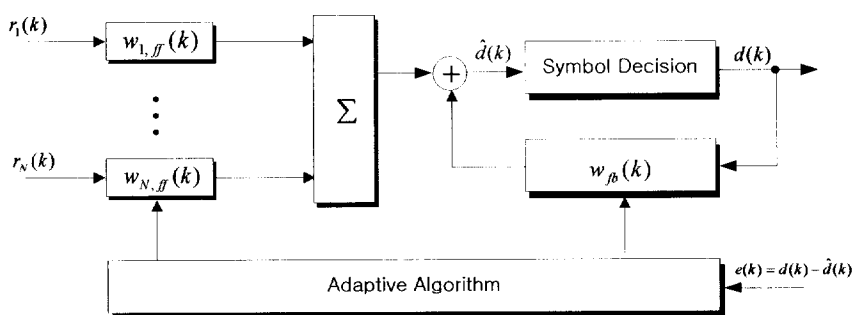


Figure 4.1. Multichannel DFE structure

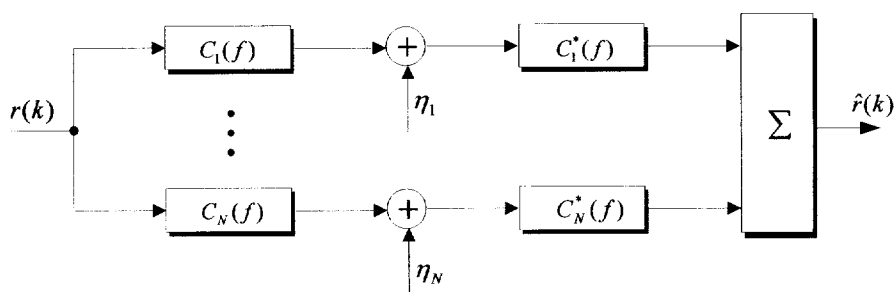


Figure 4.2. Block diagram for PPC equalizer

PPC for multiple channels uses the properties of the channel waveguide to suppress the side lobes of the channel response autocorrelation. Note that the cross-correlation of the data with the probe signal (the impulse response function) is a matched-filter process, a common procedure in digital communications. The probe signal is a linear transversal filter of a finite length. The deficiency of a linear transversal filter of a finite length in removing ISI is well known. When a small number of receivers are used, the channel response autocorrelation function has non-negligible side lobes, and PPC will generally have significant bit errors.

It is noted that multichannel DFE outperforms PPC. However, DFE is very sensitive to the choice of parameters. Error propagation sometimes causes the equalization to diverge and can not track channel characteristics.

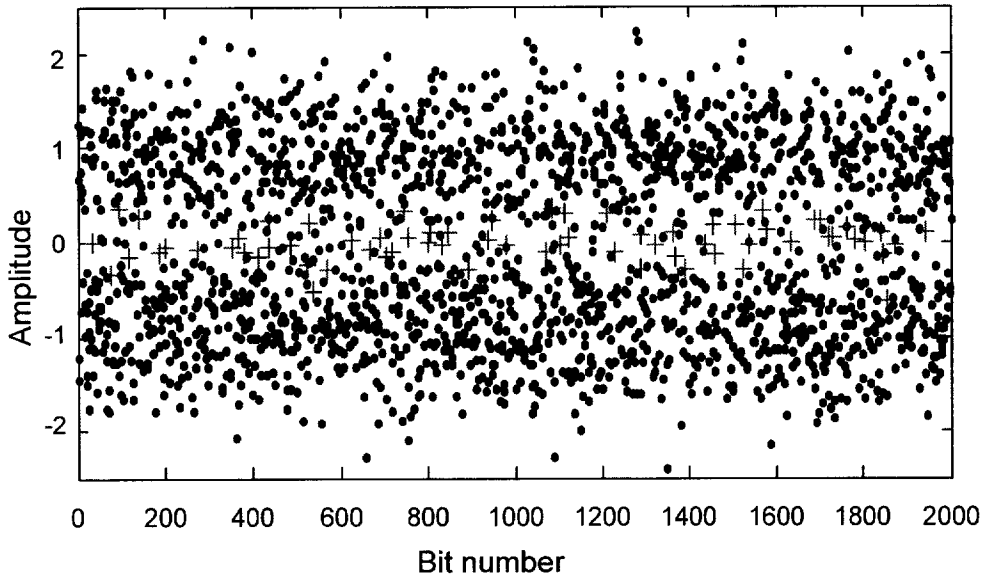
4.3 Performance comparison of PPC and DFE

The simulation was performed in the water with a constant sound speed of 1500m/s profile. It has a water depth of 100m. The source was placed at a depth of 35m. The vertical receiver array with 13 elements was equally spaced over a depth of from 87 to 99m. The source are placed at the ranges of 700m and 1000m, respectively.

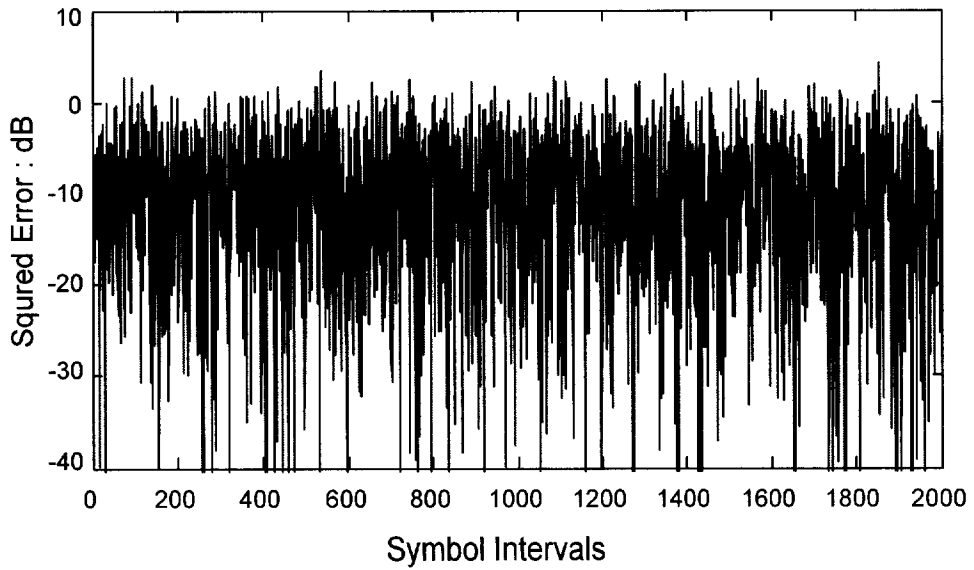
The PPC signal is obtained by convolving multipath arrivals with a cosine weighted pulse filter, allowing a small out of band energy. Seven multipath arrivals are observed with different delay times and magnitudes. Received data are created by convolving the impulse-response functions with a sequence of binary PSK signals. Random Gaussian noise is added to the received data with a SNR of 20dB.

For the channel $R=700\text{m}$, first the signals are shaped using a cosine filter. Figure 4.3 shows three channels receiver performance obtained at the same range and rate with PPC and DFE. When the three-channel equalizer (near the bottom of vertical array) is employed, DFE can eliminate ISI and achieve small MSE of -14dB. For PPC algorithm, three elements array can not reduce the ISI completely, thus MSE is close to zero and the demodulated signals can not be separated clearly which results in more errors occurred. Using three channels in a multichannel equalizer algorithm, a relatively satisfactory performance was obtained as shown by the DFE output plot, whereas using PPC algorithm can not reach the goal of error free communication. Thirteen channels are also taken as an example depicted in Figure 4.4. It is observed that the DFE output has less MSE and demodulated signals are tightly clustered than PPC. Thirteen channels DFE's MSE is approximately 4 dB lower than the previous case, i.e., three channel DFE. Hence, the symbols in Figure 4.3 are more scattered as compared with Figure 4.4. In the thirteen channel case, no errors are detected in a data block of length 3000 either for PPC or DFE.

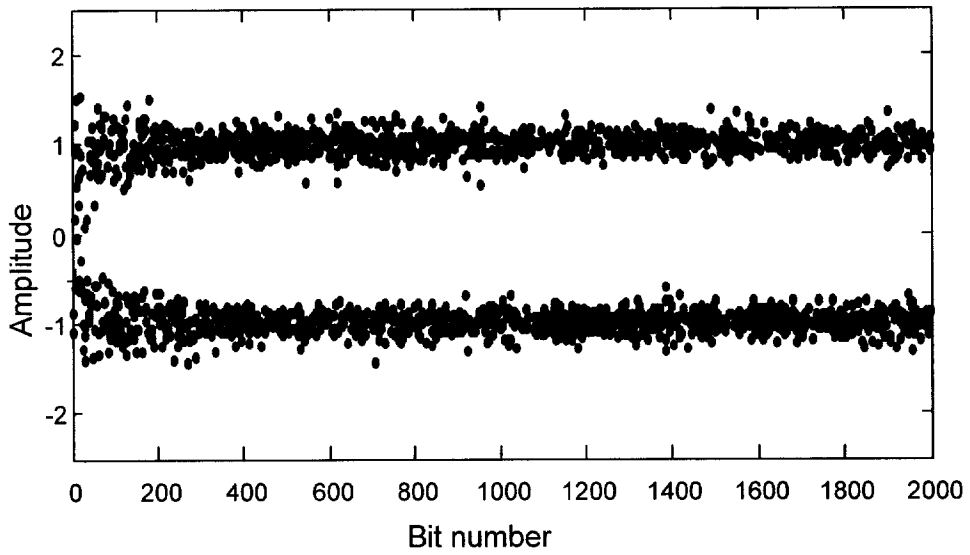
For channel $R=1000\text{m}$, Figures 4.5 and 4.6 summarize performance results.



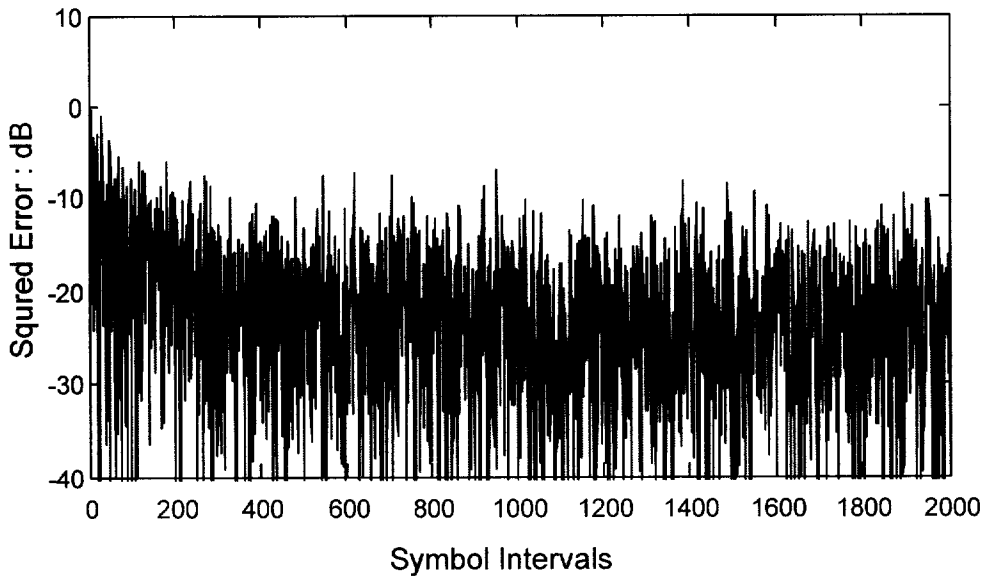
(a) Demodulated signal after PPC for $R=700m$ ($M: 3$)



(b) MSE with PPC for $R=700m$ ($M: 3$)

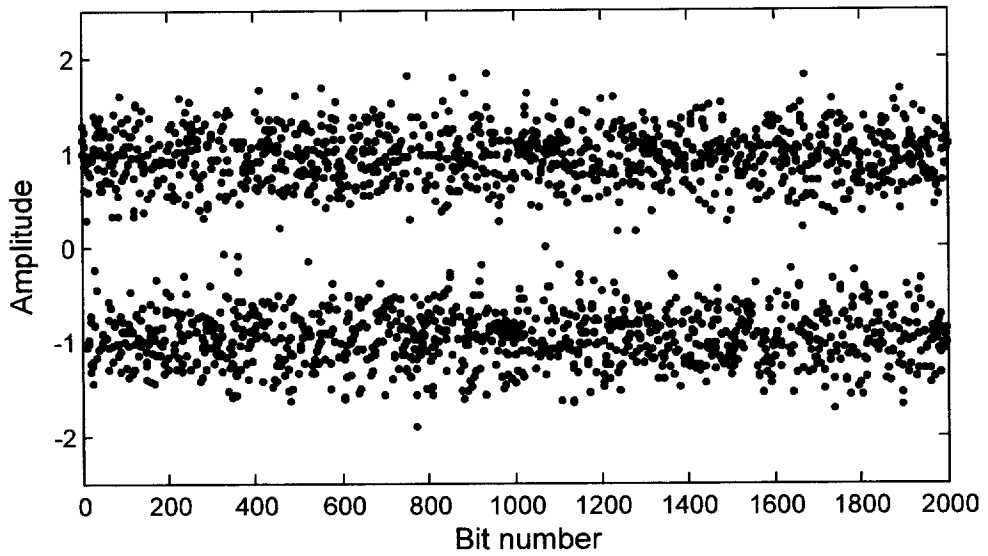


(c) Demodulated signal after DFE for $R=700$ ($M: 3$)

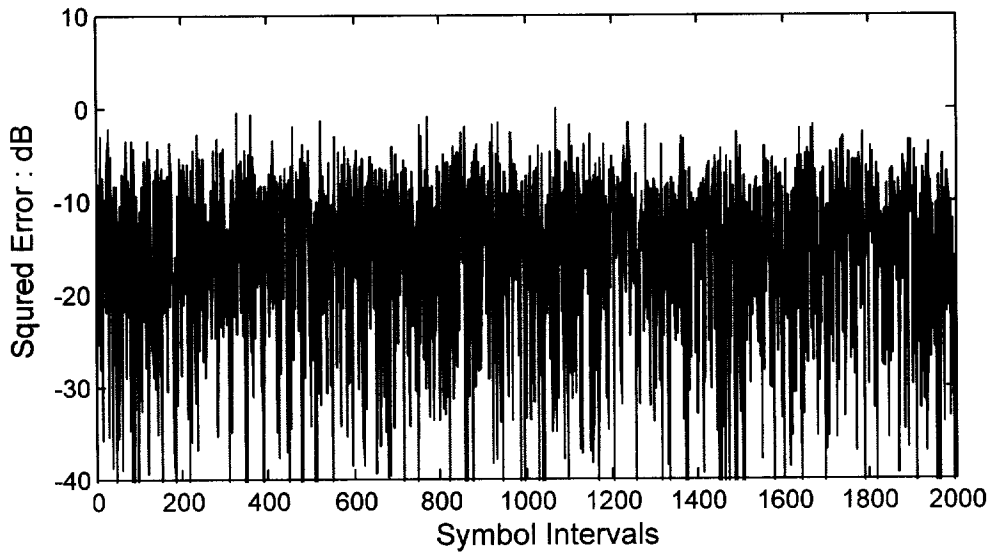


(d) MSE after DFE for $R=700m$ ($M: 3$)

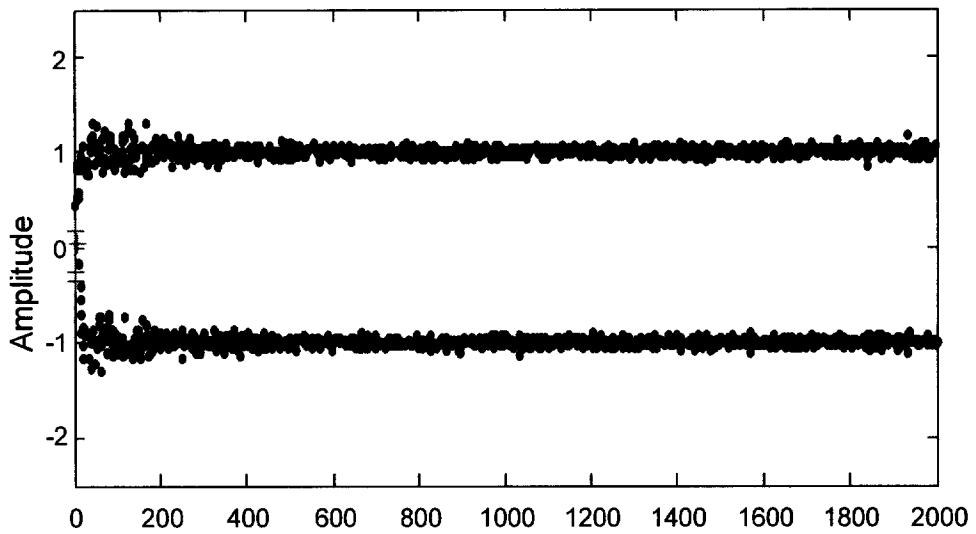
Figure 4.3. PPC and DFE performance for $M=3$ and $R=700m$



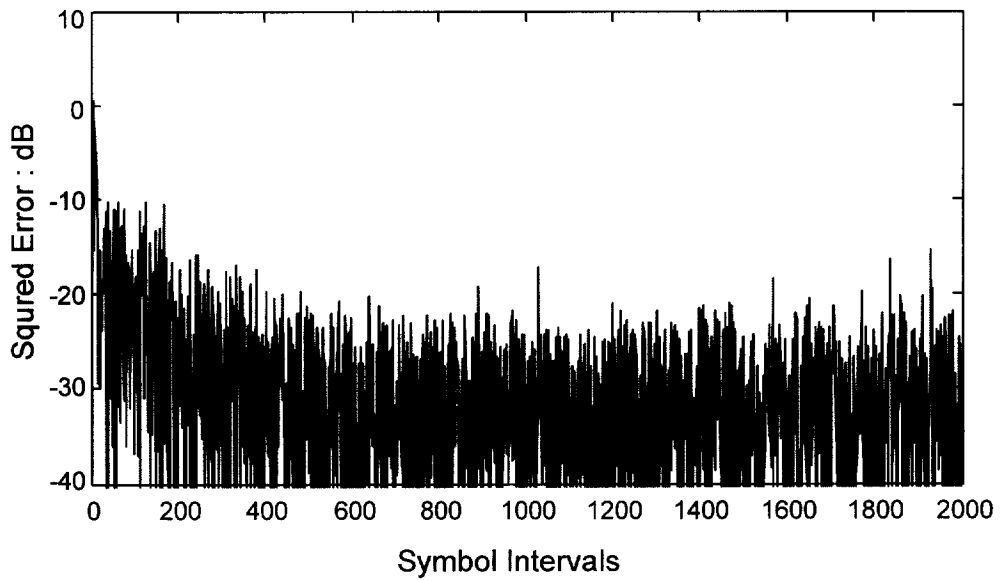
(a) Demodulated signal after PPC for $R=700m$ ($M: 13$)



(b) MSE after PPC for $R=700m$ ($M: 13$)

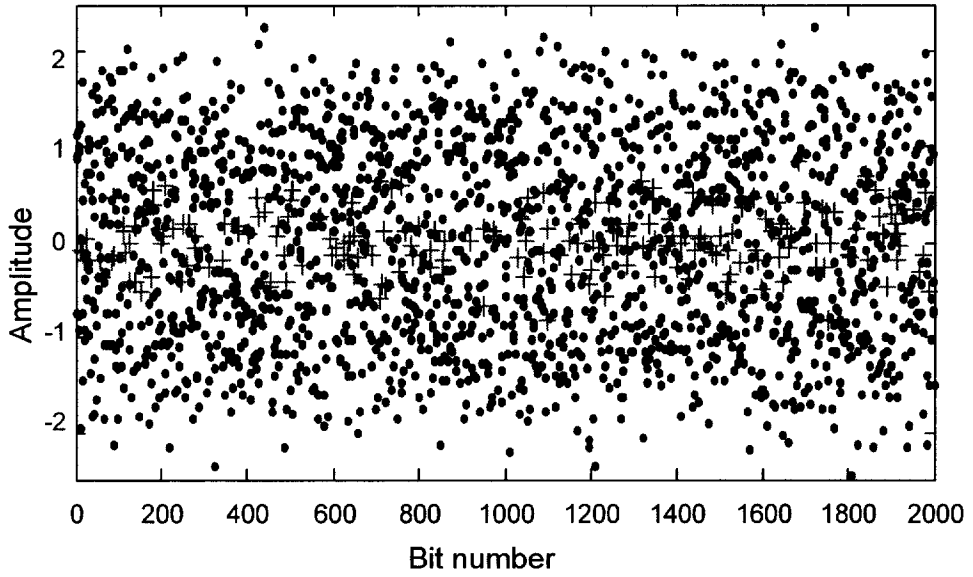


(c) Demodulated signal after DFE for $R=700m$ ($M: 13$)

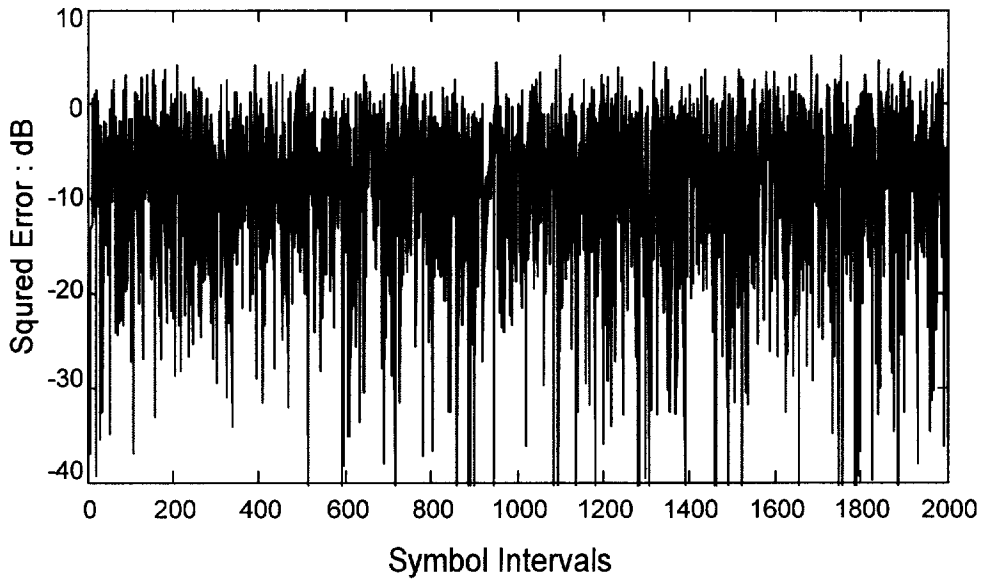


(d) MSE after DFE for $R=700m$ ($M: 13$)

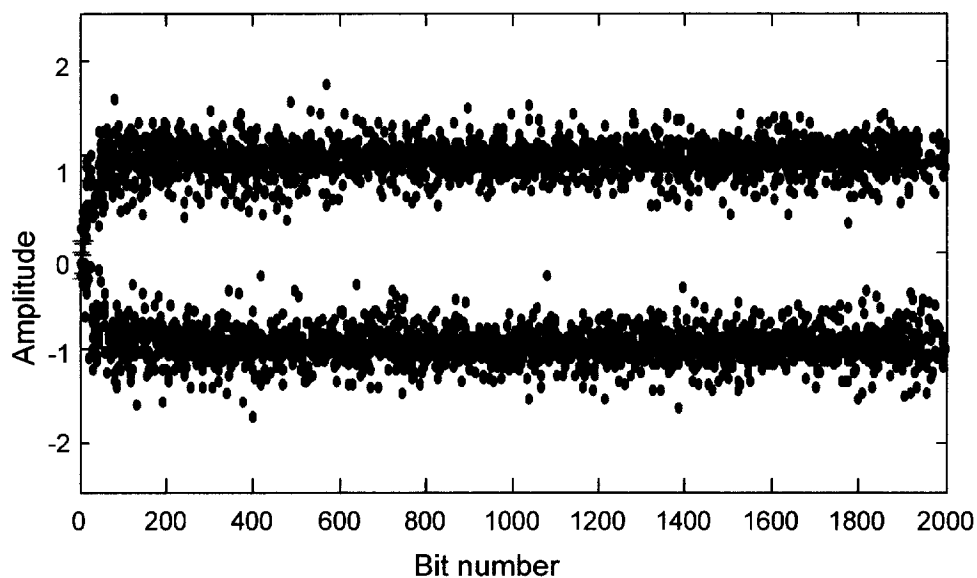
Figure 4.4. PPC and DFE performance for $M=13$ and $R=700m$



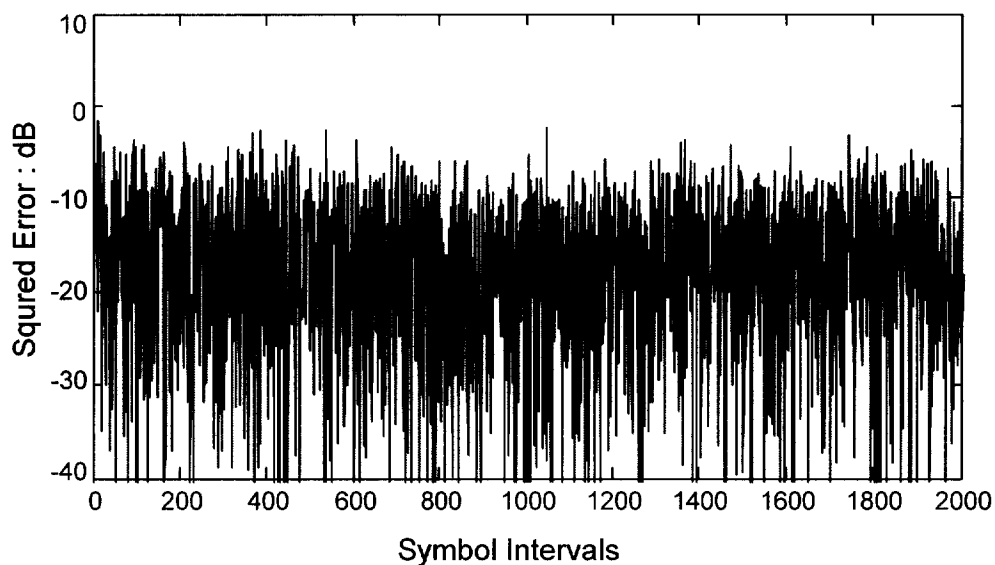
(a) Demodulated signal after PPC for $R=1000m$ ($M: 3$)



(b) MSE after PPC for $R=1000m$ ($M: 3$)



(c) Demodulated signal after DFE for $R=1000m$ (M:3)



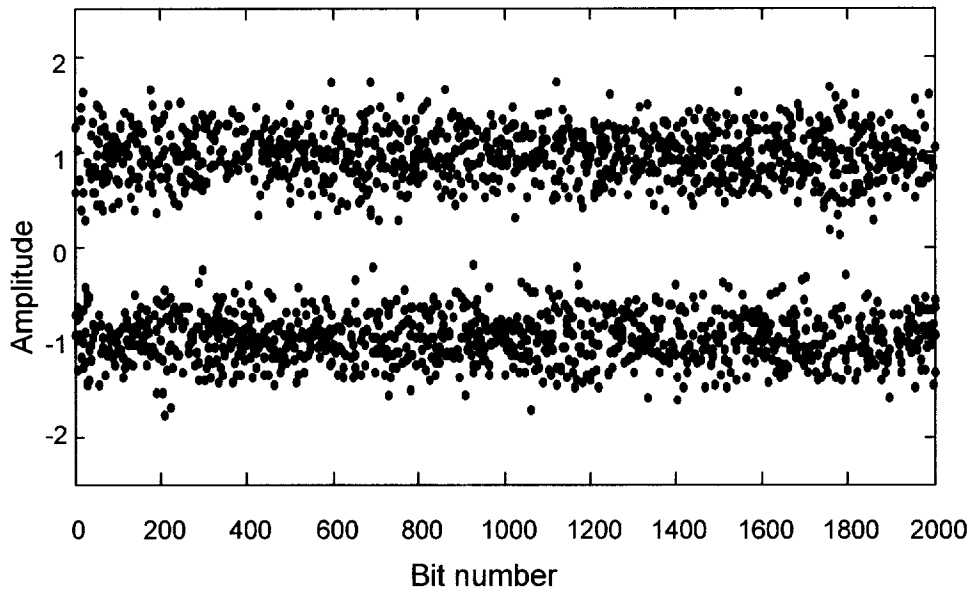
(d) MSE after DFE for $R=1000$ (M: 3)

Figure 4.5. PPC and DFE performance for $M=3$ and $R=1000m$

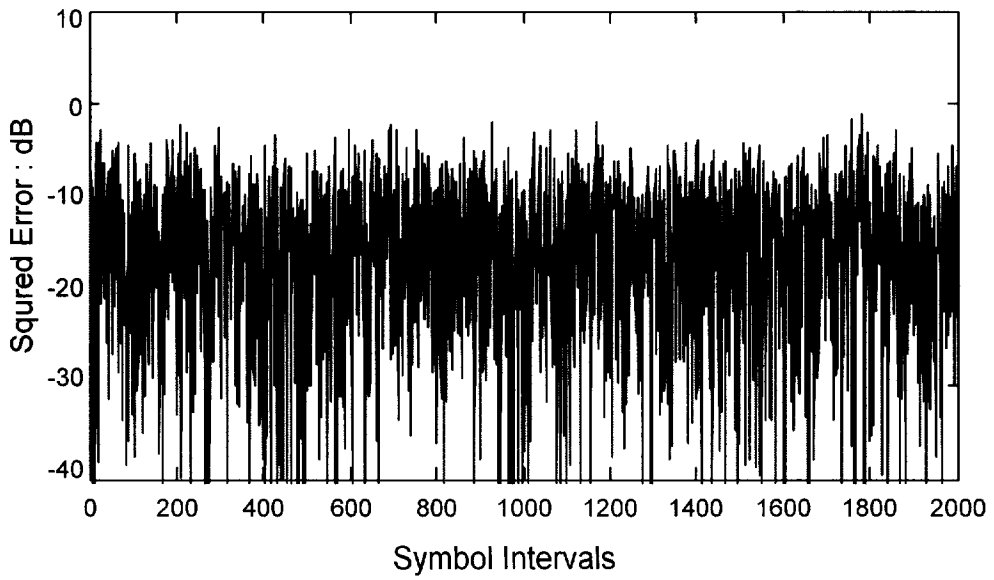
for the two cases: using 3 and 13 channels in DFE and PPC algorithm with the aid of multichannel DFE we can obtain more ideal results: small MSE and low bit errors detected. Comparing the PPC performance achieved with 3 and 13 elements demonstrates the fact that more element size can achieve better performance. Thus it is confirmed that PPC is much sensitive to the array size than multichannel DFE.

Figures 4.7a and 4.7b plot the MSE with respect to the number of array elements. It is observed that before the number of channels reaches 6 the DFE performance shows fast improvement with increase of elements, and slow increment thereafter. Increasing the number of array elements beyond 6 such as 13 offers 2 dB decrease in MSE. However in the case of PPC, performance can steadily improve. It should be noted that SNR at either 20dB or 30dB PPC provides similar performance, whereas multichannel DFE can achieve about 7dB improvement.

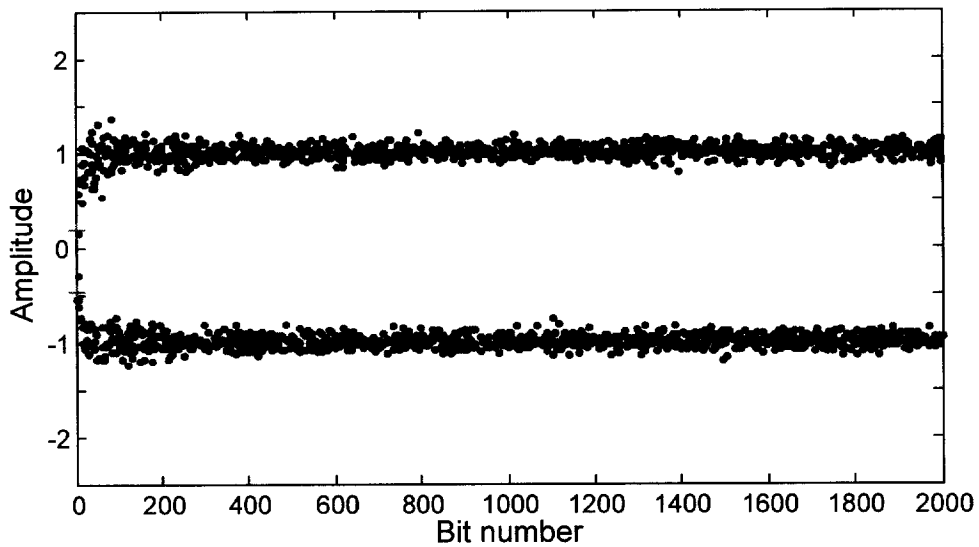
The MSE is plotted as a function of the number of array elements for the transmission rate of 1000 bps as shown in Figure 4.8. There are no errors detected either using PPC or multichannel equalizer after training. The demodulated sample variance is reduced evidently compared to the case of 2000 bps as shown in Figure 4.7a with the aid of PPC processing. Thus the decrease of transmission symbols bandwidth causes performance enhancement with PPC. It is observed that doubling the number of array elements can achieve approximate 3 dB improvement in performance. Multichannel equalizer's employment does give a rise to a little improvement in performance for 1000 bps. This implies one should choose a suitable method to make a trade off between computation complexity and transmission rate.



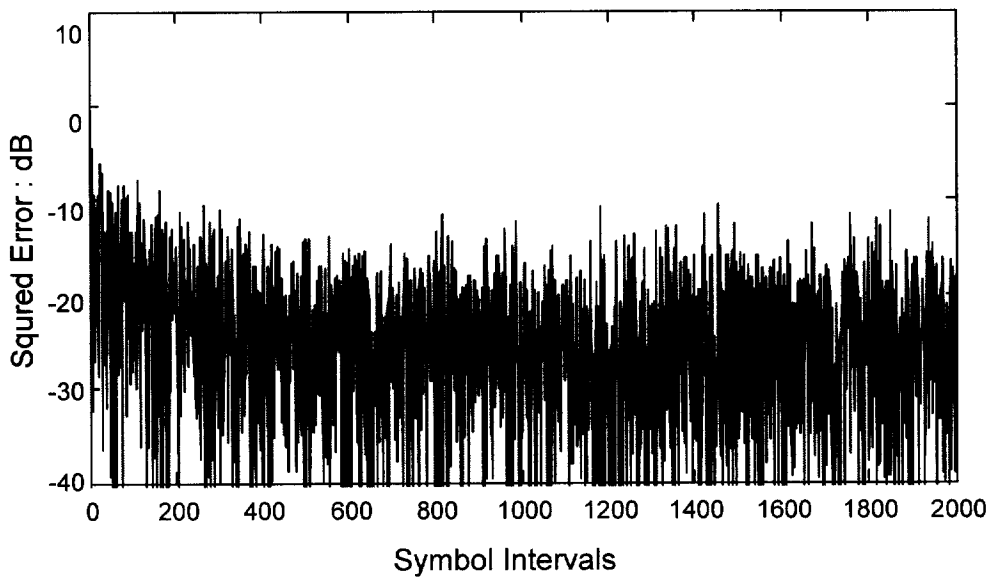
(a) Demodulated signal after PPC for $R=1000m$ ($M: 13$)



(b) MSE after PPC for $R=1000m$ ($M:13$)

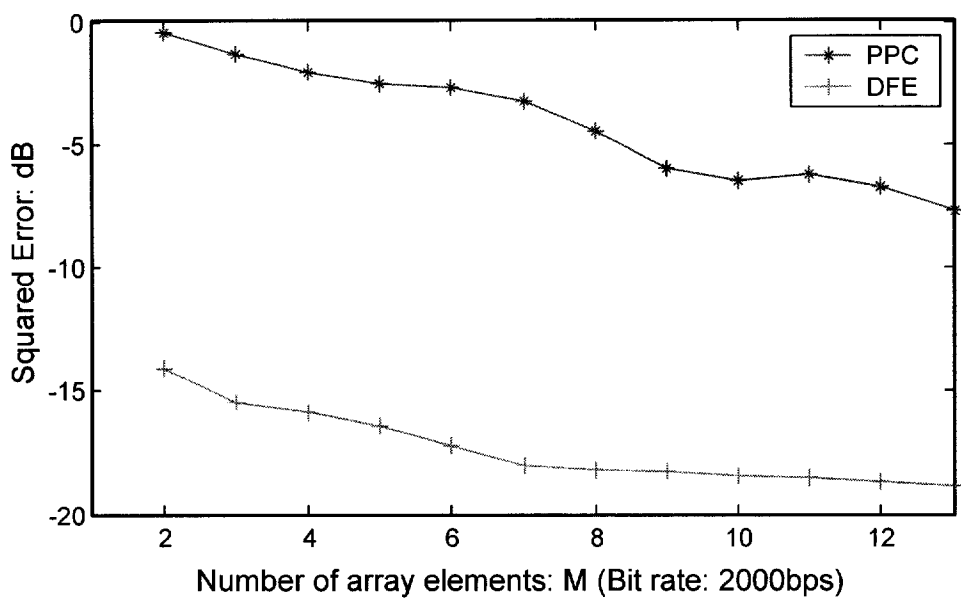


(c) Demodulated signal after DFE for $R=1000$ ($M: 13$)

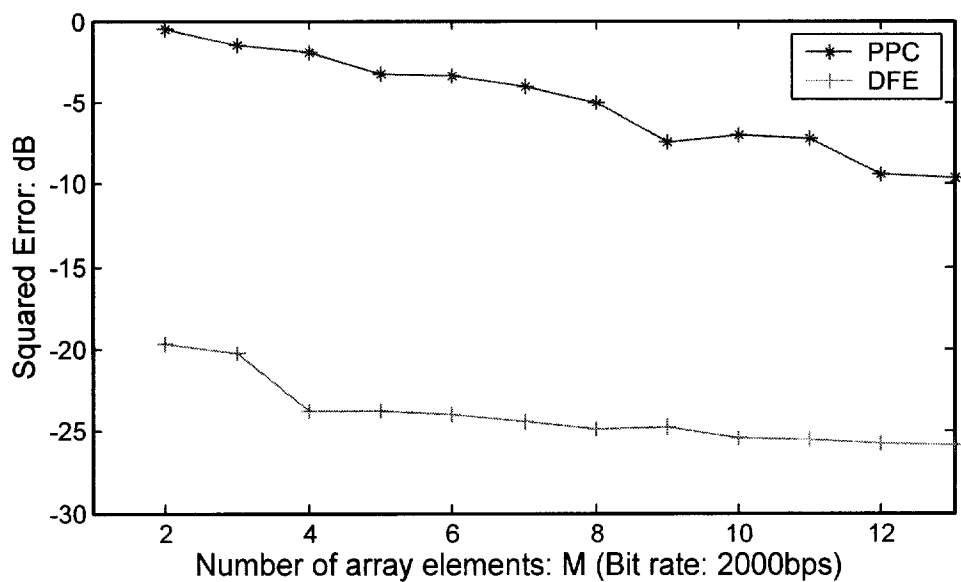


(d) MSE after DFE for $R=1000$ ($M: 13$)

Figure 4.6. PPC and DFE performance for $M=13$ and $R=1000m$



(a) SNR: 20dB



(b) SNR: 30dB.

Figure 4.7. MSE vs. number of receivers for PPC and DFE.

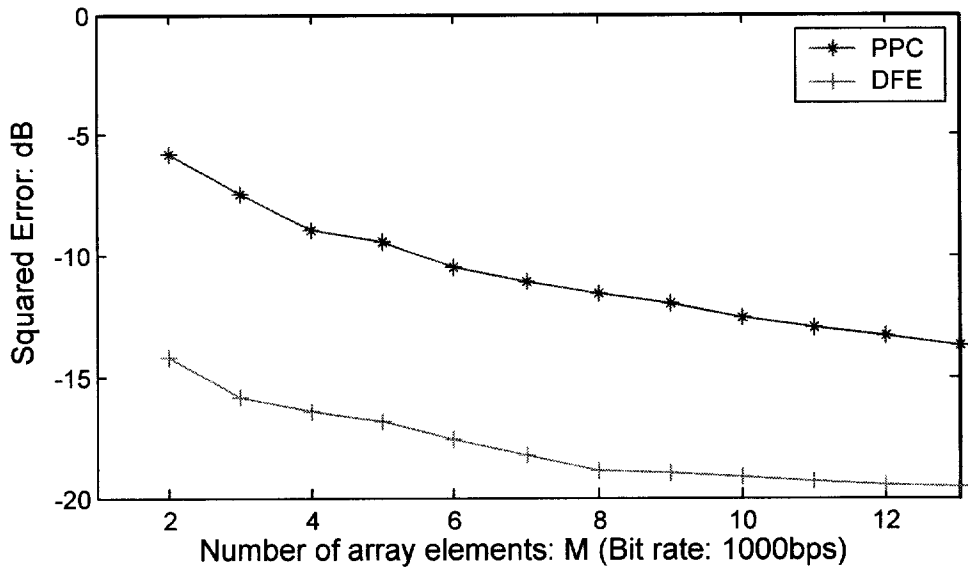


Figure 4.8. MSE vs. number of receivers for PPC and DFE (SNR: 20dB)

4.4 Conclusions

PPC and DFE performance was investigated in this simulation. In the former case, the filter coefficients are matched to time-reversed impulse response function for each receiver channel. In the latter case, the filter coefficients are determined by the MMSE criterion. PPC solution minimizes ISI by taking a coherent sum over many receivers over a large aperture vertical array. It is observed that, for a small number of receivers, PPC could not remove all the ISI. DFE can eliminate ISI completely. The advantage of DFE is its ability to reduce the MSE and BER compared with PPC. It yields a higher output SNR. In general, DFE outperforms PPC in terms of MSE. The difference in performance between PPC and DFE is due to the residual ISI [56-60] caused by the sidelobes of the function. PPC is less sensitive to SNR and more sensitive to the number of array elements and transmitted signal bandwidth compared with multichannel DFE [70].

Chapter 5

Conclusions

In this thesis the ISI caused by multipath in underwater acoustic communications is concerned on and several equalizers for reducing ISI have been discussed and simulation results demonstrate their effectiveness.

Firstly, it is found that linear and nonlinear LMS equalizer can be applied to combat ISI imposed on modulated signal over time dispersive channel. For the channel with weak ISI adaptive linear equalizer is effective in reduction of ISI, but for the channel with severe ISI employing adaptive nonlinear equalizer can remove ISI completely and obtain good performance. High data rates become possible in the case where channel variance is sufficiently slow to allow for channel tracking, the combination of adaptive equalization with more rapid convergence rate and synchronization techniques will be the subject of further study.

Secondly, how to choose the equalization algorithm suitable for multipath channel is discussed. In order to choose appropriate equalization method to achieve ideal transmission effects it is proposed that using RLS algorithm during the training period especially for the channel whose characteristics causes the received signal autocorrelation matrix large eigenvalue spread, LMS algorithm is employed during the decision direct mode. The simulation results prove that it's an effective scheme to improve the equalizer performance not improving the computation complexity largely. For the channel with deep spectral nulls, it especially shows this scheme's superiority while RLS DFE is employed for training period leading to fast convergence. Equalizer performance due to drifting distance is also analyzed and it is found that the source moving induces degrade of channel coherence resulting in smaller Euclidean distance's in signal space and more errors occurred if correlation coefficient decreases to small value.

Thirdly, diversity technique - PPC and multichannel DFE have been discussed and compared. PPC could be regarded as a special form of a linear transversal filter. The filter coefficients are matched to time-reversed impulse response function for each receiver channel. Although the PPC solution does not yield the minimum MSE, by summing over many receivers over a large aperture vertical array, ISI is reduced by the physics of waveguide propagation. The advantage of DFE is its ability to reduce the MSE and BER compared with PPC when the number of receivers is small. It yields a higher output SNR. The difference in performance is due to the residual ISI. However, DFE has its own problems, such as numerical sensitivities to the number of taps used. Adaptation of the DFE is also limited by error-propagation problem in real communication systems. The combination of adaptive equalization with more rapid convergence rate and synchronization techniques will be the subject of further study.

References

- [1] Milica Stojanovic, Josko A. Catipovic and John G. Proakis, "Phase-coherent digital communications for underwater acoustic channels," IEEE J. Oceanic Eng. vol. 19, No.1, January 1994
- [2] Milica Stojanovic, "Underwater acoustic communications," 1995
- [3] J. Catipovic, A. Baggeroer, K. von der Heydt and D.Koelsch, "Design and performance analysis of a digital acoustic telemetry system of the short-range underwater channel," IEEE J. Oceanic Eng. vol. OE-9, pp. 242-252, Oct. 1984
- [4] J. Catipovic and L. Freitag, "High data rate acoustic telemetry for moving ROV's in a fading multipath shallow water environment," in Proc. 7th Int. Symp. Unmanned Untethered Submersible Tech., pp 269-303, Washington, DC, June, 1990
- [5] Lfreitag and S.Merriam, "Robust 5000 bit per second underwater communication system for remote applications," in Proc. MTS '90 Conf., San Diego, CA, Feb. 1990
- [6] A. Vielmon, Ye (G.) Li and J. R. Barry, "Performance of alamouti transmit over time-varying Rayleigh-fading channels," IEEE T. on Wireless Comm. Vol. 3, No.5.Sep. 2004
- [7] Milica Stojanovic, "Recent advances in high speed underwater acoustic communications," IEEE, Journal, April, 1996
- [8] Simon Haykin, Adaptive filter theory, Third Edition, Prentice Hall, 1996.
- [9] John G. Proakis, Digital communications, Fourth Edition, McGraw-Hill, New York, 2001.
- [10] M. P. Fitton, A. R. Nix and M. A. Beach, "A comparison of RMS delay spread and coherence bandwidth for characterization of wideband channels," IEE 1996 The Institution of Electrical Engineers
- [11] Klaus Witrisal, "On estimating the RMS delay spread from the frequency-domain level crossing rate," IEEE Comm. Lett., 5(7), 287-289, 2001.
- [12] Steven J. Howard and Kaveh Pahlavan, "Measurement and analysis of the indoor radio channel in the frequency domain," IEEE Trans. On Instrumentation and Measurement 39(5), 751-755, 1990.
- [13] Mercedes Sánchez Varela and Manuel García Sánchez, "Study of a frequency diversity system for indoor digital TV," IEEE Trans. On Broadcasting 46(2), 165-169, 2000.
- [14] Tai-Kuo Woo, "HRLS: a more efficient RLS algorithm for adaptive FIR filtering," IEEE Comm. Letters 5(3), 81-84, 2001.

- [15] Felip Riera-Palou, James M Noras and David G M Cruickshank, "Analysis of the decision delay effect on the convergence of gradient recursive decision feedback equalizers," IEEE 2665-2668, 2000.
- [16] Gi Hun Lee, Jinho Choi, Rae-Hong Park, Lickho Song, Jae Hyuk Park and Byong-Uk Lee, "Modification of the reference signal for fast convergence in LMS-based adaptive equalizers," IEEE 645-654, 1994.
- [17] S. H. Leung and B. L. Chan, "Fast converging LMS equalizer," Electronics Letters, 29(10), 829-830, 1993.
- [18] Shun-Lee Chang and Tokunbo Ogunfunmi, "Performance analysis of nonlinear adaptive filter," IEEE 107-110, 1998.
- [19] Ki Man Kim, Il Whan Cha and Dae Hee Youn, "On the performance of the generalized sidelobe canceller in coherent situations," IEEE 465-468, 1992.
- [20] Jagdish C. Patra, Ranendra N. Pal, "A functional link artificial neural network for adaptive channel equalization," Signal Processing 43, 181-195, 1995.
- [21] Krishna R. Narayanan, Leonard J. Cimini, Jr., "Equalizer adaptation algorithms for high-speed wireless communications," IEEE 681-685, 1996.
- [22] Mark C. Austin and Ming U. Chang, "Quadrature overlapped raised-cosine modulation," IEEE Trans. On Comm. 29(3), 237-249, 1981.
- [23] Eweda Eweda, "Comparison of RLS, LMS and sign algorithms for tracking randomly time-varying channels," IEEE Trans. On Signal Processing 42(11), 2937-2944, 1994.
- [24] Norm W. K. Lo, David D. Falconer and Asrar U. H. Sheikh, "Adaptive equalizer MSE performance in the presence of multipath fading, interference and noise," IEEE 409-413, 1995.
- [25] Milica Stojanovic, J. Catipovic and J. Proakis, "Adaptive multichannel combining and equalization for underwater acoustic communications," J. Acoust. Soc. Am. 94(3), 1993.
- [26] Milica Stojanovic, Catipovic J. A., and Proakis J. G., "Reduced complexity spatial and temporal processing of underwater acoustic communication signals," J. Acoustic Soc. Am. 961-972, 1995
- [27] J. S. Kim and K. C. Shin, "Multiple focusing with adaptive time-reversal mirror," J. Acoust. Soc. Am 115(2), 600-606, 2004.
- [28] João Gomes and Victor Barroso, "Time-reversed OFDM communication in underwater channels," 2004 IEEE 5th Workshop on signal processing advances in wireless communications, 626-630, 2004.
- [29] Seongil Kim, G. F. Edelmann, W. A. Kuperman, W. S. Kodgkiss, H C. Song and T. Akal, "Spatial resolution of time-reversal arrays in shallow

- water,” J. Acoust. Soc. Am. 110 (2), 820-829, Aug. 2001.
- [30] A.J. Silva and S.M. Jesus, ”Underwater communications using virtual time reversal in a variable geometry channel,” IEEE, 2416-2421, 2002.
 - [31] John A. Flynn, James A. Ritcey, Daniel Rouseff and Warren L. J. Fox, “Multichannel equalization by decision-directed passive phase conjugation: experimental results,” J. of Oceanic Eng., 29(3), 824-836, 2004.
 - [32] Geoffrey F. Edelmann, T. Akal, William S. Hodgkiss, Seongil Kim, William A. Kuperman and Hee Chun Song, “An initial demonstration of underwater acoustic communication using time reversal,” J. of Oceanic Eng., 27(3), 602-609, 2002.
 - [33] Kevin B. Smith, Antonio A. M. Abrantes and Andres Larraza, “Examination of time-reversal acoustics in shallow water and applications to noncoherent underwater communications,” J. Acoust. Soc. Am. 113(6), 3095-3110, 2003.
 - [34] M. Heinemann, A. Larraza and K. B. Smith, “Experimental studies of applications of time-reversal acoustics to noncoherent underwater communications,” J. Acoust. Soc. Am. 113 (6), 3111-3116, 2003.
 - [35] James V. Candy, Andrew J. Poggio, David H. Chambers, Brian L. Guidry, Christopher L. Robbins and Claudia A. Kent, “Multichannel time-reversal processing for acoustic communications in a highly reverberant environment,” J. Acoust. Soc. Am. 118 (4), 2339-2354, 2005.
 - [36] W. J. Higley, Philippe Roux, W. A. Kuperman, W. S. Hodgkiss, H. C. Song and T. Akal, “Synthetic aperture time-reversal communications in shallow water: Experimental demonstration at sea,” J. Acoust. Soc. Am. 118 (4), 2365-2372, 2005.
 - [37] Daniel Rouseff, “Intersymbol interference in underwater acoustic communications using time-reversal signal processing,” J. Acoust. Soc. Am. 780-788, 2005.
 - [38] Daniel Rouseff, Darrell R. Jackson, Warren L. J. Fox, Christopher D. Jones, James A. Ritcey and David R. Dowling, “Underwater acoustic communication by passive-phase conjugation: theory and experimental results,” J. of Oceanic Eng., 26 (4), 821-831, 2001.
 - [39] Mathias Fink, Gabriel Montaldo, Mickael Tanter, “Time reversal acoustics,” 2004 IEEE Ultrasonics Symposium, 850-859, 2004.
 - [40] T. C. Yang, "Performance limitations of joint adaptive channel equalizer and phase locking loop in random oceans: initial test with data," IEEE 2000
 - [41] V. Capellano, G. Jourdain, “Comparison of adaptive algorithms for multichannel adaptive equalizers. Application to underwater acoustic

- communications," IEEE, 1178-1182, 1998.
- [42] Zoran Zvonar, David Brady and Josko Catipovic, "Adaptive equalization techniques for interference suppression in shallow water acoustic telemetry channels," IEEE, 1554-1558, 1993.
 - [43] T. C. Yang, "Performance limitations of joint adaptive channel equalizer and phase locking loop in random oceans: initial test with data," IEEE 2000.
 - [44] H. K. Yeo, B. S. Sharif, A. E. Adams, O. R. Hinton, "Comparison of adaptive algorithms performances for a multistage recursive successive interference cancellation (RSIC) multiuser detection strategy," IEEE, 2019-2023, 2000.
 - [45] João Gomes and Victor Barroso, "Ray-based analysis of a time-reversal mirror for underwater acoustic communication," IEEE, 2981-2984, 2000.
 - [46] Dale Green and Fletcher Blackmon, "Performance of channel-equalized acoustic communications in the surf zone," IEEE, 2262-2269.
 - [47] Joël Labat, Odile Macchi and Christophe Laot, "Adaptive decision feedback equalization: can you skip the training period?" IEEE Trans. of Comm. 46 (7), 921-930, 1998.
 - [48] Benoît Geller, Vittorio Caellano, Jean-Marc Brossier, Abderrahman Essebbar and Geneviève Jourdain, "Equalizer for video rate transmission in multipath underwater communications," IEEE J. of Oceanic Eng. 21 (2), 150-155, 1996.
 - [49] Daniel Rouseff, Warren L. J. Fox, Darrel R. Jackson and Christopher D. Jones, "Underwater acoustic communication using passive phase conjugation," IEEE, 2227-2230.
 - [50] John G. Proakis, Milica Stojanovic and Josko Catipovic, "Adaptive equalization algorithms for high rate underwater acoustic communications," IEEE, 157-164, 1994.
 - [51] Milica Stojanovic, J. Catipovic and J. G. Proakis, "An algorithm for multichannel coherent digital communications over long range underwater acoustic telemetry channels," IEEE, 577-582, 1992.
 - [52] J. Catipovic, "Performance limitations in underwater acoustic telemetry," IEEE J. Oceanic Eng. 15, 205-216, 1990.
 - [53] D. Slock and T. Kailath, "Numerically stable fast transversal filters for recursive least squares adaptive filtering," IEEE Trans. Sig. Proc. 39, 92-114, 1991.
 - [54] Peter Monsen, "Theoretical and measured performance of a DFE Modem on a fading multipath channel," IEEE Trans. On Comm. 25(10), 1144-1153, 1977.

- [55] Peter Monson, "Adaptive equalization of the slow fading channel," IEEE Trans. On Comm. Com-22(8), 1064-1075, 1974.
- [56] T. C. Yang, "Temporal resolutions of time-reversal and passive-phase conjugation for underwater acoustic communications," IEEE J. Oceanic Eng. 28(2), 229-241, 2003.
- [57] A. Benson, J. Proakis and M. Stojanovic, "Towards robust adaptive acoustic communications," IEEE, 1243-1248, 2000.
- [58] Mark Johnson, David Brady and Matt Grund, "Reducing the computational requirements of adaptive equalization in underwater acoustic communications," IEEE
- [59] Milica Stojanovic, J. Catipovic, J. Proakis, "Reduced complexity simultaneous beamforming and equalization for underwater acoustic communications," Oceans'93, Victoria, B.C., Oct. 1993
- [60] T. C. Yang, "Differences between passive-phase conjugation and decision-feedback equalizer for underwater acoustic communications," IEEE J. Oceanic Eng., Vol. 29, April, 2004
- [61] Young-hoon Yoon and Adam Zielinski, "Simulation of the equalizer for shallow water acoustic communication," Ocean 95, Vol. 2, pp. 1197-1203.
- [62] Abolfazl Falahati, Bryan Woodward, and Stephen C., "Underwater acoustic channel models for 4800b/s QPSK signals," IEEE J. Oceanic Eng., 1991.
- [63] Hongbin Li, Duixian Liu, Jian Li, Petre Stoica, "Channel order and RMS delay spread estimation with application to AC power line communications," Digital Signal Processing 13, PP. 284-300, 2003.
- [64] Bernard Sklar, Digital Communications, Prentice Hall P T R, 2000.
- [65] Zielinski, A., Coates, R., Wang, L. and Saleh, A., "High rate shallow water acoustic communication," Oceans, 1993, vol. III, PP432-437, 1993.
- [66] Gray Placzik and F.P. Haeni, "Surface geophysical technique used to detect existing and infilled scour and holes near bridges piers," USGS Water Resources Investigations Report ,
- [67] Herman Medwin, Fundamentals of Acoustic Oceanography, Academic Press, 1998.
- [68] M. Kocic, D. Brady, S. Merriam, "Reduced-complexity RLS estimation for shallow-water channels," IEEE J. Oceanic Eng. 16, 100-111, 1994.
- [69] Youngchol Choi and Jong-won Park, " A phase-coherent all-digital transmitter and receiver for underwater acoustic communication systems," IEEE 79-83, 2003.
- [70] Lee Freitag, Mark Johnson, Milica Stojanovic, Daniel Nagle and Josko Catipovic, "Survey and analysis of underwater acoustic channels for

coherent communication in the medium-frequency band,” IEEE 131-138, 2000.

- [71] Wael A. Al-Qaq, Michael Devetsikiotis and J. Keith Townsend, “Importance sampling methodologies for simulation of communication systems with time-varying channels and adaptive equalizers,” IEEE J. Selected Areas in Comm. 11(3), 317-327, 1993.
- [72] Geir Helge Sandmark and Arne Solstad, “Simulations of an adaptive equalizer applied to high-speed ocean acoustic data transmission,” IEEE J. Oceanic Eng. 16(1), 32-41, 1991.
- [73] Bong-Gee Song, James A. Ritcey, “Spatial diversity equalization for MIMO ocean acoustic communication channels,” IEEE J. Oceanic Eng. 21(4), 505-512, 1996.
- [74] Anthony G. Bessios, “Compound compensation strategies for wireless data communications over the multimodal acoustic ocean waveguide,” IEEE J. Oceanic Eng. 21(2), 167-180, 1996.
- [75] Josko A. Catipovic, “Performance limitations in underwater acoustic telemetry,” IEEE J. Oceanic Eng. 15(3), 205-216, 1990.
- [76] Vittorio Capellano, Gérard Loubet and Geneviève Jourdain, “Adaptive multichannel equalizer for underwater communications,” IEEE 994-999, 1996.
- [77] Milica Stojanovic and Zoran Zvonar, “Multichannel processing of broad-band multiuser communication signals in shallow water acoustic channels,” IEEE J. Oceanic Eng. 21(2), 156-166, 1996.

Acknowledgements

I am first greatly indebted to my advisor, Prof. Jong Rak Yoon, whose patience and kindness, as well as academic advice have been invaluable to me during my studying in Korea. Without his encouragement and support, I would not have finished this work. I am extremely very grateful to Prof. Shin Il Jeong, Prof. Deock-Ho Ha, Prof. Seok Tae Kim, Prof. Jea-Soo Kim as my committee members, for their thesis direction and attentive correction.

In my laboratory I was always surrounded by knowledgeable and friendly people who helped me daily. I would like to take this opportunity to thank all of them, Ji Hyun Park, Yong Ju Rho, Sung Kwan Baek, Seongwook Lee, Jong Woo Bae, Kyong Beak Ryu and so on for their numerous useful discussions and friendship. I also wish to thank Prof. Hyo Jin Seo for his advice and support. I also would like to express my gratitude to Prof. Sih Hong Doh, Prof. Kang Lyeol Ha, Prof. Byung-kee Moon for their concerning about my study. I am also very grateful to Seong Wook Heo for his encouragement and caring about my living in Pusan. I also appreciate all the Chinese students in Pukyong National University for their assistance and helpful suggestions.

There are so many more names I should mention, however, the space is limited, I would always cherish them in my memory of Korea.

This thesis is dedicated to my parents and brother. Their unconditional support has always been my impetus. My deepest appreciation is expressed to my husband Zhang Wan-song and daughter Zhang Shu-lin for their patience, support, understanding and inspiration.